

Regulation of lymphangiogenesis by WNT signalling: focus on WNT5A

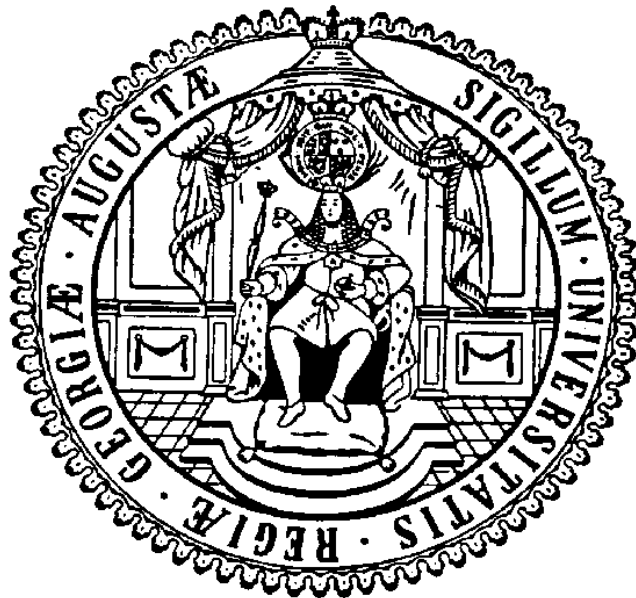
Dissertation

for the award of the degree

“Doctor rerum naturalium”

of the Georg-August-Universität Göttingen

within the doctoral program Molecular Medicine
of the Georg-August-University School of Science (GAUSS)



submitted by

Grit Lutze

from Erfurt

Göttingen, 2018

Thesis Committee

Prof. Dr. Jörg Wilting, Institute of Anatomy und Cell Biology, Center of Anatomy, UMG, Georg-August-University Göttingen

Prof. Dr. Gregor Eichele, Department of Genes and Behaviour, Max-Planck-Institute of Biophysical Chemistry, Göttingen

Prof. Dr. Ahmed Mansouri, Max-Planck-Institute for Biophysical Chemistry, Göttingen

Members of the Examination Board

Referee:

Prof. Dr. Jörg Wilting, Institute of Anatomy und Cell Biology, Center of Anatomy, UMG, Georg-August-University Göttingen

2nd Referee

Prof. Dr. Ahmed Mansouri, Max-Planck-Institute for Biophysical Chemistry, Göttingen

(if applicable) 3rd referee:

Prof. Dr. Gregor Eichele, Department of Genes and Behaviour, Max-Planck-Institute of Biophysical Chemistry, Göttingen

Further members of the Examination Board

PD Dr. Roland Dosch, Department of Developmental Biochemistry, UMG, Georg-August-University Göttingen

Prof. Dr. Dieter Kube, Department of Haematology and Oncology, UMG, Georg-August-University Göttingen

Prof. Dr. Andreas Wodarz, Department of Molecular Cell Biology, Institute I of Anatomy, University of Cologne Medical School, University of Cologne

Date of oral examination:

AFFIDAVIT

Here I declare that my doctoral thesis entitled “Regulation of lymphangiogenesis by WNT signalling: focus on WNT5A” has been written independently with no other sources and aids than quoted.

Grit Lutze

Göttingen, November 2018

List of publications

Original articles:

Manuscript under review in *Scientific Reports*

Poster Presentations:

Lutze G, Haarmann A, Demanou J A, Buttler K, Wilting J, Becker J (2018) Wnt5a mediates extension lymphangiogenesis and differentiation of lymphatics. 22nd Joint Meeting of the Signal Transduction Society, Weimar, November 5-7

Lutze G, Haarmann A, Demanou J A, Buttler K, Becker J, Wilting J (2018) Wnt5a mediates extension lymphangiogenesis and differentiation of lymphatics. 10th Kloster Seeon Meeting 'Angiogenesis': Molecular Mechanisms and Functional Interactions", Kloster Seeon, September 22-25

Lutze G, Buttler K, Wilting J (2016) Wnt signaling in lymphangiogenesis. The 38th Annual Meeting of the German Society for Microcirculation and Vascular Biology (GfMVB), Frankfurt/Main, September 26-28

Lutze G, Buttler K, Wilting J (2016) Wnt signaling in lymphangiogenesis. The 111th Annual Meeting of the Anatomical Society, Göttingen, September 21-24

Lutze G, Wilting J, Buttler K (2015) Wnt5a in Lymphangiogenesis. Joint Dutch-German Microcirculation Meeting 2015/37th Annual Meeting of the German Society for Microcirculation and Vascular Biology (GfMVB), Hanover, September 24-26; (*awarded with a poster-price*)

Table of Contents

Table of Contents	I
List of Figures	IV
List of Tables	IVI
Abbreviations	VII
1 Introduction	1
1.1 Structure and function of the lymphatic vascular system	1
1.2 Vasculogenesis, angiogenesis and lymphangiogenesis	2
1.3 Angiogenic mechanisms	4
1.4 Wnt signalling	5
1.4.1 The ‘canonical’ or β -catenin-dependent WNT signalling	7
1.4.2 The ‘non-canonical’ or β -catenin-independent WNT signalling pathways	8
1.5 WNT5A and lymphangiogenesis	9
1.6 Aims of the thesis	10
2 Materials and Methods	12
2.1 Materials	12
2.1.1 Chemicals, solutions and consumable supplies.....	12
2.1.2 Buffers and media	16
2.1.3 Inhibitors.....	18
2.1.4 Antibodies and Dyes.....	19
2.1.5 Recombinant WNT5A	21
2.1.6 Software	22
2.1.7 Equipment	23
2.1.8 Mice.....	24
2.1.9 Human dermal lymphatic endothelial cells	24
2.2 Methods	25
2.2.1 Mouse studies	25
2.2.1.1 Mouse embryo preparation.....	25
2.2.1.2 Microlymphangiography.....	25
2.2.1.3 <i>Ex vivo</i> skin cultures	26
2.2.1.4 Genotyping.....	27
2.2.1.5 Preparation of tissues for paraffin sections	27
2.2.2 Staining procedures.....	28

2.2.2.1	Whole mount staining of fresh mouse dermis	28
2.2.2.2	Immunofluorescence staining of paraffin sections.....	28
2.2.3	Studies on lymphatic endothelial cells	29
2.2.3.1	Cell culture	29
2.2.3.2	Inhibitor pre-treatment of cells	29
2.2.3.3	Cell proliferation assay	30
2.2.3.4	Cell migration studies with scratch assays	30
2.2.3.5	Tube formation assay	31
2.2.3.6	Spheroid sprouting assay	32
2.2.3.7	Immunofluorescence staining of cells.....	33
2.2.4	Molecular biology.....	34
2.2.4.1	RNA isolation	34
2.2.4.2	Reverse transcription	34
2.2.4.3	Semi-quantitative real-time PCR (qRT-PCR)	34
2.2.5	Protein biochemistry	37
2.2.5.1	Whole cell lysates	37
2.2.5.2	Concentration of supernatants.....	38
2.2.5.3	SDS-page and Western blot.....	38
2.2.6	Statistical analyses	39
3	Results.....	40
3.1	Studies on murine embryos.....	40
3.1.1	Immunohistological characterisation of embryonic murine dermal lymphatics	40
3.1.2	Superficial lymphatics of Wnt5A-null mice are malfunctioning.....	43
3.1.3	Recombinant WNT5A protein rescues maturation of dermal lymphatics in Wnt5a-null-mice.....	44
	Auxiliary finding: dermal lymphatics of Wnt5a-null mice may contain blood.....	47
3.1.4	Inhibition of Wnt-signalling retards maturation of dermal lymphatics in wild-type mice.....	47
3.2	Studies of human Lymphatic Endothelial Cells.....	49
3.2.1	Characterisation of Lymphatic Endothelial Cells	49
3.2.1.1	Immunocytology with LEC markers	49
3.2.1.2	qRT-PCR	50
3.2.1.3	Western blot and immunocytology.....	53
3.2.1.4	Immunocytology of migrating LECs.....	55
3.2.2	The PORCN inhibitor LGK974 inhibits WNT5A secretion in HD-LECs. 57	
3.2.3	<i>In vitro</i> Angiogenesis Assays – Measuring the lymphangiogenic potential of lymphatic endothelial cells	59
3.2.3.1	Spheroid Assay – Measuring the capability of sprouting.....	59

3.2.3.1.1	Sprouting of LY-LECs is WNT-dependent	59
3.2.3.1.2	Sprouting of HD-LECs is VEGF-C-dependent	60
3.2.3.1.3	Sprouting of HD-LECs is WNT-dependent.....	61
3.2.3.2	Scratch Assays – Measuring horizontal migration of LECs.....	63
3.2.3.2.1	Horizontal Migration of HD-LECs is controlled by WNT signalling.....	64
3.2.3.2.2	Horizontal migration of HD-LECs is mediated through the planar-cell-polarity (PCP) pathway via RAC and JNK.....	66
3.2.3.3	WNT5A induces phosphorylation of JNK.....	71
3.2.3.4	Tube Formation Assay – WNT5A increases network formation.....	72
3.2.4	mRNA sequencing analyses of LGK974-treated HD-LECs.....	74
3.2.4.1	Validation of WNT-regulated genes in LECs by qRT-PCR	77
4	Discussion.....	78
4.1	Development of murine dermal lymphatics is Wnt5a-mediated	78
4.2	WNT signalling potential of human lymphatic endothelial cells.....	83
4.3	PORCN inhibition with LGK974 prevents WNT5A secretion in HD-LECs.....	84
4.4	WNT signalling regulates various mechanisms of lymphangiogenesis	86
4.5	WNT5A mediates horizontal migration of HD-LECs via RAC and JNK .	89
4.6	WNT5A increases network formation of HD-LECs <i>in vitro</i>	91
4.7	WNTs regulate migration-associated and lymphangiocrine pathways.	92
5	Summary and Conclusions.....	93
6	Appendix	95
7	Bibliography.....	103
	Acknowledgements	112
	Curriculum Vitae	113

List of Figures

Figure 1: Schematic model of lymphangiogenesis in the mouse between ED 9.0 and ED 11.5.	4
Figure 2: Schematic overview of the main WNT signalling pathways.	6
Figure 3: Typical phenotype of a <i>Wnt5a</i> -null mouse embryo (B, -/-) and a littermate control embryo (A, +/+) at ED 15.5.	10
Figure 4: Example for scratch assay quantification with GNU Octave.	31
Figure 5: Example for the counting of sprouts with the circular-grid method.	33
Figure 6: Mice express <i>Wnt5a</i> in their lymphatic vessels.	41
Figure 7: Lymphatic vessels of mice express <i>Fzd5</i>	42
Figure 8: Lymphatic vessels of mice express <i>Fzd8</i>	42
Figure 9: Lymphatic vessels of mice express <i>Vangl2</i>	43
Figure 10: Interstitial injection of 2000 kDa FITC-dextran into the paw of ED 17.5 mouse embryos. ...	44
Figure 11: <i>Ex vivo</i> studies of dermis from ED 15.5 <i>Wnt5a</i> -null mice treated with recombinant WNT5A for 2 days.	45
Figure 12: Quantification of <i>ex vivo</i> studies of lymphatics in the dermis of <i>Wnt5a</i> -null mice.	46
Figure 13: Higher magnification of <i>ex vivo</i> studies of dermis from ED 15.5 <i>Wnt5a</i> -null mice treated with recombinant WNT5A for 2 days.	46
Figure 14: Lymphatic vessels of <i>Wnt5a</i> -null mice contain blood.	47
Figure 15: <i>Ex vivo</i> studies of lymphatics in the dermis of ED 15.5 C57BL/6 mice treated with the <i>Porcn</i> -inhibitor LGK974.	48
Figure 16: Quantification of <i>ex vivo</i> studies of C57BL/6 mouse dermis with the <i>Porcn</i> -inhibitor LGK974.	49
Figure 17: Anti-PROX1 and anti-CD31 double staining of LECs.	50
Figure 18: Relative expression levels of three HD-LEC lines.	52
Figure 19: Protein expression analyses of WNT-related molecules in HD-LECs.	54
Figure 20: Scratch assays: FZD5, PRICKLE1 and VANGL2 show a polarized localization in migrating HD-LECs.	56
Figure 21: LGK974 inhibits WNT5A production and secretion.	58
Figure 22: LGK974 inhibits WNT5A in serum-free conditions.	58
Figure 23: Spheroid assay with LEC2.	60
Figure 24: VEGF-C is essential for sprouting of HD-LECs.	61
Figure 25: Sprout formation of HD-LEC-spheroids after inhibition of autocrine WNT-secretion.	62
Figure 26: Application of recombinant WNT5A to HD-LEC-spheroids.	63
Figure 27: Inhibition of autocrine WNT-secretion of migrating HD-LECs.	64
Figure 28: Influence of the inhibition of autocrine WNT-secretion on migration and proliferation of HD-LECs.	65
Figure 29: Scratch assay: Application of recombinant WNT5A to migrating HD-LECs.	65

Figure 30: Effects of recombinant WNT5A protein on migration and proliferation of HD-LECs.	66
Figure 31: Is migration of HD-LECs mediated by β -catenin-dependent WNT signalling?	67
Figure 32: Activation of the β -catenin-dependent WNT signalling inhibits migration of HD-LECs, but does not influence their proliferation.	67
Figure 33: Migration of HD-LECs is independent of ROCK.	68
Figure 34: Horizontal migration of HD-LECs is independent of ROCK signalling.	69
Figure 35: Migration of HD-LECs is RAC-mediated.	70
Figure 36: Horizontal migration of HD-LECs depends on RAC signalling.	70
Figure 37: Migration of HD-LECs is JNK-mediated.	71
Figure 38: Horizontal migration of HD-LECs depends on JNK signalling.	71
Figure 39: WNT5A induces phosphorylation of JNK in HD-LECs.	72
Figure 40: WNT5A increases network formation.	73
Figure 41: Heatmap of the top 50 differentially expressed genes in HD-LECs treated with 10 μ M LGK974 compared to DMSO controls.	75
Figure 42: GSEA for the gene set "Movement of cell or subcellular component"	76
Figure 43: Validation of the mRNAseq analysis with qRT-PCR.	77

Additional Figure:

Figure A- 1: Macrophotographs of a Wnt5a-null-mouse embryo and a littermate control.	95
---	----

List of Tables

Table 1: Chemicals or solutions	12
Table 2: Consumables	15
Table 3: Recipes of buffers and medias	16
Table 4: Inhibitors	18
Table 5: Antibodies and fluorescence dyes	19
Table 6: Software	22
Table 7: Equipment	23
Table 8: Formulation of RT-PCR master mix.....	34
Table 9: qRT-PCR programme	35
Table 10: Primers.....	36
Table 11: Results of the GSEA.	76

Additional Tables:

Table A- 1: 2way ANOVA of proliferation studies with HD-LECs and the PORCN inhibitor LGK974.	96
Table A- 2: 2way ANOVA of proliferation studies with LGK974 pre-treated (10 μ M) HD-LECs and 500ng/ml WNT5A.	97
Table A- 3: 2way ANOVA of proliferation studies with an inhibitor of the β -catenin-dependent WNT signalling pathway (FH535) and two activators (Bio and IM-12).	98
Table A- 4: 2way ANOVA of proliferation studies with the ROCK inhibitors Y-27632 and Fasudil.	99
Table A- 5: 2way ANOVA of proliferation studies with the RAC inhibitors EHT 1864 and NSC23766.	100
Table A- 6: 2way ANOVA of proliferation studies with the JNK inhibitors SP600125 and JNK-IN-8.	101
Table A-7: List of differentially regulated genes in HD-LECs treated with LGK974 compared to controls, ranked according to the adjusted p value (p _{adj}).	102

Abbreviations

Abbreviation	Denotation
APC	Adenomatous polyposis coli protein
BEC	Blood endothelial cell
BS	Blocking solution
BSA	Bovine serum albumin
CAMKII	Calmodulin-dependent kinase
CKI α	Casein kinase I α
C _T	Threshold cycle
CV	Cardinal vein
DAG	Diacylglycerol
DKK1	Dickkopf-related protein 1
ED	Embryonic day
FBS	Foetal bovine serum
FZD	Fizzled receptor
GFP	Green fluorescent protein
GO	Gene ontology term
GSEA	Gene set enrichment analysis
GSK3	Glycogen synthase kinase 3
HD-LEC	Human dermal lymphatic endothelial cell
HRP	Horseradish peroxidase
IF	Immunofluorescence
IGF	Insulin-like growth factor
IP3	Inositol trisphosphate
JNK	JUN-N-terminal kinase
ko	Knock-out
LEC	Lymphatic endothelial cell
LEF	Lymphoid enhancer-binding factor
LRP	Low-density lipoprotein receptor-related protein

Abbreviation	Denotation
LY-LEC	Lymphangioma-derived lymphatic endothelial cell
LYVE-1	Lymphatic vessel endothelial hyaluronic acid receptor 1
MP	Milk powder
NFAT	Nuclear factor of activated T cells
NRP	Neuropilin
PBS	Phosphate buffered saline
PCP	Planar-cell-polarity
PIP2	Phosphatidylinositol 4,5-bisphosphate
PKC	Protein kinase C
PLC	Phospholipase C
PORCN	Porcupine protein
PRICKLE	Prickle planar cell polarity protein
PROX1	Prospero homeobox protein 1
qRT-PCR	Quantitative real-time polymerase chain reaction
RAC	Ras-related C3 botulinum toxin substrate
RHOA	Ras Homolog Family Member A
ROCK	Rho-associated coiled-coil containing protein kinase
ROR	Receptor tyrosine kinase-like orphan receptor
RT-PCR	Reverse transcription polymerase chain reaction
RYK	Related to receptor tyrosine kinase
SPTA	Spectrin alpha chain
SPTBN	Spectrin beta chain, brain
TCF	T-cell factor
VANGL	Van Gogh-like protein

Abbreviation	Denotation
VEGF	Vascular endothelial growth factor
VEGFR	Vascular endothelial growth factor receptor
WB	Western blot
WNT	Wingless-type MMTV integration site family
wt	Wild type

1 Introduction

WNT signalling has important roles in embryonic development and disease (Logan and Nusse, 2004). There are increasing numbers of studies showing that WNTs also influence both blood vessel development (angiogenesis) (Dejana, 2010) and lymphangiogenesis, but the mechanisms how WNTs regulate vessel formation have remained vague. In previous studies, it has been shown that *Wnt5a*, a member of the β -catenin-independent Wnt pathway, is essential for the development of lymphatic vessels in the dermis of mice (Buttler et al., 2013). At embryonic day (ED) 18 *Wnt5a*-null-mice possess non-functional, highly dilated lymphatics, in contrast to functional lymphatics with small lumen observed in *Wnt5a*^{+/-} and wild-type (wt) mice. However, the mechanisms by which *Wnt5a* regulates lymphangiogenesis remained unclear.

1.1 Structure and function of the lymphatic vascular system

Lymphatic vessels (lymphatics) are in addition to the primary and secondary lymphatic organs – thymus, bone marrow, spleen, lymph nodes – an important component of the lymphatic system. They can be found in almost all organs and tissues, including perineural structures (Aspelund et al., 2015; Louveau et al., 2015), but not in cornea, bone marrow and central nervous system (Alitalo et al., 2005). The lymphatic vascular system is complementary to the cardiovascular system and transports extravasated fluid back into the blood stream. Lymphatic vessels are, like the blood vessels, lined by endothelial cells (lymphatic endothelial cells - LECs). The smallest vessels are the lymph capillaries, now usually called initial lymphatics. They are often blindly ending vessels, or vascular loops, with a discontinuous basement membrane and overlapping endothelial junctions, which function as delicate interendothelial valves (Baluk et al., 2007; Tammela and Alitalo, 2010). Their main function is the drainage of interstitial fluid, and the transfer of this fluid (lymph) into larger collecting vessels. These larger, contractile

vessels (lymphatic collectors) possess a continuous basement membrane, an intima with semilunar valves, a layer of smooth muscle cells, and an adventitia, which contains nerves and nutritive blood vessels (Hasselhof et al., 2016). They carry lymph to the lymph nodes (afferent lymphatics). Efferent collectors then either drain to a vein or in a larger lymphatic duct, such as the thoracic duct, which finally drains into the confluence of the left subclavian and internal jugular vein (Wilting and Chao, 2015).

Besides fluid homeostasis, the lymphatics have several other important functions such as immune surveillance, and dietary fat absorption in the gut. They play also a role in pathological mechanisms like the dissemination and metastasis of lymphoma cells and other tumour cells. And in the last years it has also been shown that LECs can modulate immune cell activation and function by presentation of antigens (reviewed in: Aebischer et al. (2014); Card et al. (2014)).

1.2 Vasculogenesis, angiogenesis and lymphangiogenesis

Endothelial cells of lymphatic and blood vessels (LECs and BECs) are derived from the mesoderm. In the human, the development of blood cells and blood vessels starts around the middle of the third week of embryogenesis. At this time, mesenchymal haemangioblasts form clusters of cells in the chorion, in the connecting stalk and in the yolk sac. These haemangioblasts give rise to blood and vessels by forming transient structures called blood island (Pansky, 1982). The outer cells of the island differentiate to endothelial cells and the inner ones to haematopoietic cells. The blood islands connect to each other by sprouting of the endothelial cells, which fuse and form a sinusoidal network. The formation of vessels from angioblasts is called vasculogenesis (Risau and Flamme, 1995), while the outgrowth and formation of vessels from pre-existing (sinusoidal or primitive) networks is called angiogenesis (Risau, 1997).

The development of the lymphatic systems starts approximately two weeks later than the development of the cardiovascular system (Pansky, 1982). The first visible signs are the jugular lymph sacs. Already one century ago, there were two hypotheses how the lymphatic systems develops. Sabin (1902) stated that the lymphatics develop from the endothelium of the cardinal veins, whereas Huntington and McClure (1910) stated that they develop from lymphatic vesicles, and that these mesenchymal cells build the wall of the lymph vessels and connect the venous system secondarily. In recent years, our understanding of the molecular and cellular mechanisms that regulate the development and function of the lymphatic vascular system has grown enormously. *In vivo* imaging studies of zebrafish embryos (Yaniv et al., 2006) and lineage tracing experiments in mice (Srinivasan et al., 2007) confirmed Sabin's hypothesis, but it has also been shown that lymphatics have a non-venous, mesenchymal origin in avian (Schneider et al., 1999; Wilting et al., 2006), amphibian (Ny et al., 2005) and murine embryos (Buttler et al., 2013; Klotz et al., 2015; Martinez-Corral et al., 2015). Additionally, there are specialized mesoderm-derived angioblasts in a venous niche in zebrafish embryos (Nicenboim et al., 2015).

In mice, the development of the lymphatics starts at ED 9.5. At this distinct time point, cells in the cardinal and intersomitic veins start to express Prox1 (**Figure 1A**) (Wigle and Oliver, 1999). Around ED 10.5 these cells start to sprout out. This process requires the expression of Vascular endothelial growth factor C (Vegf-C, the main growth factor for lymphatics) in the surrounding tissue. The sprouting LECs then are characterised by expression of the Vascular endothelial growth factor receptor 3 (Vegfr-3, the main receptor for Vegf-C), the Lymphatic vessel endothelial hyaluronic acid receptor 1 (Lyve-1, mainly expressed on LECs), Podoplanin (a highly LEC-specific glycoprotein in the cell membrane), and they upregulate the expression of Neuropilin 2 (Nrp2, an alternative receptor for Vegf-C). Later, these cells form the jugular lymph sacs, which can be observed around ED 11.5.

The endothelial cells from the lymph sacs also sprout out and give rise to lymphatic vessels, which grow into the periphery. Additionally, lymphangioblasts (in the skin, **Figure 1B**) also differentiate from mesenchymal cells, proliferate and

form lymphatic vessels. Later, vessels from both origins interconnect and form lymphatic networks (Martinez-Corral et al., 2015).

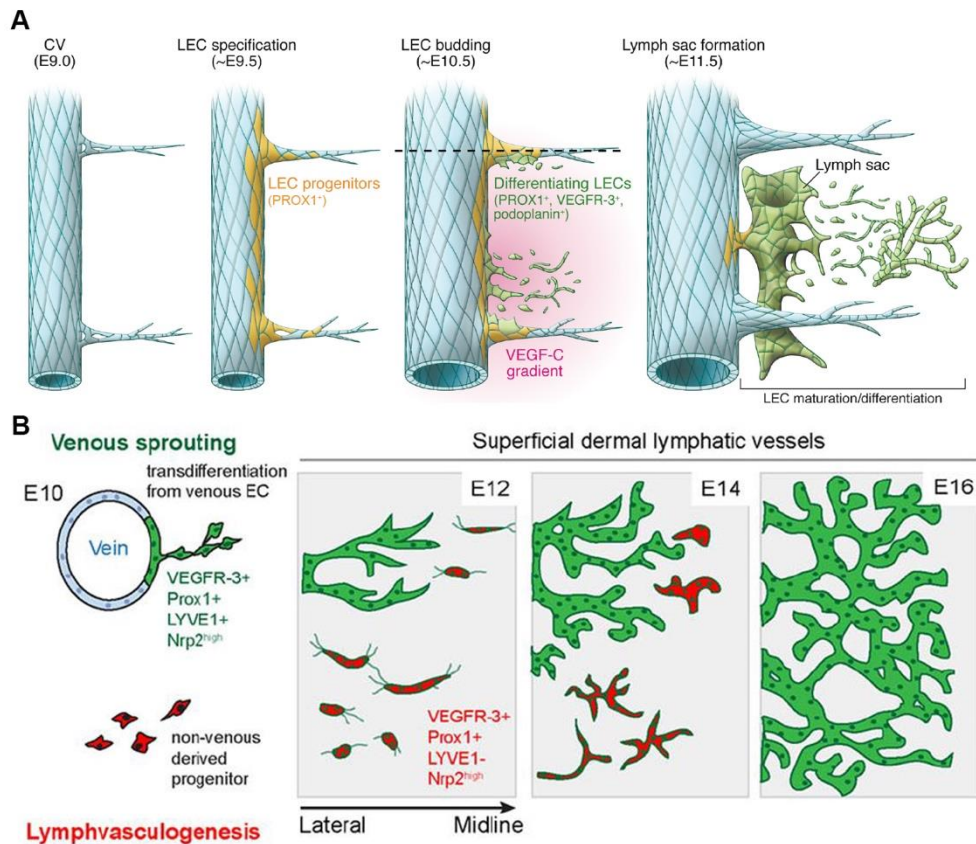


Figure 1: (A) Schematic model of lymphangiogenesis in the mouse between ED 9.0 and ED 11.5. The endothelial cells of the cardinal vein (CV) are the main source of LECs. At ED 9.5 the LEC progenitor cells start to express Prox1 and at ED 10.5 they start to bud from the CV and the intersomitic veins. This process requires Vegf-C. The differentiating LECs start to express Vegfr-3 and Podoplanin. At ED 11.5 they have formed the lymph sacs. **(B) Schematic model of lymphangiogenesis in the dermis of mice.** Besides sprouting from veins (sprouts are positive for Vegfr-3, Prox1, Lyve-1 and Nrp2) there are also non-venous progenitor cells (negative for Lyve-1), which proliferate, form vessels and connect to venous-derived vessels. The schemes were taken from (A): Y Yang and Oliver (2014) and (B): Martinez-Corral et al. (2015); with permission.

1.3 Angiogenic mechanisms

Angiogenesis is the formation of capillaries from pre-existing vessels (Risau, 1997). Angiogenic processes transform the primary vascular plexus into a mature vascular system with different lumen size and functions. This process is not only active during embryonic development, but also present in adult organisms e.g. in the female reproductive organs (Modlich et al., 1996) or during wound healing. Angiogenesis is strictly regulated. Dysregulated angiogenesis plays important

roles in diseases like rheumatoid arthritis, and in cancer. There, tumour cells induce angiogenesis, use the newly formed vessels for oxygen and nutrient supply, and also for metastasis formation (Folkman, 1995).

The main mechanisms during angiogenesis are migration and proliferation of endothelial cells. Since the first studies by Folkman and Haudenschild (1980), numerous *in vitro* assays on angiogenesis have been published. These measure proliferation – with proliferation assays, migration – with Boyden chambers or scratching/wounding of endothelial monolayers, and differentiation of endothelial cells – with 2- and 3-dimensional models, in which endothelial cells form capillary-like structures on adhesive proteins or in extracellular-matrix-modelling gels (reviewed in: WC Liu et al. (2017), Tahergorabi and Khazaei (2012)).

1.4 Wnt signalling

WNTs (Wingless-type MMTV integration site family) are secreted lipid-modified signalling glycoproteins. They are well conserved across many species (Nusse, 2005) and until now, 19 different WNT ligands, several receptors and co-receptors have been characterized in the human and in mice. WNTs are involved in numerous developmental processes, like embryonic patterning, cell growth, migration and differentiation, and, as noted above, also angiogenesis is regulated by WNT signalling (reviewed e.g. in: Wiese et al. (2018); Dejana (2010)). Dysregulation of Wnt signalling causes a variety of diseases, including cancer (reviewed in: Katoh and Katoh (2017); Polakis (2012)).

More than 15 receptors and co-receptors are involved in the WNT signalling pathway, and, together with the 19 WNT ligands, diverse combinations of ligand, receptor and/or co-receptor are possible (Niehrs, 2012). These combinations can activate multiple downstream signalling cascades. Commonly, the pathways are divided into two main branches: the ‘canonical’ or β -catenin-dependent and the ‘non-canonical’ or β -catenin-independent pathways (Asem et al., 2016). The β -catenin-independent pathways can then be subdivided into the planar-cell-polarity (PCP) pathways and the Ca^{2+} -dependent pathways (**Figure 2**). However,

this classification is only a rough guideline, because all WNT pathways are densely interconnected and can also be regulated in a tissue- or cell-type-specific manner (Niehrs, 2012).

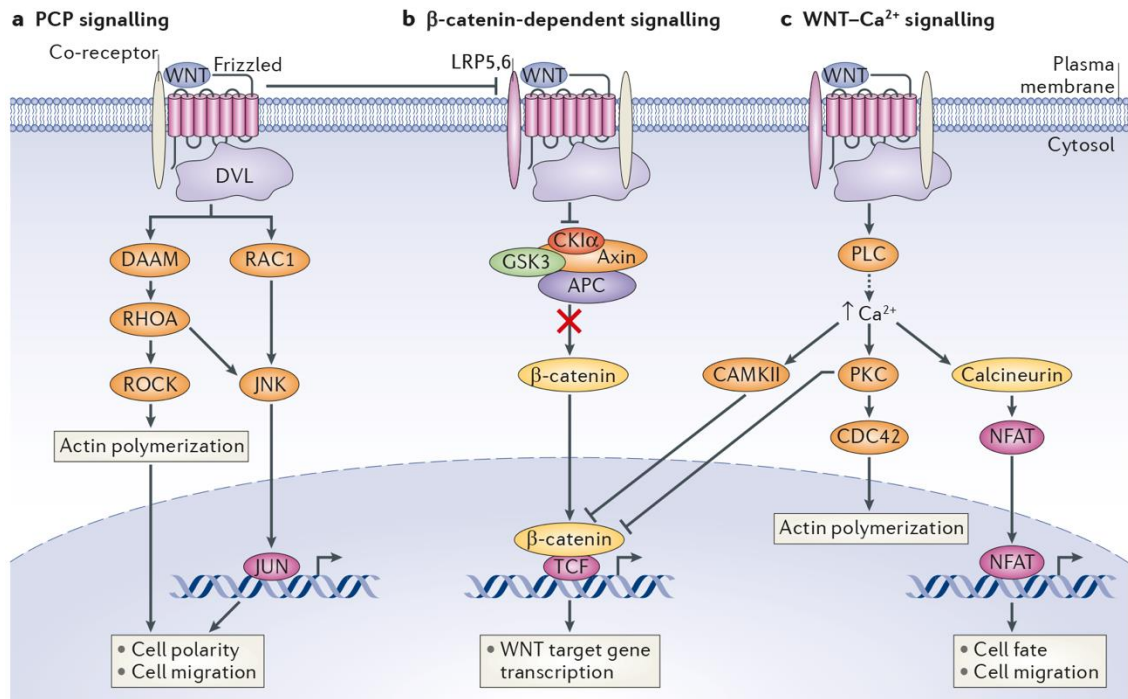


Figure 2: Schematic overview of the main WNT signalling pathways. (a) In the planar-cell-polarity (PCP) pathway, WNT activates the small GTPases (RHOA, RAC1), which activate the RHO kinase (ROCK) and/or the JUN-N-terminal kinase (JNK). This leads to actin polymerization and is mainly involved in morphogenetic movements, motility and cell polarity. **(b)** In the β -catenin-dependent WNT signalling, binding of the WNT ligand to the receptor leads to an inactivation of the β -catenin “destruction complex” (consisting of adenomatous polyposis coli (APC), Axin, the casein kinase 1 α (CK1 α) and the glycogen synthase kinase 3 (GSK3)), which leads to an accumulation of β -catenin in the cytosol and to translocation of β -catenin into the nucleus. There it activates the transcription of WNT target genes. **(c)** In WNT-Ca²⁺ signalling, the presence of WNTs leads to an activation of the Ca²⁺- and calmodulin-dependent kinase (CAMKII), protein kinase C (PKC) and Calcineurin. Calcineurin activates the transcription factor nuclear factor of activated T cells (NFAT). Both the PCP signalling and the WNT-Ca²⁺ signalling can antagonize the β -catenin-dependent WNT signalling. The scheme is taken from Niehrs (2012), with permission.

Frizzled (FZD) receptors are the principal WNT receptors and can recruit different co-receptors like low-density lipoprotein receptor-related protein 5 (LRP5) and LRP6, receptor tyrosine kinase-like orphan receptor (ROR) 1 and ROR2, and the related to receptor tyrosine kinase (RYK). LRP5 and LRP6 are usually supposed to be involved in the β -catenin-dependent WNT signalling, while RORs and RYK are involved in β -catenin-independent WNT signalling.

WNTs can mediate cell-cell communication during direct cell contact or in a short range, due to their lipophilic anchor. They can also act in an autocrine manner

(Bafico et al., 2004; Schlange et al., 2007). For secretion of WNTs, a lipid modification with palmitoleic acid is necessary. This modification is introduced by the O-acetyltransferase Porcupine (PORCN) and takes place in the endoplasmic reticulum (ER) (Kurayoshi et al., 2007; Takada et al., 2006). In recent years, small molecule inhibitors were produced, which can block the PORCN activity and prevent WNT secretion. These inhibitors may also provide new therapeutic strategies for WNT-driven cancers like melanoma or breast cancer (J Liu et al., 2013; Proffitt et al., 2013).

1.4.1 The ‘canonical’ or β -catenin-dependent WNT signalling

The β -catenin-dependent WNT pathway is the best characterised WNT pathway. For this reason, it is often also called the canonical WNT pathway. WNT1, WNT3A, and WNT8 are commonly thought to activate this pathway (Kikuchi et al., 2011), and LRP5/6 act as co-receptors in this pathway (X. He et al., 2004). The presence of canonical WNTs leads to an inhibition of the glycogen synthase kinase 3 (GSK3). One of the substrates of GSK3 is β -catenin. If GSK3 is not inhibited, β -catenin gets phosphorylated, which leads to its proteasomal degradation. Thereby, the inactivation of β -catenin involves a “destruction complex” made up of GSK3, Adenomatous polyposis coli (APC), Axin and the Casein kinase I α (CKI α). In the presence of WNTs GSK3 is inhibited. Then, β -catenin accumulates in the cytosol, enters the nucleus and associates with transcription factors like the T-cell factor (TCF) and Lymphoid enhancer-binding factor (LEF). This regulates the transcription of WNT target-genes like CyclinD1 or MYC (**Figure 2b**) (TC He et al., 1998; Shtutman et al., 1999).

1.4.2 The 'non-canonical' or β -catenin-independent WNT signalling pathways

All WNT-regulated pathways that do not use β -catenin are commonly summarised under the term 'non-canonical' or β -catenin-independent WNT signalling (Niehrs, 2012) and can be subdivided into the planar-cell-polarity (PCP) and the Ca^{2+} -dependent pathway (**Figure 2a, c**). Typical WNTs that activate the β -catenin-independent pathways are WNT5A and WNT11 (Kikuchi et al., 2011), and ROR1/ROR2 and RYK are typical co-receptors (Ho et al., 2012). The PCP pathway has often been studied. In the presence of WNTs, that activate the PCP, the small GTPases Ras Homolog Family Member A (RHOA) and/or Ras-related C3 botulinum toxin substrate 1 (RAC1) are activated, which then activate Rho-associated coiled-coil containing protein kinase (ROCK) and/or JUN-N-terminal kinase (JNK).

WNT- Ca^{2+} -signalling is the second β -catenin-independent WNT pathway. There, the presence of WNT leads to an activation of G-proteins, which activate Phospholipase C (PLC). PLC cleaves Phosphatidylinositol 4,5-bisphosphate (PIP₂) into Diacylglycerol (DAG) and Inositol trisphosphate (IP₃). IP₃ triggers Ca^{2+} release from the ER. The increasing Ca^{2+} concentration activates effectors like the Ca^{2+} - and Calmodulin-dependent kinase (CAMKII), Protein kinase C (PKC) and Calcineurin, which can activate the transcription factor Nuclear factor of activated T cells (NFAT).

It is also well established that the β -catenin-independent pathways can antagonise functions of the β -catenin-dependent pathway (Torres et al., 1996). For example, is the binding of specific non-canonical ligands to LRP5/6, which do not induce phosphorylation of LRP5/6, the basis for mutually antagonistic effects (Andersson et al., 2010; Bryja et al., 2009; DH Yang et al., 2009).

1.5 WNT5A and lymphangiogenesis

WNT5A is a specific WNT ligand that usually activates the β -catenin-independent pathways. It has also been shown that Wnt5a can inhibit the β -catenin-dependent WNT signalling (Li et al., 2010; Topol et al., 2003; Torres et al., 1996). Thereby, Ror2 may act as receptor or co-receptor of Wnt5a (Grumolato et al., 2010; A Mikels et al., 2009). Wnt5a-null-mice (constitutive homozygous Wnt5a knock-out, **Figure 3**) display complex phenotypic alterations, including skeletal defects, like craniofacial defects and limb shortening (Yamaguchi et al., 1999), and also defects of inner organs like the heart and the intestine, which is massively shortened (Cervantes et al., 2009). Interestingly, the phenotype of Ror-knock-out mice is similar to that of Wnt5a (Takeuchi et al., 2000; Yamada et al., 2010). However, it has also been shown that Wnt5a can activate the β -catenin-dependent pathway (Mikels and Nusse, 2006; van Amerongen et al., 2012).

There is increasing evidence that WNTs, and foremost WNT5A, plays an important role in lymphangiogenesis. In mice, a study of our lab has shown that the constitutive homozygous knock-out of Wnt5a leads to significant defects in morphology and function of dermal lymphatics (Buttler et al., 2013). However, Muley et al. (2017) have shown that the overexpression of Wnt5a in myeloid cells induces only very minor changes in the dermal lymphatics.

The importance of WNTs during lymphangiogenesis has also been shown in studies by Nicenboim et al. (2015), who observed that Wnt5b was necessary and sufficient for lymphatic cell-fate specification in zebrafish. They also could show that this role of Wnt5b is evolutionarily conserved, since the application of WNT5B to the culture medium of human embryonic stem cell-derived angioblasts induced increased expression of Prospero homeobox protein 1 (PROX1), the LEC-specific transcription factor (Nicenboim et al., 2015).

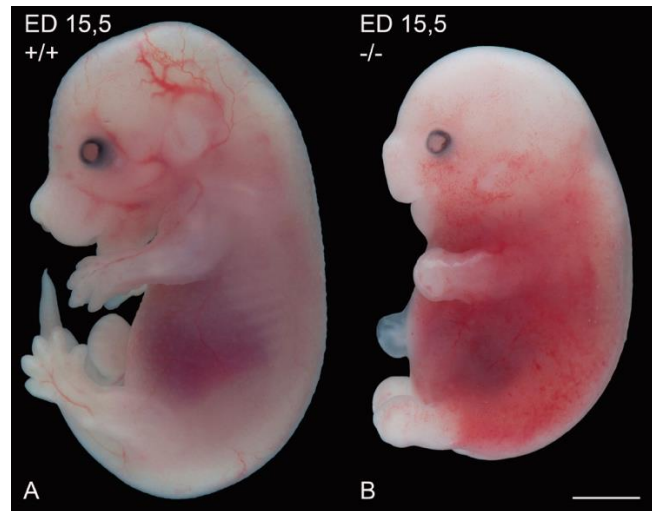


Figure 3: Typical phenotype of a *Wnt5a*-null mouse embryo (B, -/-) and a littermate control embryo (A, +/+) at ED 15.5. The *Wnt5a*-null mouse shows numerous defects, like craniofacial malformations, limb shortening and the lack of the tail. The embryo also has an oedematous appearance and shows petechial bleedings in the skin. Scale bar = 200 μ m.

1.6 Aims of the thesis

Several studies have shown that Wnts are important regulators of angiogenesis, and a few studies have shown that they also regulate lymphangiogenesis. However, the mechanisms how Wnts regulate lymphangiogenesis remained unclear. Therefore, the aim of my thesis was to study the mechanisms how WNT signaling, and specifically WNT5A, influences lymphangiogenesis in greater detail. I focussed on the functions of *Wnt5a* in the development of dermal lymphatics in murine embryos. I studied the cellular mechanisms regulated by WNTs in human LECs, and I was interested in signal transduction down-stream of WNT5A in LECs. Finally, I sought to study the transcriptional regulation by WNTs in LECs.

To follow these aims, I divided my thesis into the following parts:

In the first part, I analysed *Wnt5a*-related signalling in murine embryos and asked the following questions:

1. Which *Wnt*-related proteins are expressed in murine dermal lymphatics?

2. Is the phenotype of dermal lymphatics of Wnt5a-null mice reversible through the application of Wnt5a?
3. Can I change the phenotype of dermal lymphatics of Wild-type mice by inhibiting Wnt signalling?

To answer these questions, I characterised the expression of Wnt-related molecules in dermal lymphatics of embryonic mice using immunofluorescence staining, and used activators and inhibitors of the Wnt-signalling pathway to influence lymphangiogenesis in embryonic murine dermis in a new *ex vivo* model.

The second part of my thesis deals with the question how WNTs, and mainly WNT5A, influence the lymphangiogenic behaviour of human LECs. To gain further insight into this, I sought to answer the following questions:

1. Which WNT-related proteins are expressed in human LECs?
2. Does WNT signalling and especially WNT5A regulate lymphangiogenesis in human LECs? And if so, which angiogenic mechanisms are influenced, and which WNT signalling pathways are activated during WNT-related lymphangiogenesis?
3. Which genes are globally regulated through WNT signalling in human LECs?

Therefore, I first characterised LECs with quantitative real-time PCR, Western blot and immunocytology. Then, I performed *in vitro* angiogenesis assays, including scratch-assays, tube-formation assays and proliferation assays with LECs and analysed the influence of WNTs under these conditions. I also used these assays to get deeper insight into the intracellular down-stream signalling of WNT5A in LECs. Therefore, I used a variety of small molecule inhibitors of the WNT pathways, and also studied the effects of WNT5A application.

And finally, to analyse the influence of WNT-inhibition on the regulation of gene expression in LECs globally, I applied the WNT-secretion inhibitor LGK974 and studied the transcriptome with mRNAseq.

2 Materials and Methods

2.1 Materials

2.1.1 Chemicals, solutions and consumable supplies

Chemicals, solutions and consumables are listed in **Table 1** and **Table 2**.

Table 1: Chemicals or solutions

Chemical or solution	Manufacturer
Acetic acid, glacial	Merck KGaA, Darmstadt, DE
Acrylamide 30 % (Rotiphorese)	Carl Roth, Karlsruhe, DE
Basal Medium MV 2	PromoCell, Heidelberg, DE
Bovine serum albumin, Fraction V (BSA)	AppliChem, Darmstadt, DE
Bradford solution (Roti-Quant)	Carl Roth, Karlsruhe, DE
Bromophenol blue	Merck KGaA, Darmstadt, DE
CellTracker™ Green CMFDA	Thermo Fisher Scientific, Waltham, US
Chloroform	Merck KGaA, Darmstadt, DE
Citric acid	Carl Roth, Karlsruhe, DE
Clarity™ Western ECL Substrate	Bio-Rad Laboratories, Hercules, US
cOmplete™ protease inhibitor	Roche, Mannheim, DE
Coulter Isoton II Diluent	Beckman Coulter Life Sciences, Indianapolis, US
Crystal violet	SERVA, Heidelberg, DE
Di-sodium hydrogen phosphate anhydrous (Na ₂ HPO ₄)	AppliChem, Darmstadt, DE
Dichlorodiphenyltrichloroethane (DDT)	PanReac, AppliChem, Darmstadt, DE
Dimethyl sulfoxide (DMSO)	Sigma-Aldrich Chemie, Taufkirchen, DE

Chemical or solution	Manufacturer
EGM-2 Endothelial SingleQuots Kit	Lonza, Basel, CH
Endothelial Cell Basal Medium-2 (EBM2)	Lonza, Basel, CH
esVEGFR-2	ReliaTech, Wolfenbüttel, DE
Ethanol - ROTISOLV	Carl Roth, Karlsruhe, DE
Ethylenediaminetetraacetic acid (EDTA)	Carl Roth, Karlsruhe, DE
Fast SYBR Green Master Mix	Applied Biosystems, Waltham, US
Fluorescein isothiocyanate-dextran (FITC-Dextran; 2000 kDa)	Sigma-Aldrich Chemie, Taufkirchen, DE
Fluoromount-G	Invitrogen, Thermo Fisher Scientific, Waltham, US
Foetal bovine serum (FBS) / FBS Superior	Biochrom, Berlin, DE
Formaldehyde solution 37 %	Carl Roth, Karlsruhe, DE
Glutaraldehyde	SERVA, Heidelberg, DE
Glycerol - ROTIPURAN	Carl Roth, Karlsruhe, DE
Glycine (electrophoresis grade)	SERVA, Heidelberg, DE
Growth Medium MV 2 Supplement Pack	PromoCell, Heidelberg, DE
Hydrogen peroxide 30 % - ROTIPURAN	Carl Roth, Karlsruhe, DE
Isopropanol	Chemsolute, Th. Geyer, Renningen, DE
Isopropanol - ROTIPURAN	Carl Roth, Karlsruhe, DE
Luminol	Sigma-Aldrich Chemie, Taufkirchen, DE
Matrigel® Matrix	Corning Inc., Corning, US
Methyl cellulose	Sigma-Aldrich Chemie, Taufkirchen, DE
Milk powder	Saliter, Obergünzburg, DE
Omniscript RT Kit	Quiagen, Venlo, NL
PageRuler™ prestained protein ladder	Thermo Fisher Scientific, Waltham, US
Paraplast PLUS	Leica Microsystems, Wetzlar, DE

Chemical or solution	Manufacturer
Penicillin-Streptomycin (cell culture grade; 10 000 U/ml)	Lonza, Basel, CH
peqGOLD TriFast™	VWR Life science, Radnor, US
Phosphate buffered saline (PBS) (cell culture grade)	Lonza, Basel, CH
Ponceau S	Merck KGaA, Darmstadt, DE
Potassium dihydrogenphosphate (KH ₂ PO ₄)	Carl Roth, Karlsruhe, DE
Random Hexamer Primer	Thermo Fisher Scientific, Waltham, US
Recombinant RNasin Ribonuclease Inhibitor	Promega, Madison, US
RPMI-1640 with L-glutamine	Lonza, Basel, CH
SignalFire™ ECL Reagent	Cell Signaling Technology, Beverly, US
Sodium chloride	Carl Roth, Karlsruhe, DE
Sodium deoxy cholate	Carl Roth, Karlsruhe, DE
Sodium dodecyl sulphate (SDS)	Carl Roth, Karlsruhe, DE
Sodium orthovanadate (SOV)	Sigma-Aldrich Chemie, Taufkirchen, DE
StarPure Agarose	StarLab, Hamburg, DE
Sucrose	Carl Roth, Karlsruhe, DE
sVEGFR-3	ReliaTech, Wolfenbüttel, DE
Tetramethylethylenediamine (TEMED)	Carl Roth, Karlsruhe, DE
Tri-Sodium citrate	Merck KGaA, Darmstadt, DE
Tris base	USB, Cleveland, US
Tris HCl	Carl Roth, Karlsruhe, DE
TritonX-100	GERBU, Gaiberg, DE
Trypsin/EDTA (cell culture grade)	Lonza, Basel, CH
VEGF-C	Dr. M. Jeltsch; http://research.med.helsinki.fi/cancerbio/jeltsch/Index.html
Xylene	PanReac, AppliChem, Darmstadt, DE

Table 2: Consumables

Consumable	Manufacturer
Blotting paper sheets (330 g/m ²)	Sartorius AG, Göttingen, DE
Cell scraper	Sarstedt, Nümbrecht, DE
Chamber slides	BD Falcon, Erembodegem, BE
Cover slips	Menzel-Gläser, Braunschweig, DE
CRYO.S tubes	Greiner Bio-One, Frickenhausen, DE
Falcon tubes 15 ml, 50 ml	Sarstedt, Nümbrecht, DE
Gentle skin - powder-free examination gloves	Meditrade, Bäch, CH
ImmunoPen	Merck Millipore, Billerica, US
MicroAmp Fast Optical 96-Well Reaction Plate (0.1 ml)	Applied Biosystems, Waltham, US
Microscope slides	Labsolute, Th. Geyer, Renningen, DE
Millicell® cell culture inserts 0.4 µm, 12 mm	Merck Millipore, Billerica, US
Pasteur pipettes	Labsolute, Th. Geyer, Renningen, DE
Pipette tips (w/o filters) 10 µl, 200 µl, 1000 µl	Sarstedt, Nümbrecht, DE
PVDF membranes (pore size 0.45 µm)	Carl Roth, Karlsruhe, DE
Reaction tubes (0.2 ml, 0.5 ml, 1.5 ml, 2 ml)	Sarstedt, Nümbrecht, DE
Superfrost plus, microscope slides	Menzel-Gläser, Braunschweig, DE
Tissue culture dish (6 cm, 10 cm)	Sarstedt, Nümbrecht, DE
Tissue culture plate 12 well, 24 well, 48 well, 96 well	Sarstedt, Nümbrecht, DE
Tissue culture plate 6 well	BD Falcon, Erembodegem, BE
U-bottom 96 well suspension culture plate	Greiner Bio-One, Frickenhausen, DE
VIVASPIN 2 Centrifugal Concentrator, 10,000 MWCO PES	Sartorius AG, Göttingen, DE
µ-Slide Angiogenesis	Ibidi, Martinsried, DE

2.1.2 Buffers and media

Recipes of buffers and media used in the studies are listed in **Table 3**.

Table 3: Recipes of buffers and medias

4 % PFA solution	10 % formaldehyde solution 37 % 90 % 0.1 M Sørensen buffer
6x SDS loading buffer	350 mM Tris, pH 6.8 10 % SDS 36 % glycerol 9.3 % DTT bromophenol blue
Blocking solution I (BS I)	1 % BSA in PBS
Blocking solution II (BS II)	3 % BSA in TBS/T
Blocking solution III (BS III)	5 % BSA in TBS/T
Blocking solution IV (BS IV)	5 % MP in TBS/T
Citric acid buffer (pH 6.0)	Stock solution A: 21.01 g citric acid in 1 l ddH ₂ O Stock solution B: 29.41 g trisodium cit- rate in 1 l ddH ₂ O Working solution: 18 % stock solution A + 82 % stock solution B brought to 1 l with ddH ₂ O
EBM2 growth medium	Endothelial Cell Basal Medium-2 + EGM-2 Endothelial SingleQuots Kit
MV2 growth medium	Basal Medium MV 2+ Growth Medium MV 2 Supplement Pack
PBS (10x)	6.789 g NaCl 1.478 g Na ₂ HPO ₄ 0.43 g KH ₂ PO ₄ 1 l ddH ₂ O

Ponceau S staining solution	0.5 % (w/v) Ponceau S 1 % (v/v) glacial acetic acid
RIPA lysis buffer (stock)	140 mM NaCl 1 mM EDTA 10 mM Tris, pH 8.0 1 % Triton-X 0.1 % SDS 0.1 % sodium deoxy cholate
RIPA lysis buffer (working solution)	RIPA lysis buffer (stock) 1x cOmplete™ protease inhibitor 1 mM SOV
RPMI growth medium	500 ml RPMI 50 ml FBS 5 ml Penicillin-Streptomycin
Running buffer (10x)	250 mM Tris base 1.92 M glycine 1 % SDS
Sörensen buffer 0.3 M, pH 7,4	18.2 % Sörensen buffer A 81.8 % Sörensen buffer B
Sörensen buffer A	0.3 M KH_2PO_4
Sörensen buffer B	0.3 M Na_2HPO_4
TBS/T (10x)	1.5 M NaCl 0.035 M Tris base 0.165 M Tris HCl 1 % Tween-20
Transfer buffer (10x)	250 mM Tris base 1.92 M glycine
Transfer buffer (working solution)	10 % transfer buffer stock 20 % methanol 70 % ddH ₂ O

2.1.3 Inhibitors

Inhibitors and applied concentrations are listed in **Table 4**. DMSO was used as solvent.

Table 4: Inhibitors

Inhibitor	Manufacturer	Target	Working concentration
BIO	Sigma-Aldrich Chemie, Taufkirchen, DE	GSK-3 α/β	2 μ M
EHT 1864	Tocris Bioscience, Bristol, GB	Rac family GTPases	10 μ M
Fasudil (HA-1077) HCL	Selleck Chemicals, Houston, US	ROCK-II, PKA, PKG, PKC, MLCK	10 μ M
FH 535	Tocris Bioscience, Bristol, GB	β -Catenin/Tcf-mediated transcription	10 μ M
IM-12	Selleck Chemicals, Houston, US	GSK-3 β	10 μ M
JNK-IN-8	Merck Millipore, Billerica, US	JNK1,2,3	5 μ M
LGK974	Selleck Chemicals, Houston, US	Porcn-mediated Wnt palmitoylation	10-50 μ M
NSC 23766	Selleck Chemicals, Houston, US	Rac GTPase	100 μ M
SP600125	Santa Cruz Biotechnology, Dallas, US	JNK	10 μ M
Wnt-C59	cellagentech.com	Porcn-mediated Wnt palmitoylation	25 μ M
Y-27632 2HCL	Selleck Chemicals, Houston, US	ROCK1, ROCK2	50 μ M

2.1.4 Antibodies and dyes

Primary and secondary antibodies, and fluorescence dyes are listed in **Table 5**. All antibodies were diluted in PBS or in blocking solution.

Table 5: Antibodies and fluorescence dyes

Antibody/Stain (anti)	Manufacturer	Application and Dilution	Source	Block-ing
Alexa Fluor® 488 donkey anti goat	Life Technologies, Eugene, US	IF: 1:200	donkey	BS I
Alexa Fluor® 488 donkey anti rabbit	Life Technologies, Eugene, US	IF: 1:200	donkey	BS I
Alexa Fluor® 488 goat anti mouse	Life Technologies, Eugene, US	IF: 1:200	goat	BS I
Alexa Fluor® 488 goat anti rat	Life Technologies, Eugene, US	IF: 1:200	goat	BS I
Alexa Fluor® 594 donkey anti goat	Life Technologies, Eugene, US	IF: 1:200	donkey	BS I
Alexa Fluor® 594 donkey anti rabbit	Life Technologies, Eugene, US	IF: 1:200	donkey	BS I
Alexa Fluor® 595 goat anti mouse	Life Technologies, Eugene, US	IF: 1:200	goat	BS I
CD31/ PECAM1 (human)	BD Pharmingen, Franklin Lakes, US	IF: 1:50	mouse	BS I
CD31/ PECAM1 (mouse)	BD Pharmingen, Franklin Lakes, US	IF: 1:100	rat	BS I
CellTracker™ Green CMFDA	Thermo Fisher Scientific, Waltham, US	Cells: 0.15 µM	/	/

Antibody/Stain (anti)	Manufacturer	Application and Dilution	Source	Block- ing
DAPI (4',6-dia- midino-2-phenylin- dole)	Thermo Fisher Scientific, Wal- tham, US	IF: 1:10000	/	BS I
FZD4 (3G7), sc- 293454 (human/mouse/rat)	Santa Cruz Bio- technology, Dal- las, US	IF: 1:100 WB: 1:1000	mouse	BS IV
FZD5 (human/mouse/rat)	antikörper-on- line.de, Aachen, DE	IF: 1:100	rabbit	BS I
FZD5, #5266 (human)	Cell Signaling Technology, Bev- erly, US	IF: 1:100 WB: 1:1000	rabbit	BS I
FZD6, AF3149 (human)	R&D Systems, Minneapolis, US	IF: 1:100 WB: 1:1000	goat	BS I
FZD8 (E-17), sc- 33504, (human)	Santa Cruz Bio- technology, Dal- las, US	IF: 1:100 WB: 1:1000	goat	BS I
goat anti mouse, HRP conjugated	Santa Cruz Bio- technology, Dal- las, US	WB: 1:5000	goat	BS II ore BS IV
goat anti rabbit, HRP conjugated	DAKO, Santa Clara, US	WB 1:1000	goat	BS III
LYVE-1, Lot# 1410R24, (mouse)	ReliaTech, Wolf- enbüttel, DE	IF: 1:200	rabbit	BS I
Phospho- SAPK/JNK (Thr183/Tyr185), #4668, (human)	Cell Signaling Technology, Bev- erly, US	WB: 1:1000	rabbit	BS III
PRICKLE1 (human)	Atlas Antibodies, Sigma-Aldrich, St. Louis, US	IF: 1:200 WB: 1:1000	rabbit	BS I

Antibody/Stain (anti)	Manufacturer	Application and Dilution	Source	Block-ing
PROX1 (human)	ReliaTech, Wolfenbüttel, DE	IF: 1:500	rabbit	BS I
Rabbit anti rat peroxidase antibody	Sigma-Aldrich, St. Louis, US	WB: 1:500	rabbit	BS IV
SAPK/JNK, #9252 (human)	Cell Signaling Technology, Beverly, US	WB: 1:1000	rabbit	BS III
VANGL1 (human)	Atlas Antibodies, Sigma-Aldrich, St. Louis, US	IF: 1:100 WB: 1:1000	mouse	BS I
VANGL2 (human/mouse/rat)	Proteintech Group, Chicago, US	IF: 50 (cell) IF: 1:100 (mouse) WB: 1:1000	rabbit	BS I
Wnt-5a (C-16), sc-23698, (human/mouse/rat)	Santa Cruz Biotechnology, Dallas, US	IF: 1:100	goat	BS I
Wnt-5a (H-58), sc-30224, (human/mouse/rat)	Santa Cruz Biotechnology, Dallas, US	IF: 1:200	rabbit	BS I
Wnt-5a, MAB645 (human/mouse)	R&D Systems, Minneapolis, US	IF: 1:100 WB: 1:1000	rat	BS IV
β -Actin (C4), sc-47778	Santa Cruz Biotechnology, Dallas, US	WB: 1:5000	mouse	BS II

2.1.5 Recombinant WNT5A

Recombinant Human/Mouse Wnt5a was purchased from R&D Systems (Minneapolis, US), diluted in PBS with 1% BSA. Activity of the protein was measured by R&D by its ability to inhibit Wnt3a-induced alkaline phosphatase production in MC3T3-E1 mouse preosteoblastic cells.

2.1.6 Software

Software is listed in **Table 6**.

Table 6: Software

Software	Developer
Adobe Photoshop CS6	Adobe Systems, San José, US
AngioTool 0.5a	Open source, Zudaire et al. (2011)
AxioVision Release 4.6.3 SP1	Carl Zeiss Microscopy, Jena, DE
EndNote X7.8	Thomson Reuters, New York City, US
Fiji, version 2.0.0-rc64/1.51s	Open source; Schindelin et al. (2012)
GNU Octave, version 4.0.3 (with “image” package)	Open source, Eaton et al. (2017)
GraphPad Prism 5.03	GraphPad Software, La Jolla, US
Image Lab™, version 6.0.1	Bio Rad Laboratories. Inc, Hercules US
Leica Application Suite Advanced Fluorescence 2.6.0.7266	Leica Microsystems, Wetzlar, DE
Leica Application Suite Advanced Fluorescence 3.2.0.9652	Leica Microsystems, Wetzlar, DE
Microsoft® Office for Mac 2016	Microsoft Corporation, Redmont, US

2.1.7 Equipment

Equipment is listed in **Table 7**.

Table 7: Equipment

Name	Manufacturer	Instrument
Axio Imager.Z1	Carl Zeiss Microscopy, Jena, DE	Microscope
Biometra T personal	Biometra, Göttingen, DE	PCR-Thermocycler
BioPhotometer	Eppendorf AG, Hamburg, DE	Photometer
Centrifuge 5415	Eppendorf AG, Hamburg, DE	Centrifuge
Centrifuge 5417R	Eppendorf AG, Hamburg, DE	Centrifuge
ChemiDoc Touch Imaging System	Bio Rad Laboratories. Inc, Hercules US	Western blot imaging system
Citadel 2000	Thermo Fisher Scientific, Waltham, US	Tissue processor
Coulter counter Z1 single	Beckman Coulter Life Sciences, Indianapolis, US	Cell counter
Leica DMI6000 B	Leica Microsystems, Wetzlar, DE	Microscope
Leica M205 FA	Leica Microsystems, Wetzlar, DE	Microscope
Leica MZ 9 5	Leica Microsystems, Wetzlar, DE	Microscope
Leica RM2245	Leica Microsystems, Wetzlar, DE	Microtome
Leica S6 E	Leica Microsystems, Wetzlar, DE	Microscope

Name	Manufacturer	Instrument
Mikrowellen Herd GT 8804	General Technic	Microwave oven
Molecular Devices Thermo max microplate reader	Molecular Devices, San Jose, US	ELISA Microplate reader
Rotina 380 R	Hettrich Zentrifugen, Tuttlingen, DE	Centrifuge
StepOnePlus Real-Time PCR System	Applied Biosystems, Waltham, US	Real Time PCR machine
Thermomixer compact	Eppendorf AG, Hamburg, DE	Thermomixer

2.1.8 Mice

I used the following mice: C57BL/6, and B6;129S7-*Wnt5a*^{tm1Amc}/J (*Wnt5a*-null-mice). The *Wnt5a*-deleted-mice were obtained from the Jackson Laboratory, Bar Harbor, USA (JAX stock #004758) and were originally produced by Yamaguchi et al. (1999). All mice were kept in the Central Animal Facility of the University Medical Centre Göttingen with a 12 h dark-light-cycle, and with water and food *ad libitum*. All rights of the German Animal Welfare Act (TierSchG) and the German regulations on the welfare of animals used for experiments or for other scientific purposes (TierSchVersV) were kept.

2.1.9 Human dermal lymphatic endothelial cells

Human dermal lymphatic endothelial cells (HD-LECs) from 4 different donors (HD-LEC-C2, HD-LEC-C3, HD-LEC-C4 and LEC7) were used. HD-LEC-C2, HD-LEC-C3 and HD-LEC-C4 were purchased from PromoCell and cultured in MV2. LEC7 were also purchased from PromoCell but cultured in EBM2 with 250 ng/ml VEGF-C.

The initial assays (spheroid assays) were performed with lymphatic endothelial cells isolated from tissue of a patient with a lymphatic malformation, also called lymphangioma (lymphangioma-derived lymphatic endothelial cells - LY-LECs). These cells (LEC2) were cultured in EBM2 with 250 ng/ml VEGF-C. During the course of my studies, genetic analyses revealed that these cells possess an activating mutation in the *PIK3CA* gene (Blesinger et al., 2018). Therefore, the main body of my studies was performed on healthy LECs.

2.2 Methods

2.2.1 Mouse studies

2.2.1.1 Mouse embryo preparation

Pregnant mice were sacrificed and the embryos removed from the uterus at ED 15.5-18.5. The amniotic sac and placenta were removed and the embryos stored in PBS at 4°C. From each embryo, a specific part of the body was used for genotyping. The embryos were subjected to various techniques. For whole mount immuno-staining, the skin of the back and the abdomen of the embryos was carefully dissected. For *ex vivo* skin cultures of the skin, ventral and dorsal segments of the skin were dissected, cultured and stained as described below.

2.2.1.2 Microlymphangiography

To test the functionality of the superficial lymphatics of the embryos, microlymphangiography was performed. It was performed as described in Buttler et al. (2013). Therefore, 2000 kDa fluorescein isothiocyanate-dextran (FITC-dextran, 25 mg/ml in PBS) was injected with a fine glass pipette into the interstitium of the paws of the fore and hind limbs at ED 16.5 and ED 17.5. A Leica M205 FA microscope with ET GFP filter cube (excitation range 450-490 nm, emission range 500-550 nm) was used for visualization of FITC-dextran uptake and transport.

Photographs were taken directly after application and every 5 minutes for 30 minutes. Wnt5a-null-embryos were compared to wildtype (wt, +/+) and heterozygous (+/-) littermates with normal phenotype. At least n = 6 embryos of each genotype were studied.

2.2.1.3 Ex vivo skin cultures

Development of dermal lymphatics was studied *ex vivo*. First, 24 well plates were prepared. Each well was filled with 500 μ l MV2 culture medium containing 1 % penicillin/streptomycin. Then, a Millicell[®] cell culture insert was placed into the well and 200 μ l MV2 with 1 % penicillin-streptomycin was added onto the insert. Skin specimens of approx. 2x2 mm were isolated from ED 15.5 wild-type and Wnt5a-null embryos. Corresponding dermal specimens were taken from the right and the left side of each embryo, and used as experimental vs. control groups. Each skin specimen was separately placed on a cell culture insert with the epidermis facing the insert. All specimens were cultured for 48 h at 37°C and 5 % CO₂.

To study WNT5A effects, dermis from Wnt5a-null mice was treated with 500 ng/ml recombinant Wnt5a protein in the culture medium (n = 26). After 24 h, 10 ng of Wnt5a in 50 μ l culture medium were added to each well. In the controls (n = 26), 0.1 % BSA was applied with the medium.

To study the effects of the inhibition of Wnt signalling, I used dermis of ED 15.5 wild-type C57BL/6 mice, and cultured the specimens as described above. For the inhibition of Wnt secretion, 25 μ M (n = 14) or 50 μ M (n = 14) of the porcupine inhibitor LGK974 diluted in DMSO was added to the culture medium. In the corresponding controls, equal amounts of DMSO were added to the medium.

After 48 h, the dermal lymphatics were studied. For this reason, whole-mount staining of the specimens was performed with anti-Lyve-1 antibodies. Nuclei were counter-stained with DAPI. The staining procedure is described in 2.2.2.1.

Photographs of the lymphatic networks were taken with a Zeiss Axio Imager.Z1. For analysis and comparison, the free software AngioTool 0.5a was used. The vessel-covered area and the number of branching points were determined in each picture.

2.2.1.4 Genotyping

The genotyping followed Version 2.0 of the genotyping protocol provided by the Jackson Laboratory (Bar Harbor, US) for the Wnt5a-null-mice strain (https://www2.jax.org/protocolsdb/f?p=116:5:0::NO:5:P5_MASTER_PROTOCOL_ID,P5_JRS_CODE:23556,004758).

2.2.1.5 Preparation of tissues for paraffin sections

Freshly dissected mouse dermis was fixed with 4 % PFA overnight, and transferred into a tissue processor. There, the tissues were dehydrated and transferred in warm Paraplast plus (program of the tissue processor: 3 h 70 % ethanol, 1 h 80 % ethanol, 1 h 90 % ethanol, 1 h 96 % ethanol, 2x 2 h 100 % ethanol, 1.5 h isopropyl alcohol, 30 min and 2x 45 min xylene, 30 min Paraplast plus and 7 h Paraplast plus). Afterwards the tissue was transferred and embedded in fresh Paraplast plus. After cooling, paraffin sections were cut with a microtome and transferred to microscope slides.

2.2.2 Staining procedures

2.2.2.1 Whole mount staining of fresh mouse dermis

The skin samples were fixed for 1-2 h with cold PFA (4 % in PBS) for whole mount staining and, thereby, carefully flattened with a slotted spatula or two fine forceps. After rinsing three times with cold PBS for 15 min, the samples were blocked with 1 % BSA in PBS (BS I), with gentle agitation at 4°C overnight, and then incubated with the primary antibodies in BS I, again with gentle agitation at 4°C overnight. In some cases, the blocking step was omitted and the samples were incubated only in a solution of the primary antibodies with BS I, with gentle agitation at 4°C for 4 days. After rinsing with PBS at 4°C overnight, the samples were incubated with secondary antibodies and DAPI on a shaker at 4°C overnight, followed by overnight washing. The samples were finally mounted on a glass slide and covered with Fluoromount-G.

2.2.2.2 Immunofluorescence staining of paraffin sections

Slides with paraffin sections were heated for one minute at 42°C on a heating plate. The paraffin was removed with two rinsing steps in xylene for five minutes each. The slices were rehydrated in descending ethanol series (100 %, 96 %, 80 %, 60 %, five minutes each) and washed with ddH₂O. For some antibodies, an antigen-retrieval procedure was used. For this purpose, the slides were boiled four times for five minutes with citric acid buffer at pH 6.0 in a microwave oven at 240 W. After cooling down to room temperature they were washed twice for five minutes with ddH₂O and three times for five minutes with PBS.

One section on each slide was separated with an ImmunoPen-line (negative control) and then all sections were blocked with BS I for one hour at room temperature in a dark wet chamber. A solution of the primary antibodies in BS I was applied to all sections, for the negative control only BS I was applied. The slides were stored in a dark wet chamber for one hour at room temperature or overnight at 4°C. After two rinsing steps, the secondary antibodies together with DAPI were

applied to all sections for one hour at room temperature in a dark wet chamber. After two rinsing steps, the sections were mounted with Fluoromount-G and covered with coverslips.

Photographs were taken with an Axio Imager.Z1 (Zeiss). Photographs of the negative controls were taken under the same conditions as the objects and served as a control for unspecific binding of the secondary antibodies.

2.2.3 Studies on lymphatic endothelial cells

2.2.3.1 Cell culture

HD-LECs were cultured in growth medium at 37°C in 5 % CO₂. Medium was changed every 2-3 days and cells split (ratio: 1:2 - 1:3) at 80-90 % confluence. For all experiments only HD-LECs from passages 3-9 were used. Cell numbers were determined in a Coulter counter. Therefore, 100 µl of trypsinized cells were diluted in 10 ml Isoton 2 and counted.

For cryo-conservation, cells were centrifuged and re-suspended in FBS containing 10 % DMSO and collected in cryo-tubes. Cells were frozen in cryo-boxes containing isopropanol for a constant cooling of approximately 1°C/min, and stored for at least 24 h at -80°C. The tubes were then transferred to liquid nitrogen for long-term storage.

2.2.3.2 Inhibitor pre-treatment of cells

For activation experiments with WNT5A, HD-LECs were pre-treated for 3 (to 4) days with 10 µM LGK974. This inhibits all autocrine WNT secretion, which turned out to be absolutely necessary to study effects of WNT5A.

2.2.3.3 Cell proliferation assay

Proliferation assays were performed as described previously (J. Becker et al., 2006). 5,000 cells per well were seeded into 96 well culture plates in 50 μ l culture medium. After 12 h (t_0), various substances were applied to the cultures (compared to controls treated with solvent) and the first portion of the cells (6-8 wells) was fixed. Every 24 h ($t_1 = 24$ h, $t_2 = 48$ h, $t_3 = 72$ h), a further portion of the cells was fixed. Cells were stained with crystal violet and extinction measured photometrically with a microplate reader at 570 nm. To study WNT5A effects, 25 μ l culture medium with 500 ng/ml recombinant WNT5A was added to the wells at both t_1 and t_2 . All assays were performed with three HD-LEC lines and 6-8 replicates.

2.2.3.4 Cell migration studies with scratch assays

The scratch assay is a commonly used assay to measure horizontal cell migration. 50,000 cells per well were seeded into 24 well plates and grown to confluence. For better visibility, cells were stained with CellTracker™ Green (CMFDA) according to the manufacturer's instructions before scratching. For this purpose, 1.5 μ M CMFDA were added to serum-free culture medium and incubated for 45 minutes at 37°C in 5 % CO₂. Scratches were then performed with a 100 μ l pipette tip. Wells were washed with PBS and fresh medium with or without various test substances was added to each well. Directly after scratching photographs were taken with Leica DMI600B using L5 filter cube (for GFP) and with phase contrast. At the microscope, the positions for each scratch were stored. After 24 h, photographs were taken with phase contrast and L5 filter cube at the same positions.

For quantification of cell migration, the area of the scratch, which was covered by cells (closed area) was measured with GNU Octave, version 4.0.3 after 24 h (**Figure 4**). GNU Octave was kindly provided by MSc. Adem Saglam. Because of the slight variability of the scratches, the width of each scratch was determined in the 0 h photographs. With the line drawing tool and the "measure" function in Fiji, the width of each scratch was determined at three positions. The mean of the measurements was calculated with Excel and classified into categories.

Category 1 contained scratches $< 500 \mu\text{m}$, category 2 contained scratches $< 600 \mu\text{m}$ and $\geq 500 \mu\text{m}$, category 3 contained scratches $< 700 \mu\text{m}$ and $\geq 600 \mu\text{m}$, category 4 contained scratches $< 800 \mu\text{m}$ and $\geq 700 \mu\text{m}$, category 5 contained scratches $< 900 \mu\text{m}$ and $\geq 800 \mu\text{m}$, category 6 contained scratches $< 1000 \mu\text{m}$ and $\geq 900 \mu\text{m}$, and category 7 contained scratches $< 1100 \mu\text{m}$.

To reduce variability, categories 1 and 7 were excluded from the analyses. Thereby, $100 \mu\text{m}$ corresponded to approx. one row of cells on each side of the scratch.

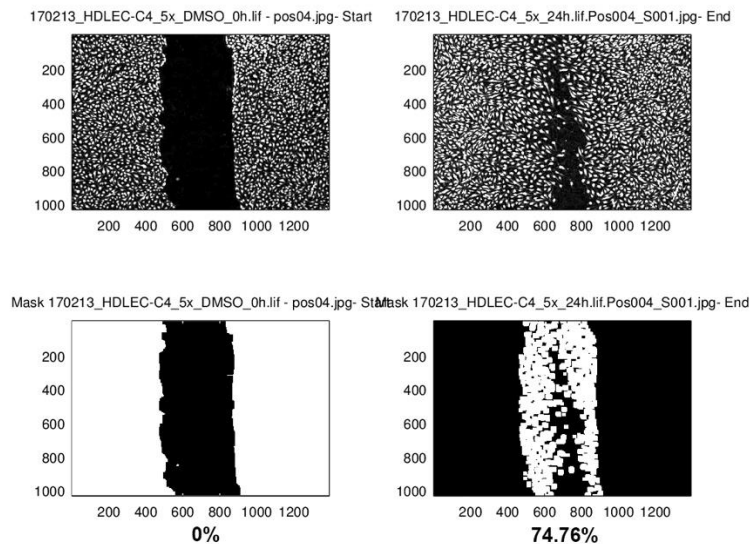


Figure 4: Example for scratch assay quantification with GNU Octave. The script provides the percentage of the closed area of the scratch, which is 74.76 % in this example.

2.2.3.5 Tube formation assay

Kubota et al. (1988) were the first that noticed that endothelial cells form tube-like structures when plated on a basement membrane-like matrix. Now, the tube formation assay is a widely used assay to study angiogenesis *in vitro*. The assay was performed on ibidi angiogenesis slides, and the protocol provided with the slides was optimized for LECs. $10 \mu\text{l}$ Matrigel were used for coating of the slides and allowed to polymerise overnight at 37°C . The next day, 5,000 cells dispersed in MV2 (+ test substance or solvent) were seeded in each well.

LECs were pre-treated with 10 μ M LGK974 for three days, and labelled with CellTrackerTM Green CMFDA immediately before the assay. After 9 h, formation of networks was documented. The cell-covered area, number of tubes, number of branching points and the total tube length were quantified with the WimTube analysis software (Onimagin Technologies SCA, Córdoba, Spain). All assays were performed with three HD-LEC lines and five replicates.

2.2.3.6 Spheroid sprouting assay

The spheroid sprouting assay is a commonly used *in vitro* angiogenesis assay. Korff and Augustin (1998) first provided a protocol for generating spheroids with a defined blood endothelial cell number, and this protocol was optimized here for LECs.

For the formation of spheroids, 3,000 LECs in a mixture of 80 % EBM2 and 20 % methyl cellulose solution (1,2 % methyl cellulose in EBM2) were seeded in a round-bottom 96 well plate. After 24-48 h, the spheroids were harvested with a 1 ml pipette. The pipette tip was cut off and the spheroids were collected in a falcon tube and centrifuged at 500 g for 3 min. The supernatant was discarded. The spheroids were dispersed in a mixture of 2 parts EBM2 (plus test substance) and 1 part of Matrigel, and 50 μ l of this mixture was pipetted onto a flat 96 well plate.

After 30 minutes of polymerisation (solidifying) at 37°C, a photo was taken of each of the spheroids (t₀) and after 24h later, a second photo was made (t₁). The assay was performed at least 3 times with at least 5 replicates.

In some experiments growth factor-reduced conditions were used. For this purpose, no serum was added to the cell culture medium and growth factor-reduced Matrigel was used.

To measure both the number of sprouts and the sprout length, I designed a method that makes use of a circular grid. I applied the plug-ins “*concentric circles*” and “*cell counter*” in Fiji. With *concentric circles*, I produced a grid where the inner circle corresponded to the core of each individual spheroid, and all consecutive

circles followed at a distance corresponding to 0.5x radius of the core circle (**Figure 5**). Next, with *cell counter* I calculated the intersections of sprouts with the circles, starting with circle 1 (circle next to the core circle). Thereby, both left and right sides of each sprout crossing the circle are noted; numbers were therefore divided by 2. Different colour coding was used with different circles (**Figure 5**). For the analyses, the sprouts in the t1 photos were counted. In photographs of spheroids of lymphangioma-derived cells, only the endpoints of the sprouts were counted.

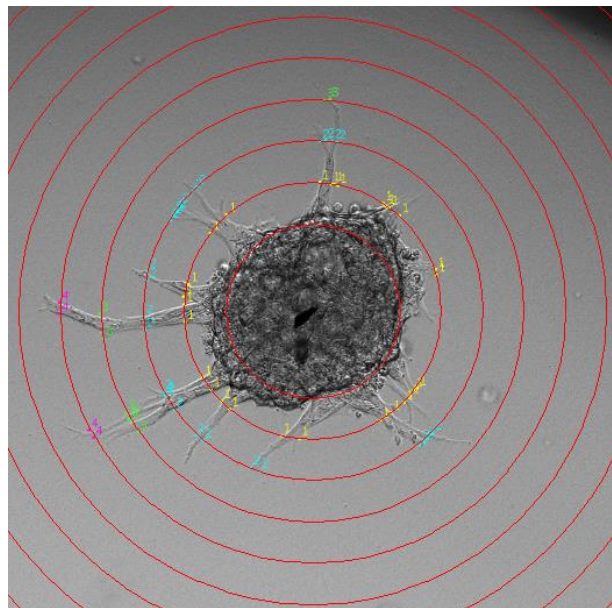


Figure 5: Example for the counting of sprouts with the circular-grid method. Both left and right sides of a sprout that intersects a circle, was counted using the cell-counter plug-in of Fiji. Different colours were used for the intersections to mark circles of increasing distance. For calculation of sprouts reaching each circle, the intersection numbers were divided by 2 (because left end right sides of sprouts were marked).

2.2.3.7 Immunofluorescence staining of cells

For immunofluorescence staining, LECs were seeded on chamber-slides and grown to 100 % confluence. After fixation with 4 % PFA (1-30 min, depending of the antibodies used) and three rinsing steps with PBS, BS I was added for 30 min. For detection of nuclear antigens, 0.05 % Tween or 0.1 % Triton-X was added to the last rinsing step. Then the chambers were removed. The further staining protocol was the same as in 2.2.2.2 after the antigen-retrieval.

2.2.4 Molecular biology

2.2.4.1 RNA isolation

Total RNA was isolated with peqGOLD TriFast™ according to the manufacturer's protocol. Thereby, cells were washed with cold PBS, lysated with peqGOLD TriFast™, mixed with chloroform and centrifuged. The clear, upper phase with the RNA was transferred in a new reaction tube and the RNA-precipitation was performed with isopropyl alcohol. The isolated RNA pellets were washed with ethanol, dissolved in RNase-free water and the RNA concentration was determined with BioPhotometer (Eppendorf).

2.2.4.2 Reverse transcription

2 µg of each RNA were mixed with the RT-PCR master mix (**Table 8**) and filled up with water to a final volume of 20 µl. The samples were then placed into the thermocycler (and reverse transcription of mRNA to cDNA occurred).

Programme of the thermocycler: 60 min - 37°C, 10 min - 70°C, 4°C ∞.

Table 8: Formulation of RT-PCR master mix

2 µl	Buffer
2 µl	dNTPs
2 µl	Random Primer Mix (0.2 µg/ml)
1 µl	Omiscrypt
0.5 µl	RNase

2.2.4.3 Semi-quantitative real-time PCR (qRT-PCR)

The qRT-PCR was performed with SYBR Green in a StepOnePlus Real-Time PCR System.

SYBR Green binds to the double-stranded DNA and causes fluorescence. Every PCR cycle doubles the amount of target DNA and fluorescence is measured after

every cycle. Increase of fluorescence-intensity is directly dependent on the amount of amplified DNA and allow therefore quantification. The first cycle where intensity exceeds background fluorescence is called the “threshold cycle” or C_T . So, a lower C_T -value reflects more initially available template cDNA which corresponds to mRNA levels.

For relative quantification of the PCR products, not only the amount fluorescence of the target gene but also of a reference transcript (here β -actin) is measured to ensure equal abundance of total RNA in the samples. According to the $\Delta\Delta C_T$ - Method, each sample value is subtracted from the value of the respective value of the reference transcript (ΔC_T). For comparison, one of the samples is defined standard and all Sample values (including itself) are subtracted by this value ($\Delta\Delta C_T$; resulting in 0 for the standard sample). By calculating $2^{-\Delta\Delta C_T}$ the standard becomes 1 (2^0) and the expression levels of the other samples become values higher than one (in case of higher expression) or lower than one (in case of reduced expression compared to the standard sample) (Livak and Schmittgen, 2001).

For the PCR reaction and the simultaneous fluorescence detection, the detection system and corresponding 96 well plates were used.

For each reaction 10 μ l Fast SYBR Green Master Mix, 0.1 μ l primer (concentration 0.01 nmol/ μ l, forward and reverse primers mixed) and 5 μ l cDNA, which correlates to 10 ng RNA, were mixed and filled up with water to a final volume of 15 μ l. The cDNA was diluted 1 to 10 for qRT-PCR.

All analyses were performed in triplicates. The corresponding qRT-PCR programme is shown in **Table 9**.

Table 9: qRT-PCR programme

Initial Denaturation	95°C/20 sec
Denaturation and Elongation	95°C/3 sec 60°C/30 sec (40 cycles)
Melt Curve Stage	95°C/15 sec 60°C/1 min 95°C/15 sec

The primers used for qRT-PCR are listed in **Table 10** and have been generated by IBA GmbH (Göttingen, DE).

Table 10: Primers

Primer	Sequence
AKTIN	Fwd: 5' TCC CCC AAA GTT CAC AA 3' Rev: 5' AGG ACT GGG TTC TCC TT 3'
DDK1	Fwd: 5' GCA CCT TGG ATG GGT ATT CCA 3' Rev: 5' GCA CAG TCT GAT GAC CGG AG 3'
FZD3	Fwd: 5' ACG TGA TGG CAG GTA CAC G 3' Rev: 5' TGA CAT GCT GCC ATG AGG TA 3'
FZD4	Fwd: 5' GAC AAC TTT CAC ACC GCT CA 3' Rev: 5' TGC ACA TTG GCA CAT AAA CA 3'
FZD5	Fwd: 5' CTG GGG ACT GTC TGC TCT TC 3' Rev: 5' GAC GGT TAG GGC TCG GAT T 3'
FZD6	Fwd: 5' TGG GTC TCT GAT CAT TGT CG 3' Rev: 5' TTC TGG TCG AGC TTT TGC TT 3'
FZD8	Fwd: 5' GAT GGG ATT GCA CGG TTT GG 3' Rev: 5' CCC GTA TTT ACG TGG GGT GT 3'
IGF1	Fwd: 5' ACT AGC AGT CTT CCA ACC CA 3' Rev: 5' TGG TGT GCA TCT TCA CCT TCA 3'
LRP5	Fwd: 5' GAC AAC GGC AGG ACG TGT AA 3' Rev: 5' AGA TCC TCC GTA GGT CCG TC 3'
LRP6	Fwd: 5' CTC CGG CGA ATT GAA AGC AG 3' Rev: 5' TAA GTC CCA CAG GCT GCA AG 3'
PRICKLE1	Fwd: 5' AAC CAG AGC AAA GTG TTC GG 3' Rev: 5' TGG CCT TGG CTT GTT TTC TC 3'
PRICKLE3	Fwd: 5' CAT CTC CGA CGA CGA CTC AG 3' Rev: 5' CTC TGG GAG GCA GCT GAA AA 3'
ROR1	Fwd: 5' CAA CAA ACG GCA AGG AGG TG 3' Rev: 5' ACT CTG GAC TTG CAG TGG GA 3'
ROR2	Fwd: 5' GAC CCT TTA GGA CCC CTT GA 3' Rev: 5' GGC CTT GGA CAA TGG TGA TA 3'
RYK	Fwd: 5' AGT TCG TTG GAT GGC TCT TG 3' Rev: 5' GAG TTC CCA CAG CGT CAC TC 3'

Primer	Sequence
SPTA1	Fwd: 5' AGG GCT TAC TTT CTG GAT GGA 3' Rev: 5' TAG TTG ACG CTT CAT CGC CT 3'
SPTBN5	Fwd: 5' AAT GAG TGC ACG ACC AAG GA 3' Rev: 5' CCC CTG AAG TTT GGT GTT GC 3'
VANGL1	Fwd: 5' CCA AAT TCC GAG CAG CCA AG 3' Rev: 5' CTG GCC AGT GGC ATT GTT AC 3'
VANGL2	Fwd: 5' CTG TCT ACA ACC CTG CCC TC 3' Rev: 5' GGT GCT GTT TTC CTC TCC GA 3'
WNT11	Fwd: 5' CTG CAG AGC TCA CCT GAC TT 3' Rev: 5' GTT GCA CTG CCT GTC TTG TG 3'
WNT3A	Fwd: 5' AGT GCC CCA CTC GGA TAC TT 3' Rev: 5' AAT ACT GTG GCC CAA CAG CC 3'
WNT5A	Fwd: 5' AGG GCT CCT ACG AGA GTG CT 3' Rev: 5' GAC ACC CCA TGG CAC TTG 3'
WNT5B	Fwd: 5' TTC TGA CAG ACG CCA ACT CC 3' Rev: 5' GGC TGG GCA CCG ATG ATA AA 3'

2.2.5 Protein biochemistry

2.2.5.1 Whole cell lysates

Cells were trypsinized, centrifuged and the pellets washed with PBS containing 1 mM SOV, and transferred into a reaction tube. This was centrifuged for 10 min at 2,000 rpm at 4°C. The supernatant was discarded and the pellet dissolved in RIPA lysis buffer (working solution). After 30 min incubation on ice, the tube was centrifuged for 15 min at 15,000 rpm at 4°C. The supernatant with the dissolved proteins was collected in a new reaction tube.

For the WNT5A stimulation experiments, HD-LECs were lysed directly in the culture plates.

After washing twice with ice-cold PBS + 1 mM SOV, 150-500 μ l RIPA lysis buffer (working solution) were added to the plates, which were kept constantly on ice. After 10 min, the cells were scraped off with a cell scraper and transferred to a reaction tube together with the buffer. This was kept on ice for another 20 min. After 15 min centrifugation at 15,000 rpm at 4°C, the supernatant with the dissolved proteins was transferred to a new reaction tube.

The protein concentration of each supernatant/lysate was measured with Roti-Quant according to the manufacturer's instructions. The optical densities were measured with the Eppendorf BioPhotometer and the concentrations calculated with help of a standard curve performed with BSA as a calibration protein.

2.2.5.2 Concentration of supernatants

For verification of WNT5A attendance in supernatants, the supernatants of cells were collected (with or without LGK974 the application of 10 μ M LGK974) after three days.

In a second method, growth medium of the cells was exchanged with serum-free medium (with or without LGK974) and the supernatants were collected after 24 hours. This was performed three times, with at least one day of normal growth medium between each collection. And at the end the supernatants were combined.

Then all supernatants were concentrated with VIVASPIN 2 Centrifugal Concentrator (10,000 MWCO PES) according to the manufacturer's protocol. The protein concentrations were determined with Roti-Quant as described (2.2.5.1).

2.2.5.3 SDS-page and Western blot

Proteins were size-fractionated with sodium dodecyl sulphate polyacrylamide gel electrophoresis (SDS-PAGE) (Laemmli, 1970). Polyacrylamide gels composed of 5 % stacking gel and 10 % (12 % for WNT5A) separation gel were used. 50 μ g

protein of each sample was mixed with the appropriate amount of 6x sample buffer, denatured at 95°C for 5 min, centrifuged for 5 min at 14,000 rpm and then loaded onto the gel. PageRuler™ prestained protein ladder was used to determine protein sizes.

Following electrophoresis, the Bio-Rad Tank Blot system was used to transfer the proteins to a PVDF membrane. The membranes were soaked with blocking buffer for 1 h at room temperature. The membranes were then incubated with primary antibodies diluted in the appropriate blocking buffer and gently shaken at 4°C overnight. After three rinsing steps of at least five minutes each, the membranes were incubated with HRP-conjugated secondary antibodies diluted in the appropriate blocking buffer. After another three rinsing steps of at least five minutes each, the membranes were incubated with Clarity™ Western ECL Substrate for five minutes and imaged with the ChemiDoc Imaging System.

For the detection of WNT5A, 6x sample buffer without DDT was used. The lysates were not denatured with heat and SignalFire™ ECL Reagent was used for development of the signal.

2.2.6 Statistical analyses

Statistical analyses were performed with GraphPad Prism 5.03. All data sets were tested for normality with the Shapiro-Wilk normality test. When all data sets of one comparison passed the normality test, they were evaluated with an unpaired t-test. If one of the relevant data sets was not normally distributed, the Mann-Whitney test was used.

The proliferation assays were analysed with two-way ANOVA with a Bonferroni post hoc test (control vs. treatment).

3 Results

The aim of my studies was to analyse the influence of WNT signalling, and specifically WNT5A, on lymphangiogenesis. Therefore, I split my thesis into two main parts:

Firstly, I analysed Wnt5a-related signalling in murine embryos. Initial studies on dermal lymphatics of Wnt5a-null-mice were published by our lab some years ago (Buttler et al. (2013). I characterised the dermal lymphatics of embryonic mice with a focus on Wnt signalling in greater detail. And, I applied an activator and an inhibitor of the Wnt signalling pathway to murine embryonic dermis to analyse the influence of Wnts on dermal lymphatics.

In the second part of my thesis, I studied the intracellular down-stream signalling of WNT5A in human lymphatic endothelial cells (LECs). I characterised the cells, performed *in vitro* angiogenesis assays, and applied activators and inhibitors of both the β -catenin-dependent and β -catenin-independent WNT pathways. Finally, I analysed the effects of the inhibition of autocrine WNT-signalling on gene expression in LECs.

3.1 Studies on murine embryos

This part of my thesis focuses on the influence of Wnt signalling on the development and function of murine dermal lymphatics.

3.1.1 Immunohistological characterisation of embryonic murine dermal lymphatics

First, I analysed dermal lymphatics of mice under the light of Wnt signalling in more detail. Therefore, I used whole-mount staining as described in 2.2.2.1. In previous studies, our lab has shown that dermal lymphatics of murine embryos are positive for Wnt5a (Buttler et al., 2013). I expanded this experimental approach with numerous antibodies. Staining of tissues with antibodies against

Wnt5a was difficult. I tested three different antibodies (anti-WNT5A (C-16), Santa Cruz Biotechnology; anti-WNT5A (H-58), Santa Cruz Biotechnology; anti-WNT5A, R&D Systems), but only one of them (H-58, Santa Cruz Biotechnology) showed convincing results. In line with in situ hybridization data (see: <http://www.genepaint.org/cgi-bin/mgrqcgi94>) Wnt5a is expressed in numerous cells of embryonic mouse dermis, including lymphatic endothelial cells (**Figure 6**).

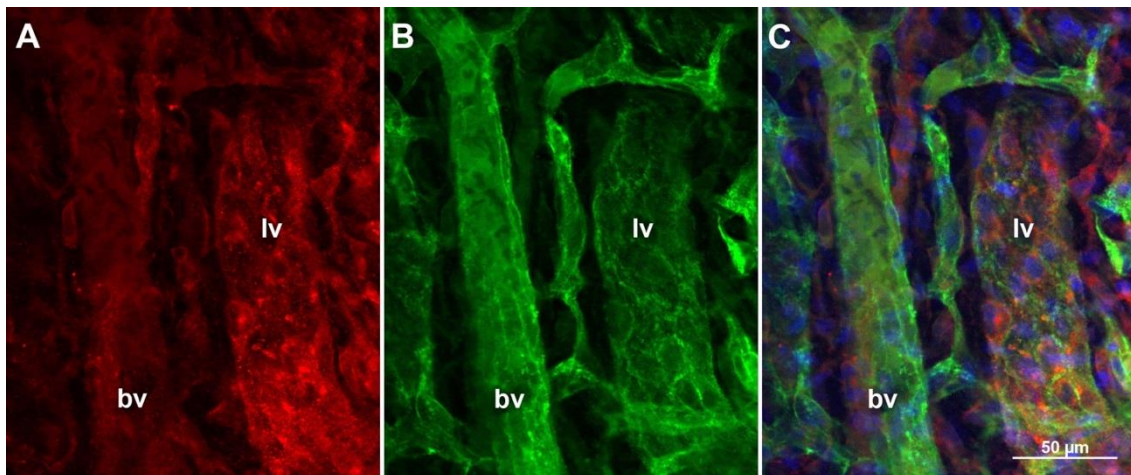


Figure 6: Mice express Wnt5a in their lymphatic vessels. (A) Anti-Wnt5a (red) whole-mount staining of dermis of a mouse at ED 18.5 (anti-WNT5A; H-58, Santa Cruz Biotechnology). The lymphatic vessel (lv) shows a stronger expression of Wnt5a than the blood vessel (bv). (B) Anti-CD31 staining (green). The lymphatic vessel (lv) typically shows weaker expression than the blood vessels (bv). (C) Merged picture. Counter-staining of nuclei with DAPI (blue).

Frizzleds (Fzd) are high-affinity receptors for Wnt ligands. To characterise the expression of Fzd receptors in lymphatic vessels, I stained whole-mounts of murine dermis with various anti-Fzd antibodies using a double staining protocol with endothelial cell-specific antibodies. Thereby, I received the clearest results with antibodies against Fzd5 and Fzd8. Co-staining with an endothelial specific antibody (CD31) showed that dermal lymphatic vessels of mice express Fzd5 (**Figure 7**) and co-staining with Lyve-1 antibodies revealed expression of Fzd8 in dermal lymphatics (**Figure 8**). Thereby, both Fzd receptors are not only expressed in the lymphatic vessels, but also in numerous other dermal cell types. My data show that major players of the β -catenin-independent Wnt signalling are present in murine dermis, including the lymphatic vessels.

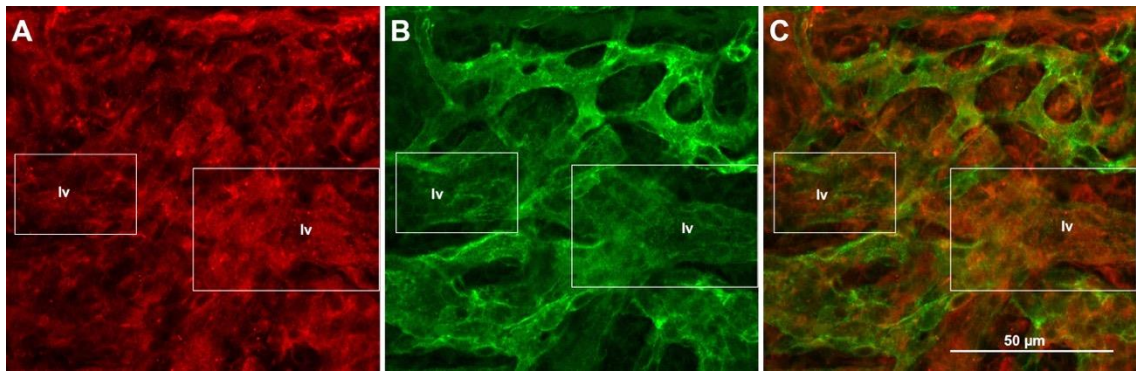


Figure 7: Lymphatic vessels of mice express Fzd5. (A) Anti-Fzd5 (red) whole-mount staining of murine dermis at ED 18.5. The boxes mark Fzd5-positive lymphatic endothelial cell. (B) Anti-CD31 (green) whole-mount staining of the same specimen. The lymphatic vessels (lv) show the typical weaker expression of CD31 than the blood vessels. The boxes mark CD31-positive lymphatic endothelial cell. (C) Merged picture.

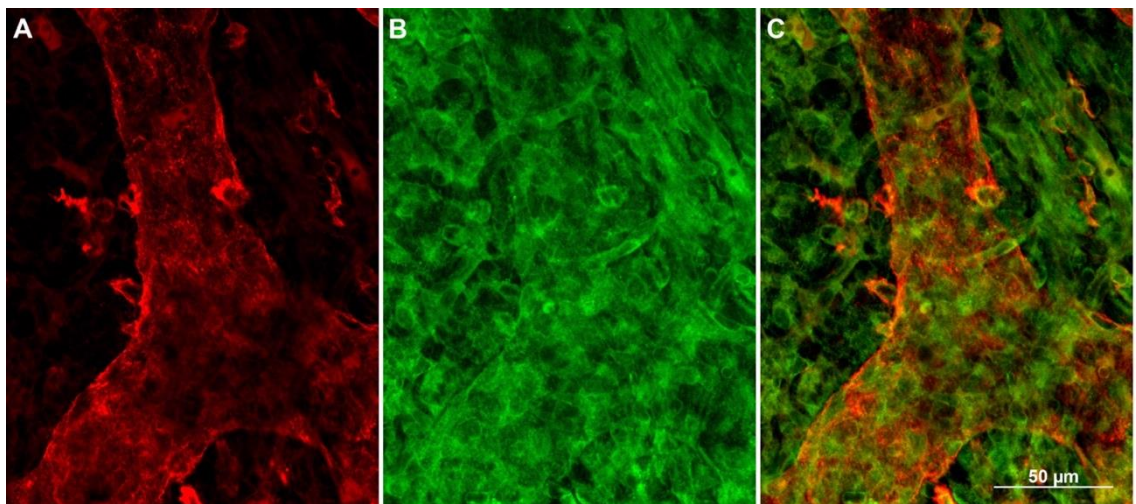


Figure 8: Lymphatic vessels of mice express Fzd8. (A) Anti-Lyve-1 (red) whole-mount staining of dermis of mice at ED 18.5. The endothelial cells of the lymphatic vessel show a strong expression of Lyve-1. (B) Anti-Fzd8 (green) whole-mount staining of the same specimen. (C) Merged picture. The Lyve-1-positive LECs of the lymphatic vessel are also positive for Fzd8.

Another protein that is often mentioned in the context of planar-cell-polarity is Vangl2. Whole-mount double staining of murine dermis with an anti-Vangl2 antibody and CD31 revealed that dermal lymphatics express Vangl2 (**Figure 9**). However, like the other investigated proteins, Vangl2 is almost ubiquitously expressed in the dermis of mice.

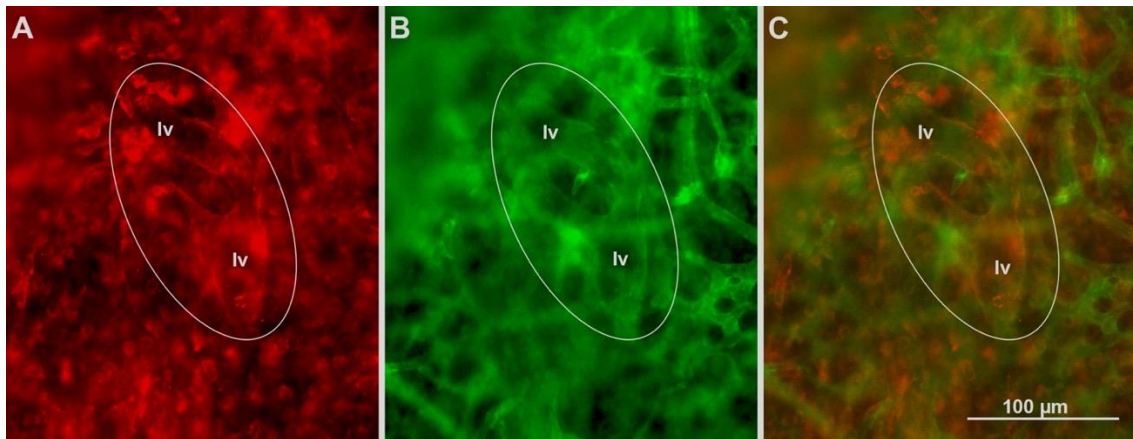


Figure 9: Lymphatic vessels of mice express Vangl2. (A) Anti-Vangl2 (red) whole-mount staining of dermis of mice at ED 18.5. The lymphatic endothelial cells of the lymphatic vessel (lv) express of Vangl2. (B) Anti-CD31 (green) whole-mount staining of dermis of mice at ED 18.5. The lymphatic vessel (lv) shows the typical weaker expression of CD31 than the blood vessels. (C) Merged picture. The lymphatic endothelial cells of the lymphatic vessel (lv) show co-expression of Vangl2 and CD31.

3.1.2 Superficial lymphatics of Wnt5A-null mice are malfunctioning

To analyse the functionality of the superficial lymphatics, 2000 kDa FITC-dextran was injected into the interstitial space of the paws of both the front and hind limbs of ED 16.5 and ED 17.5 embryos, as described in 2.2.1.2. In healthy appearing mice (wt and *Wnt5a*^{+/-}), FITC-dextran was taken up into the lymphatics immediately after injection and transported proximally. Thereby, *Wnt5a*^{+/-} embryos possess a phenotypically normal appearance and cannot be distinguished from wt-mice. In contrast, *Wnt5a*-null-mice are massively malformed. They are characterised by craniofacial malformations, limb shortening and the lack of the tail. This phenotype was first described by Yamaguchi et al. (1999). Macrophotographs of a *Wnt5a*-null mouse embryo and a littermate control can be seen in the appendix (Figure A- 1).

Figure 10 shows the embryos after the injection of FITC-dextran. The upper row shows the uptake of the of FITC-dextran in an ED 17.5 heterozygous-*Wnt5a*-mouse after 2 min, 10 min, 15 min and 30 min. After 15 minutes a second injection was made into the paw of the lower limb and after another 15 minutes the superficial connecting vessel between the lumbar and axillar region was visible

(arrowhead in **Figure 10**). The lower row shows pictures of an injection of FITC-dextran into the upper limb bud of a *Wnt5a*-null-mouse (ED 17.5) after 1 min and 15 minutes. In contrast to the heterozygous mouse no uptake is visible. This clearly shows that the lymphatics are malfunctioning and do not drain the tissue.

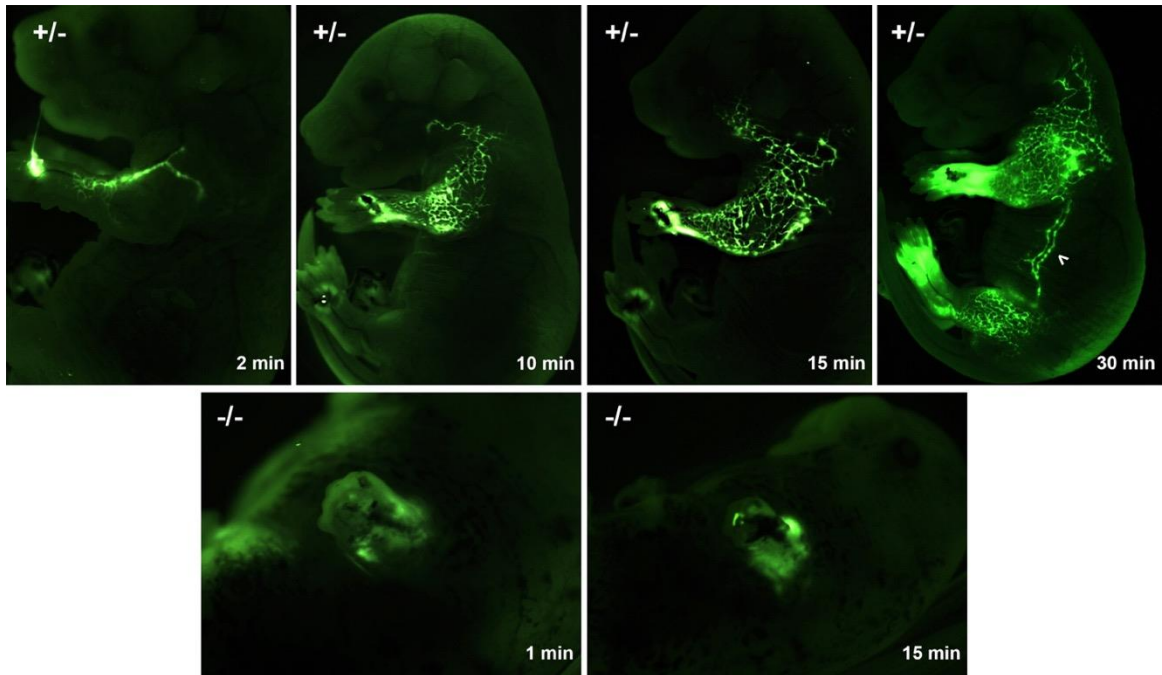


Figure 10: Interstitial injection of 2000 kDa FITC-dextran into the paw of ED 17.5 mouse embryos. Upper row: Pictures of a *Wnt5a*^{+/-} embryo 2 min, 10 min, 15 min and 30 min after the injection. After 15 minutes a second injection was made in the paw of the lower limb. The arrowhead marks the interconnection of the inguinal and axillary regions. **Lower row:** Pictures of *Wnt5a*-null-embryos 1 min and 15 min after the injection.

3.1.3 Recombinant WNT5A protein rescues maturation of dermal lymphatics in *Wnt5a*-null-mice

Pieces of approximately 2x2 mm of dorsal thoracic dermis of ED 15.5 *Wnt5a*-null-mice were cultured and treated with 500 ng/ml recombinant WNT5A for 2 days as described in 2.2.1.3. Dermis from the contralateral side was used as controls. In contrast to normal dermis, the dermis of *Wnt5a*-null-mice was oedematous and soft. Both culturing and whole-mount immunostaining was difficult and several specimens showed a high background after staining with Lyve-1 antibodies. Therefore, a large number of experiments could not be evaluated. Finally, from 10 experiments, I was able to compare 7 WNT5A-treated specimens

from 4 different embryos, derived from 3 different litters, with corresponding controls. **Figure 11** shows representative pictures of the analysed specimens. After 2-day culture, an immature vascular plexus was visible in the untreated controls. The vessels had a large diameter and lots of small “loops” with short connections between the individual vessels (**Figure 11**, upper row). In contrast, after treatment with WNT5A, the vascular network appeared more mature, with thinner and longer vessels, with less but larger “loops” and longer interconnections (**Figure 11**, lower row).

To quantify the effects, the vessel-covered area and the number of branching points of the specimens were analysed with AngioTool 0.5a. The vessel-covered area was significantly smaller in the WNT5A-treated dermis (thinner and longer vessel = maturation) (**Figure 12A**, $n \geq 5$, Mann Whitney test, $p = 0.0025$). The number of branching points was slightly lower (less and larger “loops” = more mature network), but this was statistically not significant (**Figure 12B**, $n \geq 5$, Mann Whitney test, $p = 0.1038$).

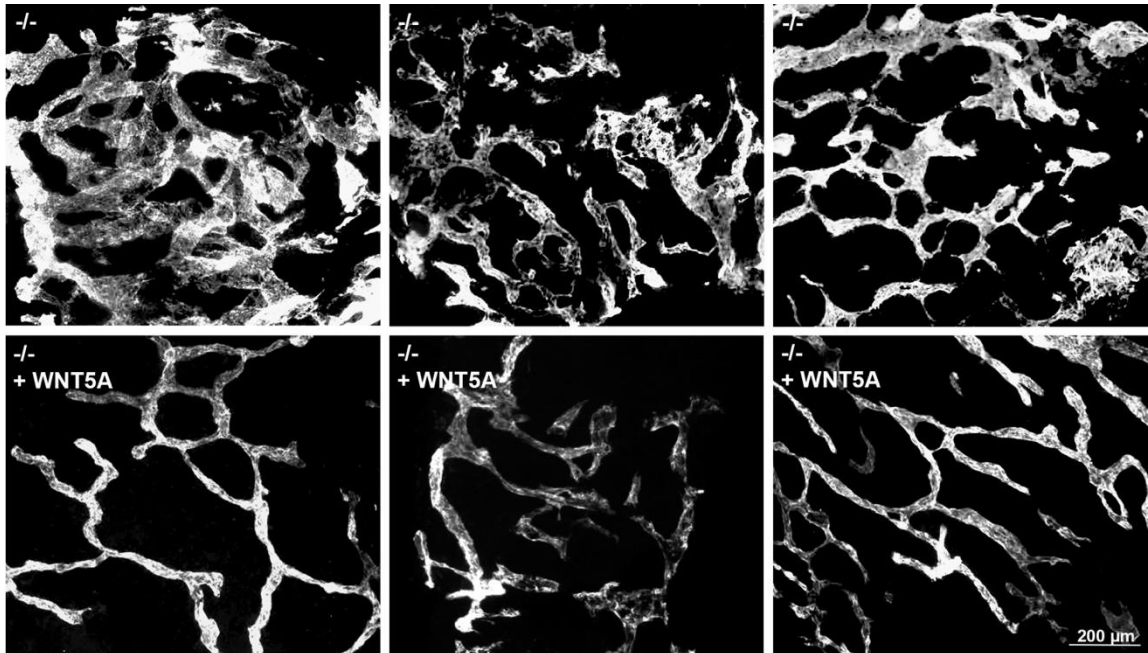


Figure 11: *Ex vivo* studies of dermis from ED 15.5 *Wnt5a*-null mice treated with recombinant WNT5A for 2 days. Representative pictures are shown. Lymphatic vessels were stained with anti-Lyve-1-antibody. The upper row shows controls treated with BSA, and the lower row the experimental specimens.

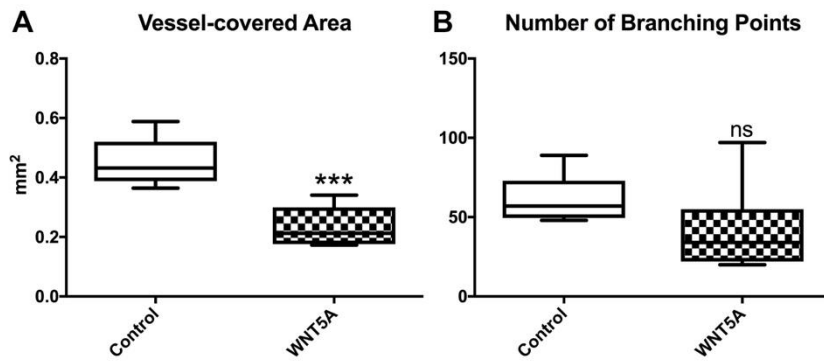


Figure 12: Quantification of *ex vivo* studies of lymphatics in the dermis of *Wnt5a*-null mice; controls vs. WNT5A-treated. (A) Vessel-covered area in mm². (B) Number of branching points. The vessel-covered area is significantly lower in WNT5A-treated dermis (Mann-Whitney test, * $p \leq 0.001$).**

Higher magnifications of the vessels showed that the endothelial cells of the dermal lymphatic vessels possessed an elongated shape after the application of recombinant WNT5A (**Figure 13**).

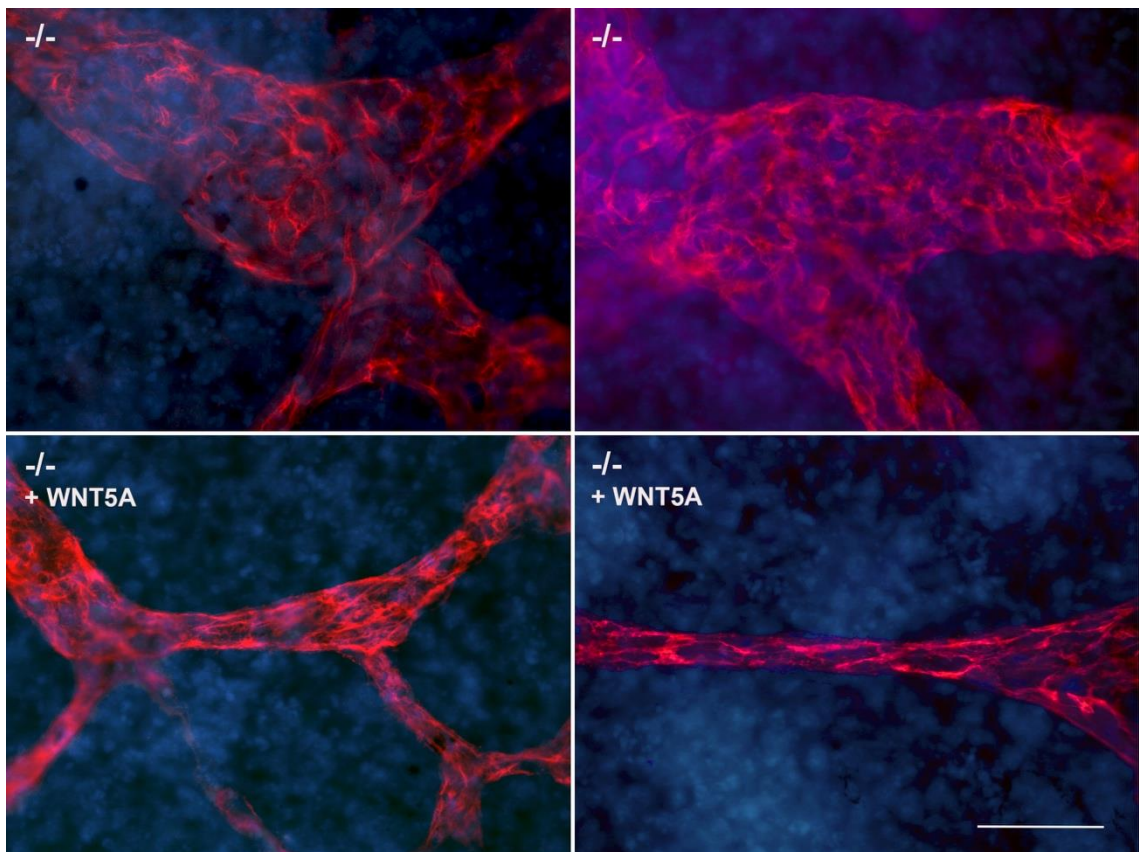


Figure 13: Higher magnification of *ex vivo* studies of dermis from ED 15.5 *Wnt5a*-null mice treated with recombinant WNT5A for 2 days. Representative pictures are shown. Lymphatic vessels were stained with anti-Lyve-1-antibody (red), counter-staining with DAPI (blue). The upper row shows controls treated with BSA, and the lower row shows specimens after treatment with WNT5A. Application of WNT5A led to an elongation of the LECs. Scale bar = 50 μm .

Auxiliary finding: dermal lymphatics of *Wnt5a*-null mice may contain blood

During my tests of *Wnt5a* antibodies, I made the observation that the lymphatic vessels of *Wnt5a*-null mice are often filled with blood (**Figure 14**). This finding goes in line with the observation that the *Wnt5a*-null embryos show numerous petechial bleedings in the skin (Appendix, **Figure A- 1, upper row**). These studies were performed in cooperation with Jules A. Demanou Toukam, whom I supervised during his medical doctoral thesis at the UMG, Göttingen.

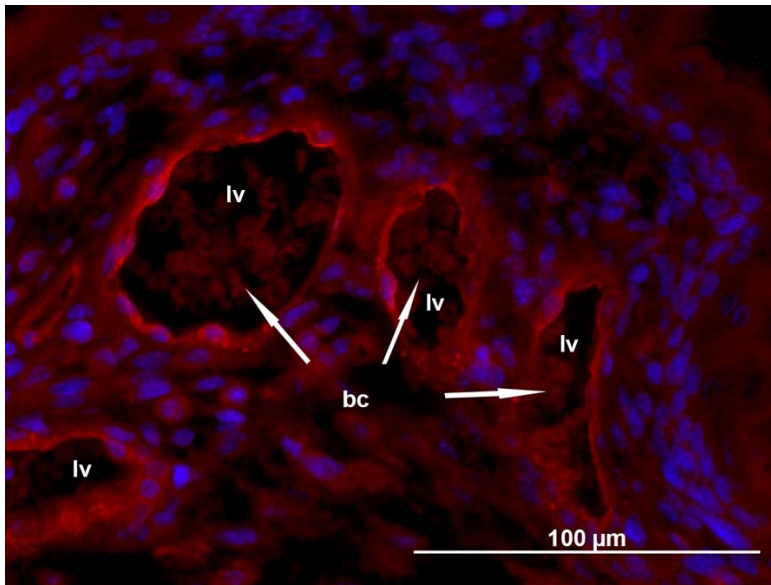


Figure 14: Lymphatic vessels of *Wnt5a*-null mice contain blood. Anti-Lyve-1 staining (red) of a paraffin section of the dermis of a *Wnt5a*-null mouse at ED 18.5. The lymphatic vessels (lv) are filled with blood cells (bc). Counter-staining of nuclei with DAPI (blue).

3.1.4 Inhibition of Wnt-signalling retards maturation of dermal lymphatics in wild-type mice

Pieces of approximately 2x2 mm of dorsal thoracic dermis of ED 15.5 wild-type (wt) C57BL/6 mice were cultured and treated with 25 μM or 50 μM Porcupine (Porcn) inhibitor LGK974 for 2 days as described in 2.2.1.3. LGK974 completely prevents secretion of Wnts (J Liu et al., 2013). The dermal lymphatic vessels of

the untreated specimens were thin and only a small number of “loops” and interconnections between individual vessels were visible (**Figure 15, upper row**). The specimens treated with 25 μM LGK974 showed often larger vessel diameters, and occasionally immature “loops” (**Figure 15, row in the middle**). Interestingly, the specimens treated with 50 μM LGK974 showed many large-diameter vessels with numerous immature “loops” and connections between neighbouring vessels. 14 specimens from 4 mice were quantified.

Figure 16 shows the vessel-covered area and the number of branching points determined with AngioTool 0.5a. Treatment with 25 μM LGK974 did not significantly influence the determined parameters (n = 14; vessel-covered area: t-test, $p = 0.1858$; number of branching points: Mann-Whitney test, $p = 0.1305$). However, treatment with 50 μM induced a significant increase in both the vessel-covered area (= larger vessel diameters) (n = 14, t-test, $p = 0.0004$) and the number of branching points (= many immature “loops”) (n = 14, Mann Whitney test, $p = 0.0244$). This led to the conclusion that the treatment with LGK974 prevents maturation of dermal lymphatics.

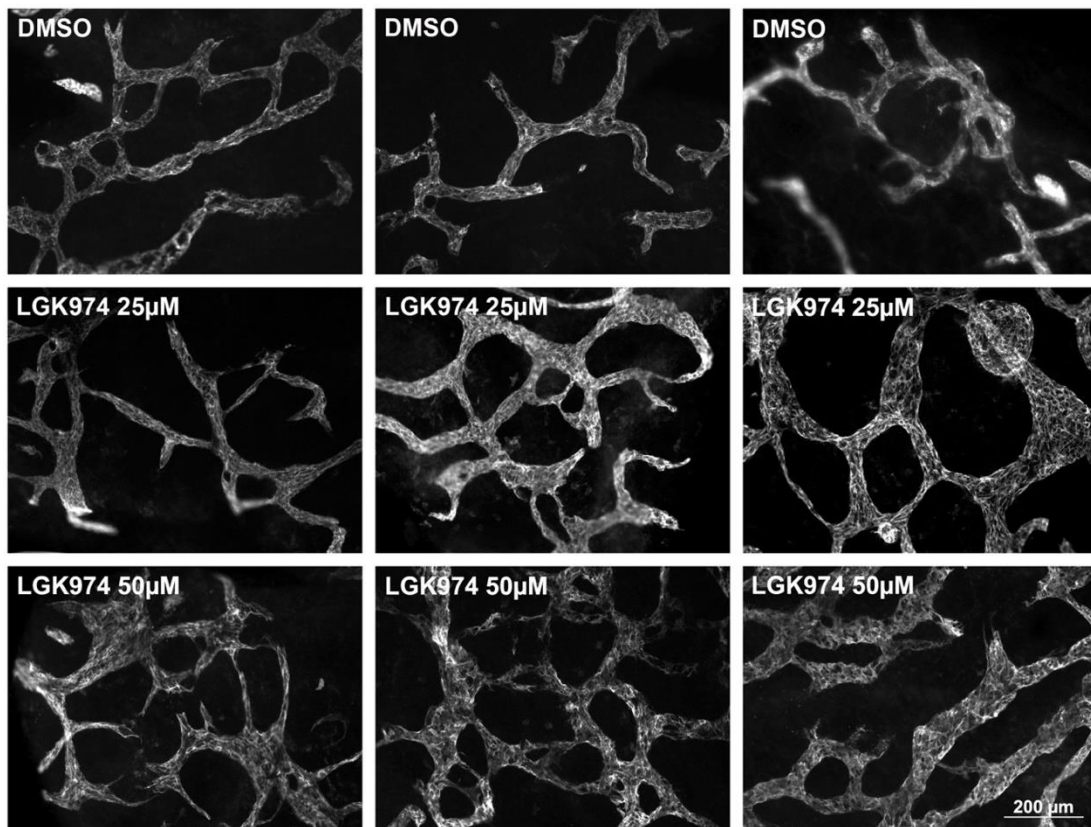


Figure 15: *Ex vivo* studies of lymphatics in the dermis of ED 15.5 C57BL/6 mice treated with the Porcn-inhibitor LGK974. Representative pictures are shown. Lymphatic vessels were stained with anti-Lyve-1-antibody. The upper row shows the 2-day-cultured controls, the middle row shows specimens treated with 25 μM LGK974, and the bottom row shows specimens treated with 50 μM LGK974.

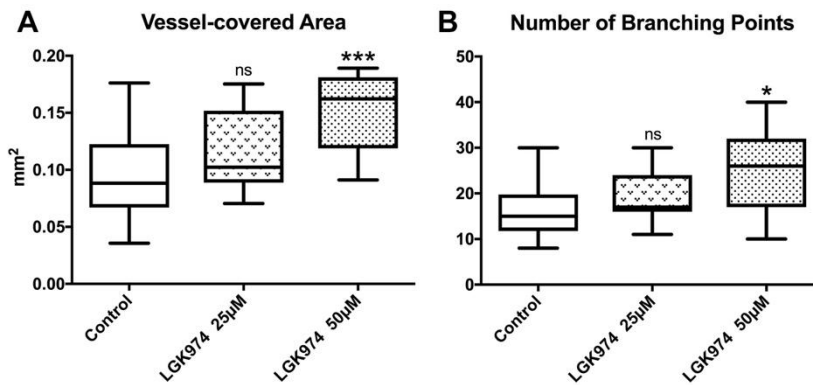


Figure 16: Quantification of *ex vivo* studies of C57BL/6 mouse dermis with the Porcn-inhibitor LGK974. Shown are (A) the vessel-covered area in mm² and (B) the number of branching points. Both are significantly higher in dermis treated with 50 µM LGK974 (t-test and Mann Whitney test, *p ≤ 0.05, ***p ≤ 0.001).

3.2 Studies of human Lymphatic Endothelial Cells

The second part of my thesis investigated the question how WNTs, and manly WNT5A, influence the lymphangiogenic behaviour of human LECs. First, I performed a molecular characterisation of the LECs, which were then used in various *in vitro* lymphangiogenesis assays.

3.2.1 Characterisation of Lymphatic Endothelial Cells

In this part of my thesis I characterised HD-LECs under the light of WNT signaling. Therefore, I performed immunocytology, qRT-PCR and Western blot expression analyses with the HD-LECs, which were later used in all *in vitro* angiogenesis assays.

3.2.1.1 Immunocytology with LEC markers

As a prerequisite for all studies on human LECs, I studied the purity of the cell cultures. I tested several LEC lines, which were bought from PromoCell. These

cells are isolated from foreskin and may contain blood vascular endothelial cells (BECs) as well. Each cell line represents one individual. Therefore, I wanted to perform the assays with at least three LEC lines. Typical markers for human LECs are CD31/PECAM1 and the transcription factor PROX1 (Wilting et al., 2002). BECs express CD31 higher than LECs, and they do not express PROX1. For all further studies, I chose LEC lines, which were almost 100% CD31 and PROX1 double-positive (**Figure 17**). This also holds true for the LEC line (LEC2), which was isolated in our lab several years ago, and originates from a child suffering from lymphangioma (LY-LEC) (**Figure 17**) (Norgall et al., 2007).

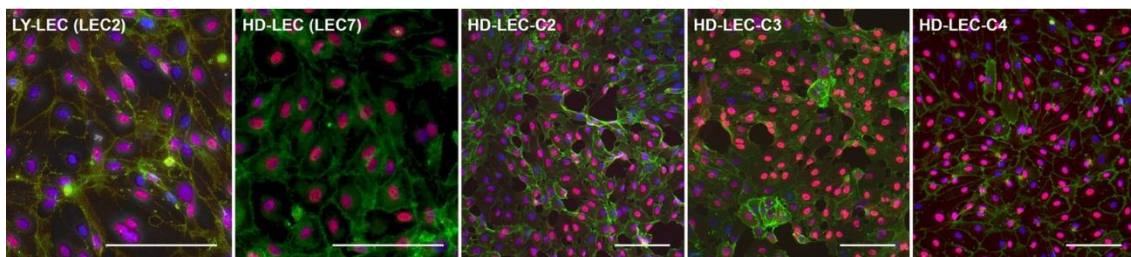


Figure 17: Anti-PROX1 and anti-CD31 double staining of LECs. All LECs showed the typical expression pattern with PROX1-positive nuclei (red) and CD31-positive cell membranes (green). Counter staining of the nuclei with DAPI (blue). Scale bar = 100 μ m

3.2.1.2 qRT-PCR

Next, I studied the expression of WNT-related molecules in LECs in greater detail. I analysed the mRNA expression with semi quantitative real-time PCR (qRT-PCR). The method (see 2.2.4.3) provides a relative quantification of the mRNA expression levels, calibrated to the expression of a house-keeper gene, here β -actin. For comparison, the expression levels of a pool of a large number of cell lines, which we culture in our lab, was set as 'one'. This pool of cells contained neuroblastoma cell lines (where WNT signalling is up regulated in many cell lines = positive control; see: Jürgen Becker and Wilting (2018)), as well as BECs and LECs. Buttler et al. (2013) had shown that LY-LECs express WNT5A, ROR1, ROR2 and RYK. Among many others, I included these molecules in my studies, which I performed with the same HD-LECs, which were also used in all *in vitro* angiogenesis assays (HD-LEC-C2, HD-LEC-C3 and HD-LEC-C4).

Figure 18 shows the relative expression levels of WNT-related molecules in HD-LECs, as compared to the cell-pool, set as 'one'.

The expression levels in the three LEC lines were always lower than in the neuroblastoma-containing cell pool; but clear values were measurable with most of the probes. Thereby, HD-LEC-C4 constantly showed lowest expression. The mRNA expression of the WNT-ligands WNT3A (β -catenin dependent WNT), WNT5A and WNT5B (β -catenin independent WNTs) could be verified. Additionally, HD-LECs expressed the WNT receptors FZD3, FZD4, FZD5, FZD6 and FZD8, as well as the co-receptors ROR1 and RYK. The cells also expressed the mRNA of the PCP signalling-related molecules VANGL1, PRICKLE1, PRICKLE3. As well as DKK1, LRP5 and LRP6, which belong to the β -catenin-dependent signalling pathway. No mRNA expression of WNT11 and ROR2 was detectable in the tested HD-LECs.

Results

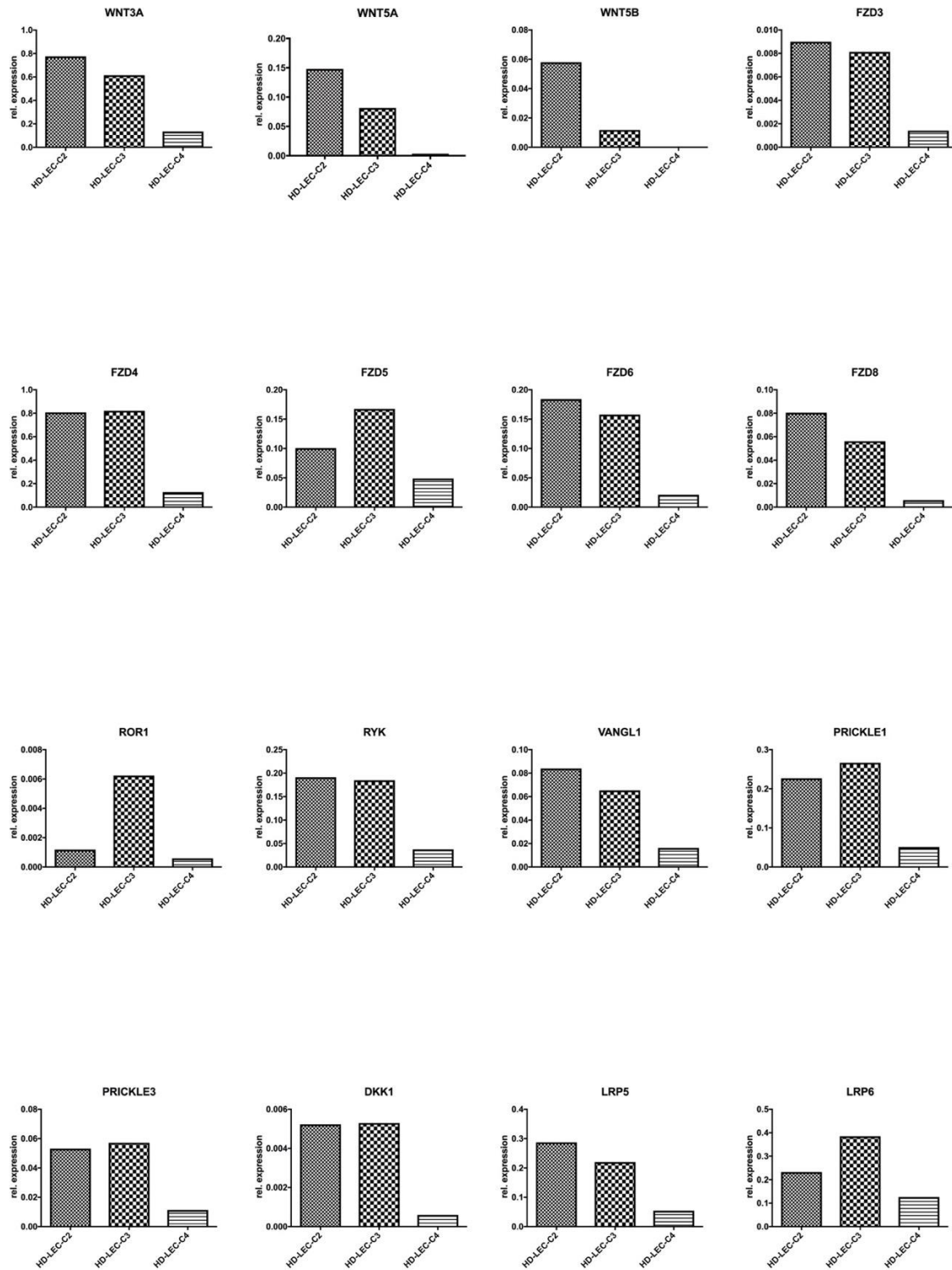


Figure 18: Relative expression levels of three HD-LEC lines. In all graphs, the relative expression is compared to of a pool of various cell lines, consisting of numerous neuroblastoma cell lines and mixed endothelial cells (expression level of pooled cells was set to 1; not shown).

3.2.1.3 Western blot and immunocytology

Protein expression of WNT-related proteins was studied with both Western blot analyses (see 2.2.5.3) and immunofluorescence staining of cells (see 2.2.3.7). The results are shown in **Figure 19**. All analysed molecules could be detected in Western blots and in immunofluorescence stainings (picture of PRICKLE1 immunofluorescence staining can be found in **Figure 20**). Immunocytology staining of WNT5A was not possible in HD-LEC. Three different anti-WNT5A antibodies showed no proper staining (tested antibodies: anti-WNT5A (C-16), Santa Cruz Biotechnology, anti-WNT5A (H-58) Santa Cruz Biotechnology, anti-WNT5A, R&D Systems).

WNT5A detection in Western blots was possible, but the HD-LEC-C4 cell line showed a variable expression of WNT5A (weak expression: **Figure 19**, strong expression **Figure 21A**).

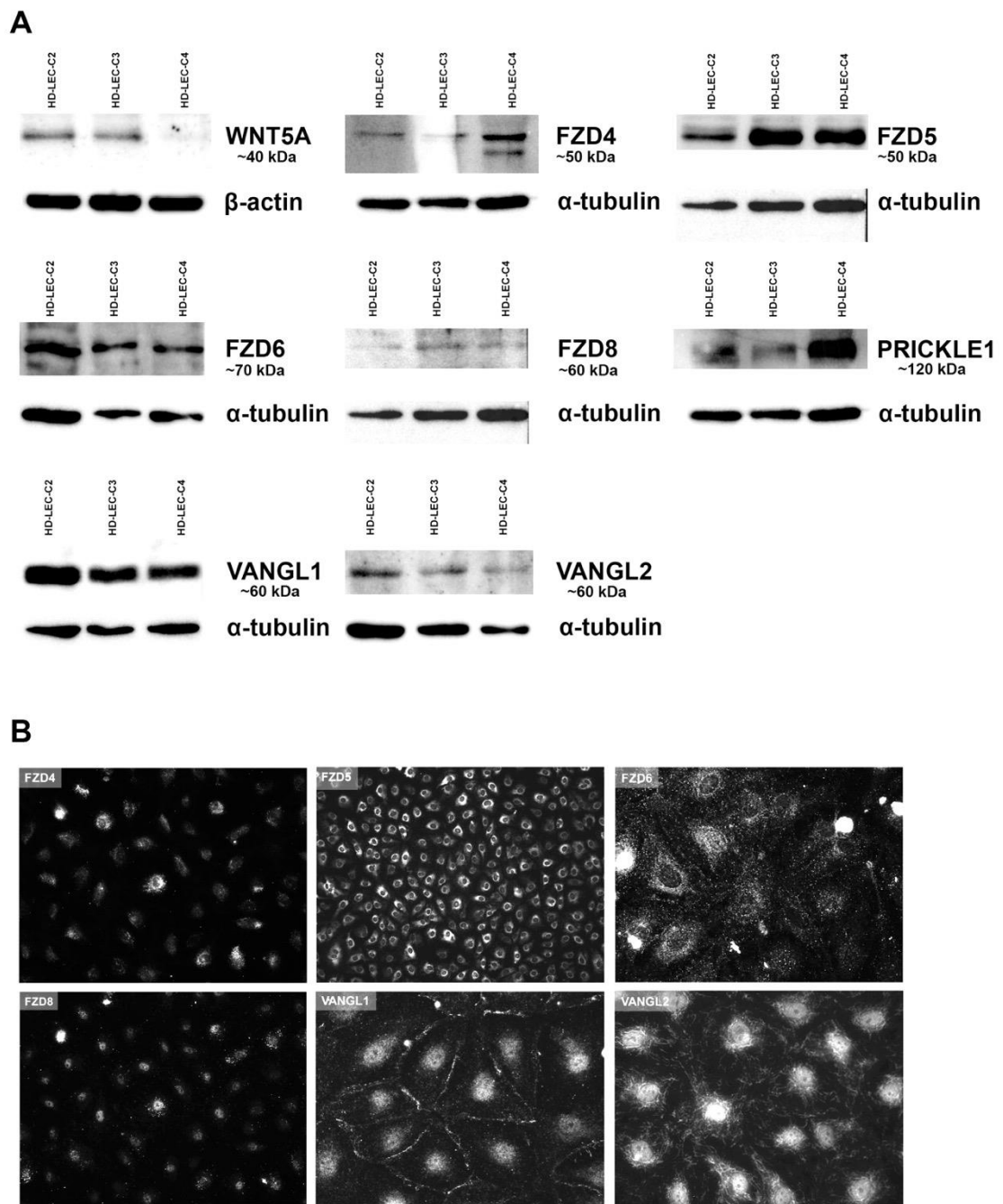


Figure 19: Protein expression analyses of WNT-related molecules in HD-LECs. (A) Western blots showing WNT5A, FZD4, FZD5, FZD6, FZD8, PRICKLE1, VANGL1 and VANGL2 in HD-LECs lysates. Note the highly similar expression levels in all three HD-LEC lines. WNT5A expression of HD-LEC-C4 varied in the analysed Western blots (see 3.2.1.3). **(B)** Immunocytology with antibodies against FZD4, FZD5, FZD6, FZD8, VANGL1 and VANGL2 in HD-LEC monolayers. All analysed proteins show perinuclear accumulation in the cytoplasm. VANGL1 is also expressed at the cell membrane.

3.2.1.4 Immunocytology of migrating LECs

Several of the above analysed molecules are associated with the WNT-PCP-pathway, and it has been shown that FZDs, VANGLs and PRICKLs may have a polarized localizations in epithelial cells, such Fzd6 and Vangl1 in mouse tracheal epithelial cells (Vladar et al., 2012) (reviewed in: Y Yang and Mlodzik (2015)). To test this in LECs, I analysed FZD5, VANGL2 and PRICKLE1 with immunofluorescence staining in migrating LECs, using the scratch assay described in 2.2.3.4. Notably, LECs in the first 3-4 rows adjacent to the scratch presented a polarized morphology. Thereby, FZD5 was enriched in the trailing end of the cells (**Figure 20A and A`**), whereas in non-migrating cells there was no accumulation of the protein at any side of the cells (**Figure 20A``**). PRICKLE1 was highly expressed in the nucleus of all LECs, and additionally, there was a punctate localisation in the cell membrane of the trailing end of migrating LECs (**Figure 20B**). VANGL2 was usually localised in the cytoplasm around the nucleus, but prominently also in a directed, street-like manner in the leading compartment of the cells (**Figure 20**).

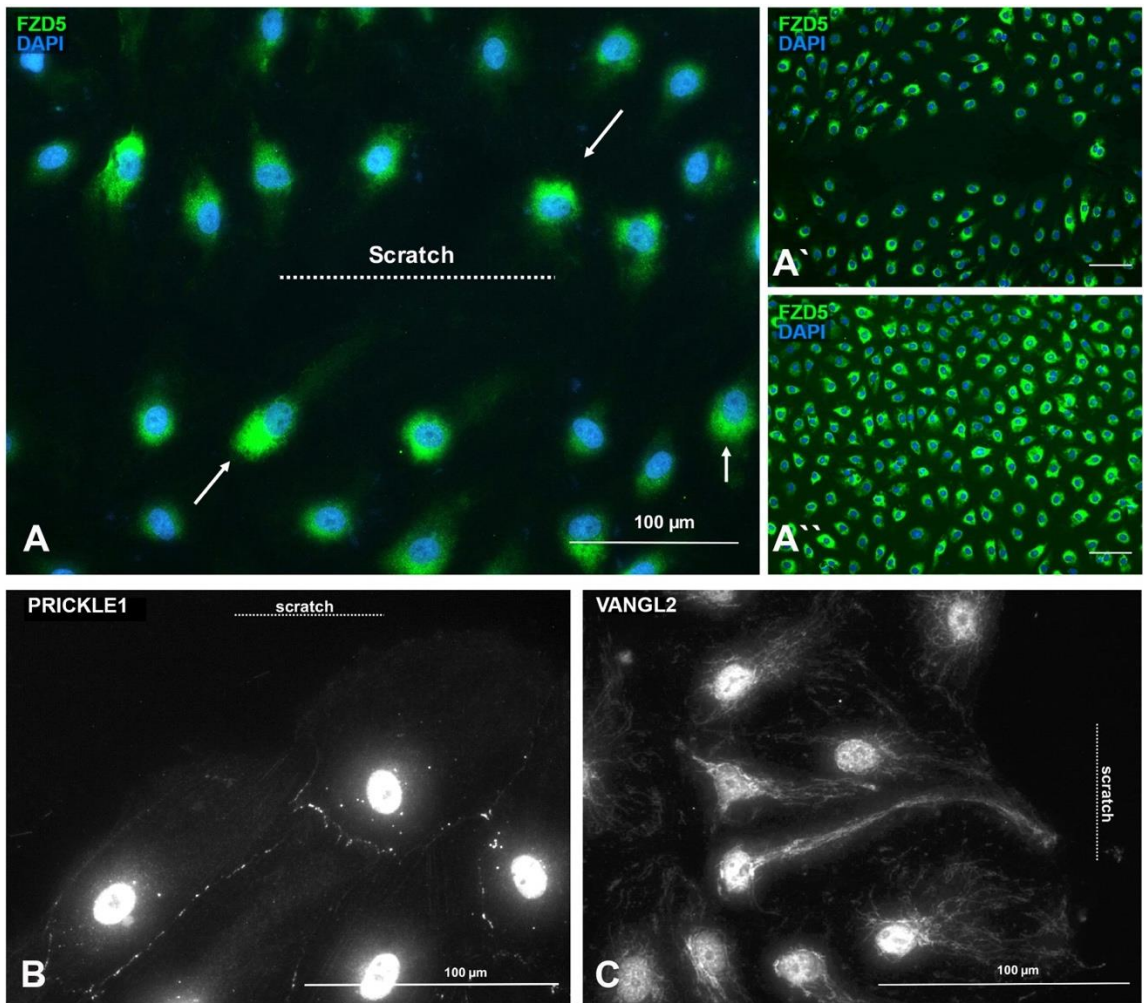


Figure 20: Scratch assays: FZD5, PRICKLE1 and VANGL2 show a polarized localization in migrating HD-LECs. (A –A`) FZD5 is enriched in the trailing end (arrows) of migrating cells. **(A``)** In non-migrating cells of the monolayer there is no polar distribution of FZD5. **(B)** Besides the strong expression of PRICKLE1 in the nucleus, there is a punctate staining in the cell membrane of the trailing end of migrating LECs. **(C)** Note strong expression of VANGL2 around the nucleus, and in the leading compartment of the cells towards the scratch. Scale bar = 100 μm

3.2.2 The PORCN inhibitor LGK974 inhibits WNT5A secretion in HD-LECs

In my *in vitro* and *ex vivo* studies I used the small molecule drug LGK974 to prevent the secretion of all WNT proteins, including WNT5A. LGK974 is a highly specific inhibitor of PORCN, which is involved in the processing/palmitoylation of WNTs (Liu et al., 2013). To test if LGK974 inhibits the secretion of WNT5A in HD-LECs I treated the cells with 10 μ M of the drug. I collected the supernatants, concentrated them with VIVASPIN 2 Centrifugal Concentrators (see 2.2.5.2), and also used the cells to prepare cell lysates. By Western blot analyses and application of WNT5A-specific antibodies, I analysed if LGK974 had reduced the amount of WNT5A in the supernatants. I expected that the amounts of WNT5A in the cell lysates remained unchanged (as shown by Liu et al. (2013) for Wnt3a), because LGK974 inhibits the palmitoylation of WNTs, which is important for their secretion but not for their production.

First, I analysed the amount of WNT5A in two HD-LEC lines, cultured in MV2, and treated them for 3 days with 10 μ M LGK974 (**Figure 21**). LGK974 clearly inhibited WNT5A secretion (**Figure 21B**, upper image). The huge amount of BSA in the FBS produced a strong band in the supernatants (visible in the Ponceau staining at 55 kDa in **Figure 21B**, lower image). Therefore, the amount of WNT5A that had passed the BSA fraction appeared rather small.

However, in the lysates of these LECs treated for 3 days with 10 μ M LGK974, WNT5A was reduced significantly (**Figure 21A**).

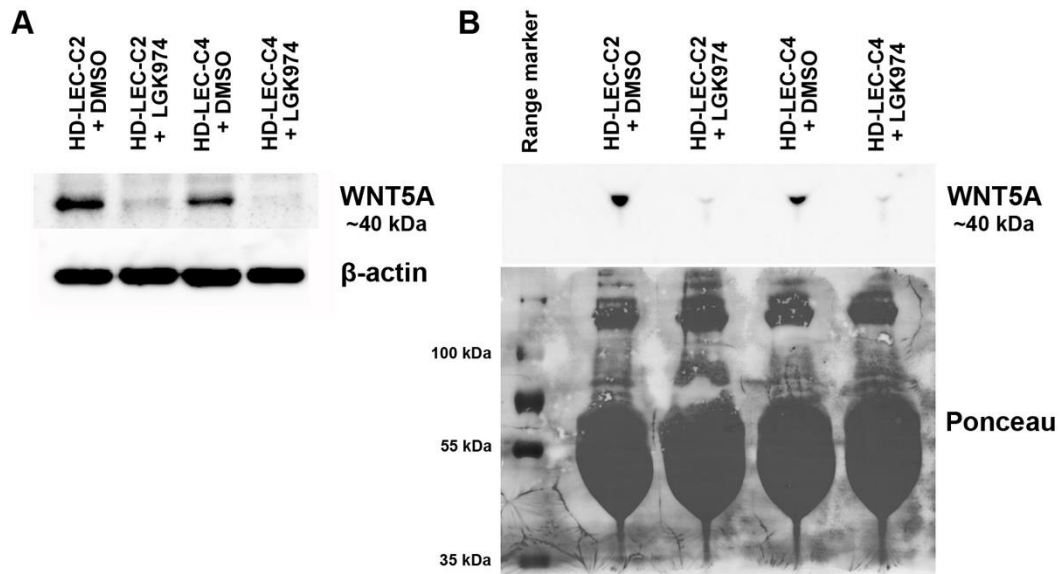


Figure 21: LGK974 inhibits WNT5A production and secretion. Western blot analysis of HD-LECs treated for 3 days with 10 μ M LGK974. Application of LGK974 reduces significantly the amount of WNT5A in cell lysates (**A**) and in supernatants (**B**). Both β -actin and Ponceau staining are shown as loading controls. Note the large fraction of BSA at 55 kDa in the Ponceau staining.

Because of the large BSA fraction in the supernatants, and due to the fact that it is not known how many active WNT proteins are present in serum, I also analysed supernatants of LECs treated with LGK974 under serum-free conditions. Therefore, I treated HD-LECs three times for 24 h with LGK974 in serum-free medium, pooled all collected supernatants and concentrated them. Again, under these conditions 10 μ M LGK974 significantly reduced both the amount of WNT5A in the cell lysates (**Figure 22A**) as well as the secretion of WNT5A (**Figure 22B**).

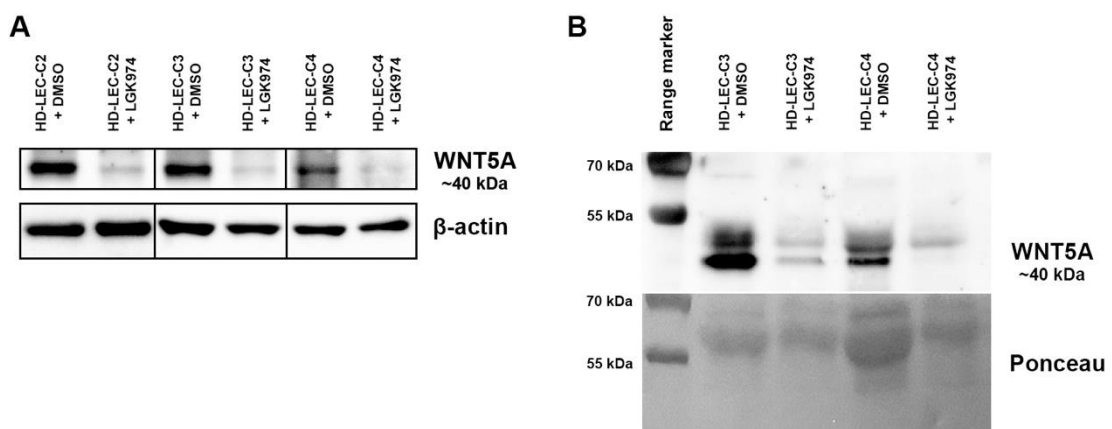


Figure 22: LGK974 inhibits WNT5A in serum-free conditions. Western blot analysis of HD-LECs treated three times for 24 h with 10 μ M LGK974. Application of LGK974 reduces significantly the amount of WNT5A in cell lysates (**A**) and in supernatants (**B**). Both β -actin and Ponceau staining were used as loading controls.

3.2.3 *In vitro* Angiogenesis Assays – Measuring the lymphangiogenic potential of lymphatic endothelial cells

Angiogenesis is the formation of new blood vessels from pre-existing vessels. It plays an important role in embryonic development, growth and wound healing. It plays also an important role in the malignancy of tumours. There are many *in vitro* angiogenesis assays which measure the main angiogenic mechanisms like sprouting, migration, proliferation and tube formation. I used three common assays and adopted them for LECs.

3.2.3.1 Spheroid Assay – Measuring the capability of sprouting

The spheroid assay was performed as described in 2.2.3.6. Initial assays were performed with lymphangioma-derived LY-LECs (LEC2). These were then diagnosed to have a monoallelic activating mutation of the *PIK3CA* gene (Blesinger et al., 2018). Therefore, in following experiments I used HD-LECs (LEC7) from a healthy donor.

3.2.3.1.1 Sprouting of LY-LECs is WNT-dependent

Spheroids of LEC2 were produced in round-bottom plates using serum-free EBM2, mixed with growth factor-reduced Matrigel and 25 μ M LGK974, 25 μ M WNT-C59 (PORCN inhibitors) or DMSO (as solvent control), and then transferred into 96 well plates. Photographs were taken after 0 h and 24 h, and the number of endpoints of the sprouts were counted with the *cell counter* plug-in of Fiji. Representative examples are shown in **Figure 23**. Quantification in **Figure 23D** shows that autocrine WNT-inhibition with Wnt-C59 and LGK974 inhibits the sprouting of LY-LECs significantly (Mann Whitney test, Wnt-C59: $p < 0.0001$, LGK974: $p < 0.0001$, $n \geq 6$ each).

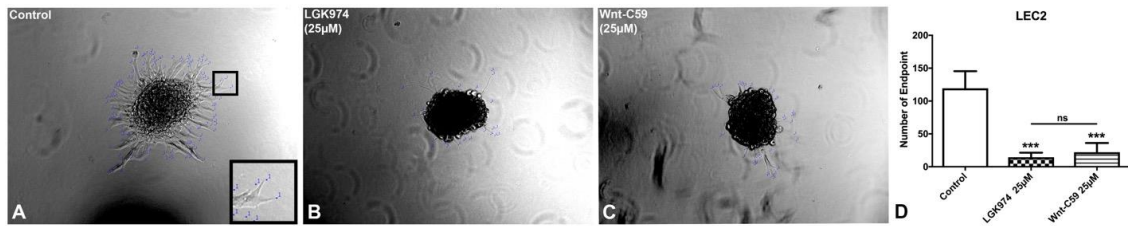


Figure 23: Spheroid assay with LEC2. (A-C) Representative pictures of LEC2 spheroid after 24 h. The spheroids were transferred in growth-factor reduced Matrigel with 25 μM LGK974 (B), 25 μM Wnt-C59 (C) or the corresponding amount of DMSO as control (A). The blue dots mark the counted endpoints. (D) For quantification, the number of endpoints of sprouts were counted. Application of LGK974 or Wnt-C59 reduced the number of endpoints of sprouts highly significantly (mean with SD, $n \geq 6$ spheroids; Mann Whitney test, $***p \leq 0.001$).

3.2.3.1.2 Sprouting of HD-LECs is VEGF-C-dependent

Since the PIK3CA is likely to interact with the WNT-pathway in a manner, which is not fully understood, I decided to switch from LY-LECs to healthy HD-LECs. First, I used the same experimental conditions as for LY-LECs, but no sprouting occurred (Figure 24A). I then tested different conditions and found that growth factors (from Matrigel), and especially VEGF-C, are necessary to induce sprouting of HD-LECs. In fact, no sprouting was visible in the absence of VEGF-C (Figure 24A, not quantified), and sprouting was significantly reduced when 250 ng VEGF-C were mixed with soluble VEGF-receptors (esVEGFR-2, sVEGFR-3), which can bind VEGF-C (Figure 24C and D, not quantified).

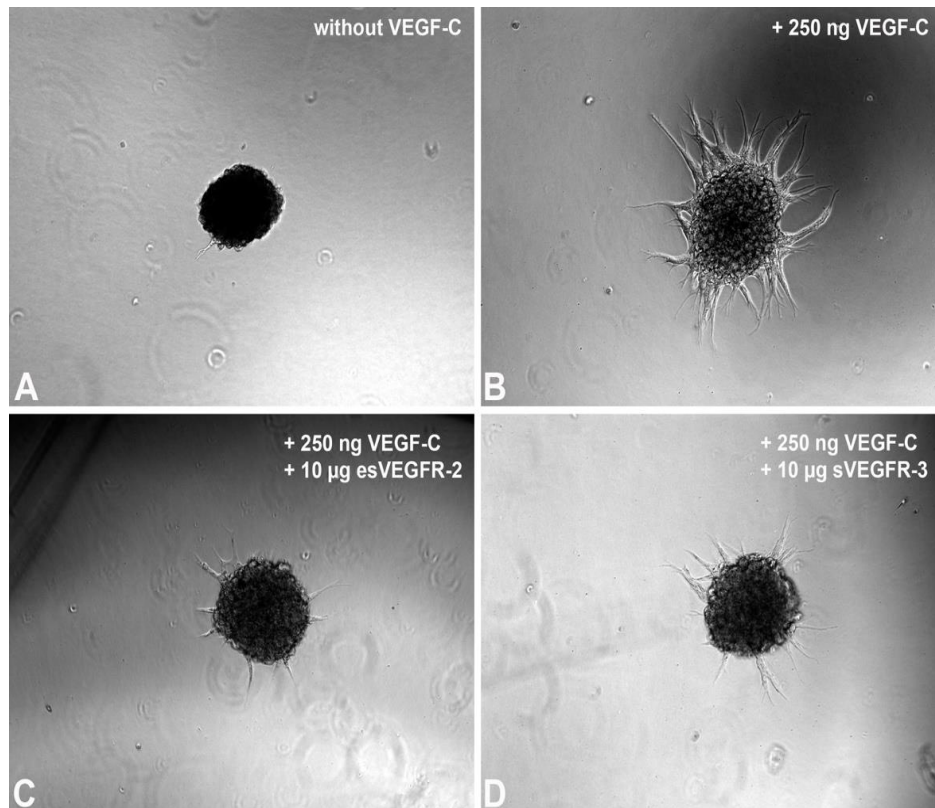


Figure 24: VEGF-C is essential for sprouting of HD-LECs. Spheroids were transferred in growth factor-reduced Matrigel and the influence of VEGF-C was examined after 24h. **(A)** No sprouting was visible in the absence of VEGF-C. **(B)** VEGF-C stimulates sprouting. **(C,D)** Soluble VEGF-Receptor-2 and -3 inhibit VEGF-C-induced sprouting.

3.2.3.1.3 Sprouting of HD-LECs is WNT-dependent

The next step was to analyse if WNTs play a role during sprouting of HD-LECs. Therefore, I transferred the HD-LECs in normal Matrigel with 250 ng VEGF-C. This induced the sprouting. I used the same PORCN inhibitors (Wnt-C59 and LGK974) like in 3.2.3.1.1, which inhibit the autocrine WNT-secretion. I observed that in HD-LECs WNTs play an important role during sprouting, because auto-crine WNT-inhibition with Wnt-C59 and LGK974 inhibits sprouting significantly (**Figure 25**).

For the quantification of sprouting of HD-LECs I designed a specific method, which allows not only the quantification of the number of sprouts, but also their length (see 2.2.3.6). **Figure 25D-I** shows the evaluation of WNT secretion-inhibited spheroids. Both, Wnt-C59 and LGK974 significantly reduced the number and length of sprouts (**Figure 25D-I**, $n = 21$ spheroids; Mann Whitney test:

Type 1: DMSO vs. LGK974 $p = 0.0042$, DMSO vs. Wnt-C59 $p = 0.0116$;
 Type 2: DMSO vs. LGK974 $p = 0.0009$, DMSO vs. Wnt-C59 $p = 0.002$;
 Type 3: DMSO vs. LGK974 $p < 0.00001$, DMSO vs. Wnt-C59 $p = 0.0002$;
 Type 4: DMSO vs. LGK974 $p = 0.0005$, DMSO vs. Wnt-C59 $p = 0.0005$;
 Type 5: DMSO vs. LGK974 $p = 0.4878$, DMSO vs. Wnt-C59 $p = 0.4878$;
 Total number: DMSO vs. LGK974 $p = 0.0011$, DMSO vs. Wnt-C59 $p = 0.0051$).
 Although LGK974 appeared to be more potent when used at the same concentration as Wnt-C59, this effect was not statistically significant (**Figure 25I**, $n = 21$ spheroids; Mann Whitney test, LGK974 vs. Wnt-C59 $p = 0.6994$).

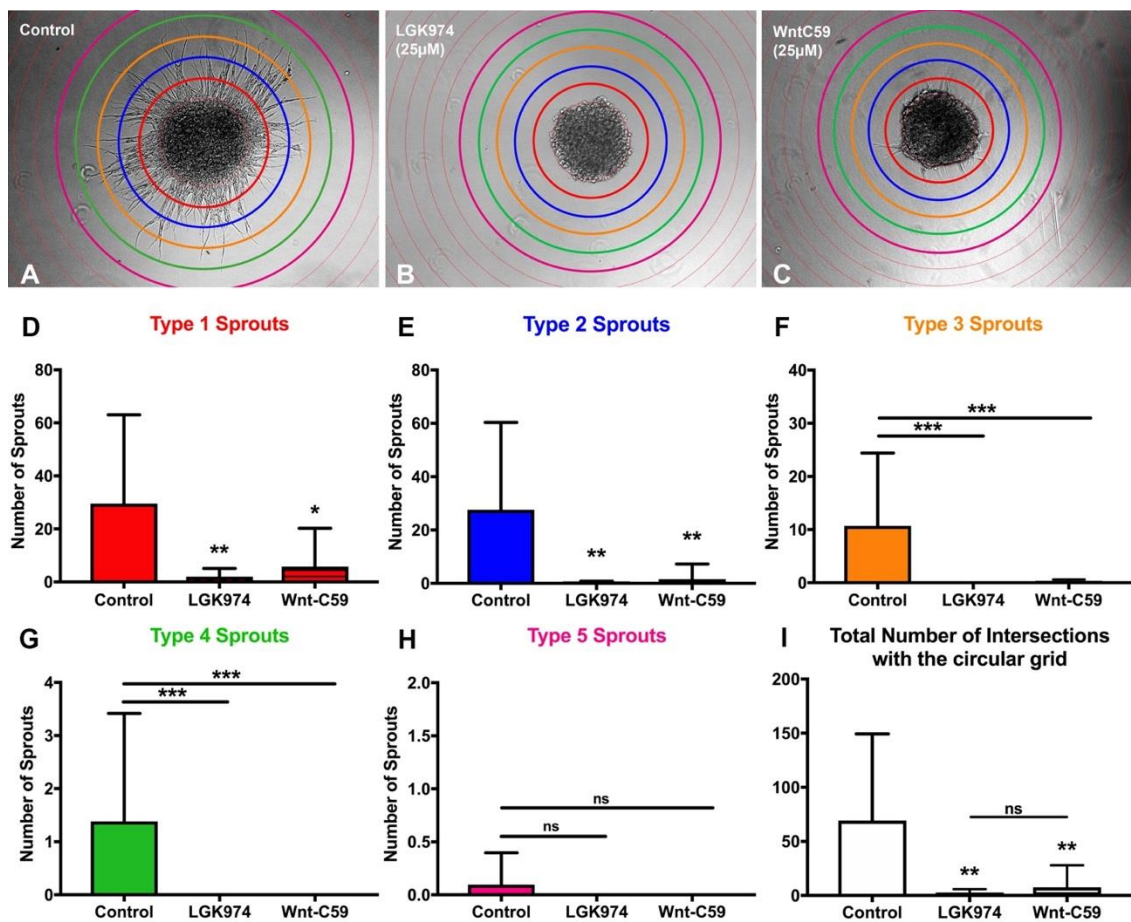


Figure 25: Sprout formation of HD-LEC-spheroids after inhibition of autocrine WNT-secretion. (A-C) Representative pictures of spheroids of HD-LECs after 24 h. Spheroids were grown in normal Matrigel supplemented with 250 ng VEGF-C. A circular grid was applied as described in (2.2.3.6). Effects of 25 μM LGK974 (**B**), 25 μM Wnt-C59 (**C**) or equal amounts of the solvent DMSO (**A**). (**D-I**) Quantification of sprouts crossing consecutive circles of the grid. The PORCN-inhibitors LGK974 (25 μM) or Wnt-C59 (25 μM) reduce sprout number and length significantly (mean with SD, $n = 21$ spheroids each; Mann Whitney test, * $p \leq 0.05$, ** $p \leq 0.01$, *** $p \leq 0.001$). *Type 1 sprouts*: as long as or longer than the half of the radius of the spheroid core (red), *Type 2 sprouts*: as long as or longer than the radius of the spheroid core (blue), *Type 3 sprouts*: as long as or longer than the 1.5-fold radius of the spheroid core (orange), *Type 4 sprouts*: as long as or longer than the 2-fold radius of the spheroid core (green), *Type 5 sprouts*: as long as or longer than the 2.5-fold radius of the spheroid core (magenta).

Next, I studied the effects of recombinant WNT5A protein in the spheroid assays. I used HD-LECs (LEC7) and tested if the application of recombinant WNT5A protein to the Matrigel counteracted the inhibitory effects of LGK974 or Wnt-C59, but this was not the case (**Figure 26**, not quantified, $n = 3$). However, it is likely that WNT5A protein did not readily penetrate the Matrigel to reach the cell surface. I therefore used scratch assays to study WNT5A effects.

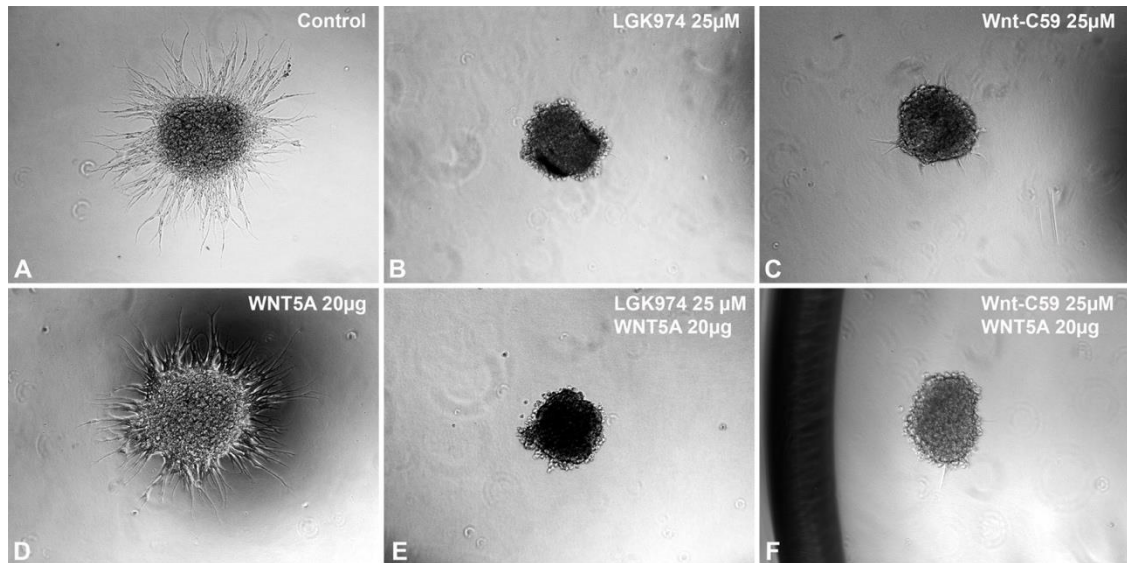


Figure 26: Application of recombinant WNT5A to HD-LEC-spheroids. Representative pictures of spheroids out of HD-LECs are shown. The spheroids were transferred in normal Matrigel with 250 ng VEGF-C and with 25 μ M LGK974 (**B**), 25 μ M Wnt-C59 (**C**) or the equal amount of DMSO as control (**A**). Application of recombinant WNT5A to the Matrigel did not alter sprout formation, neither alone (**D**), nor in inhibitor-treated spheroids (**E-F**).

3.2.3.2 Scratch Assays – Measuring horizontal migration of LECs

The scratch assay is a migration assay which measures horizontal migration of monolayers of cells. The assay was performed as described in 2.2.3.4. Normal, healthy HD-LECs (HD-LEC-C2, HD-LEC-C3, HD-LEC-C4) were used in these assays. I applied various inhibitors to examine the influence of WNT and WNT-related pathway members on the horizontal migration ability of HD-LECs. I used inhibitors that influence either the β -catenin-dependent signalling (via TCF and GSK3) or the β -catenin-independent WNT signalling (via ROCK, RAC and JNK).

3.2.3.2.1 Horizontal Migration of HD-LECs is controlled by WNT signalling

To examine if WNTs play a role during horizontal migration, I performed scratch assays. I applied the PORCN inhibitor LGK974 in two different concentrations (10 μ M and 25 μ M). Both concentrations inhibited migration significantly (**Figure 27 and Figure 28A**, $n \geq 33$ each; t-test, DMSO vs. LGK974 10 μ M $p = 0.0203$, DMSO vs. LGK974 25 μ M $p < 0.001$). In order to test if these effects might be induced by differences in proliferation, I performed proliferation assays as described in 2.2.3.3. The proliferation assays showed that after 24 h, when the scratch assays were analysed, there were absolutely no differences between the proliferation rates of the controls and the inhibitor-treated LECs (**Figure 28B and Table A-1**, $n \geq 21$ each; two-way ANOVA with Bonferroni post-hoc test, DMSO vs. LGK974 10 μ M $p = 0.9801$, DMSO vs. LGK974 25 μ M $p = 0.2515$). The assay also showed that HD-LECs possess a doubling time of approx. 36 h. Therefore, it is evident that the effects measured in the scratch assays after 24 h reflect alterations in migration, but not proliferation.

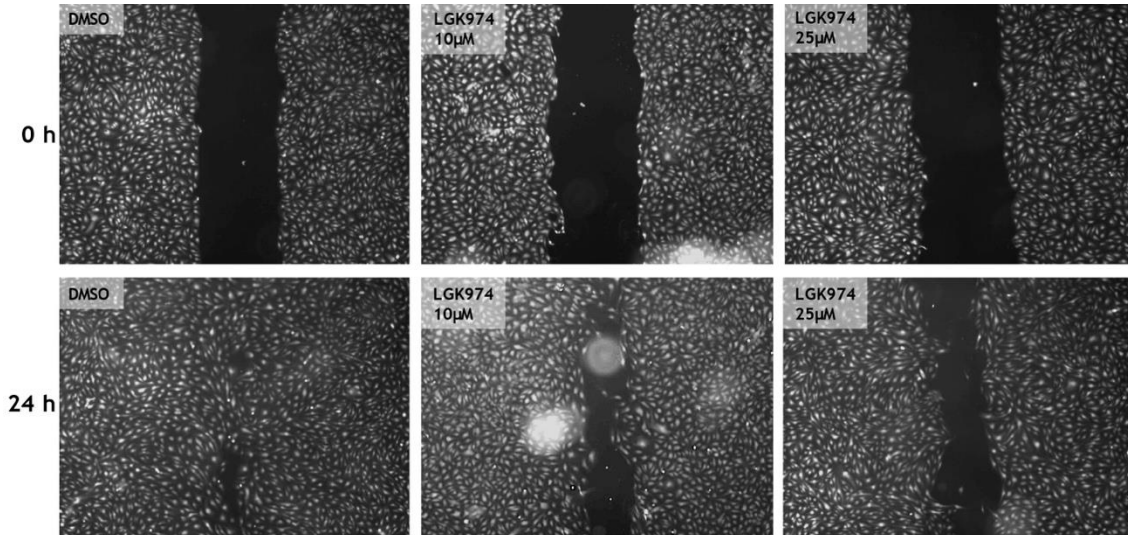


Figure 27: Inhibition of autocrine WNT-secretion of migrating HD-LECs. Representative pictures of scratch assays with HD-LECs treated with solvent or LGK974 in two concentrations (10 μ M and 25 μ M) after 0 h (upper row) and 24 h (lower row) are shown. Note inhibition of scratch closure by LGK974.

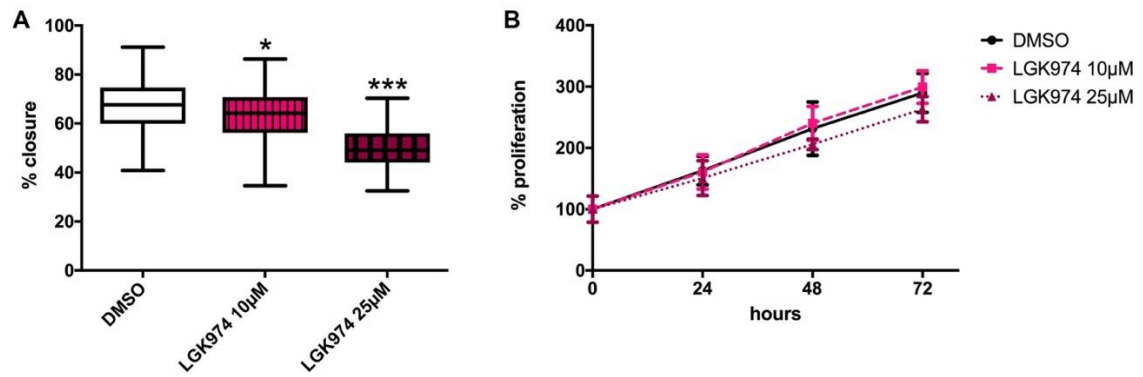


Figure 28: Influence of the inhibition of autocrine WNT-secretion on migration and proliferation of HD-LECs. (A) Scratch assay: Quantification of scratch closure by HD-LECs after application of two concentrations of LGK974 (10 µM and 25 µM) after 24 h. Percentage of scratch closure is shown. Inhibition of PORCN with LGK974 reduces migration significantly ($n \geq 33$ each; t-test, $*p \leq 0.05$, $***p \leq 0.001$). **(B)** Proliferation studies: After 24 h, 48 h and 72 h LGK974 treatment (10µM and 25µM) no differences occurred as compared to DMSO controls after 24 h (mean with SD, $n \geq 21$ each, two-way ANOVA with Bonferroni post-hoc test)

To test if WNT5A is the WNT family member that regulates migration, LGK974 pre-treated HD-LECs were used in scratch assays and stimulated with 500ng/ml recombinant WNT5A protein after the scratch was made. The results are shown in **Figure 29** and **Figure 30A**. The application of WNT5A stimulated migration significantly (t-test, LGK974^{pre} vs. LGK974^{pre} + WNT5A, $p = 0.0042$), although WNT5A was not able to rescue the inhibitor effects completely (t-test, DMSO vs. LGK974^{pre} + WNT5A, $p = 0.0058$). Best rescue effects of WNT5A were observed in LECs pre-treated with 10 µM inhibitor. Importantly, pre-treatment with 10 µM LGK974 and application of 500 ng/ml WNT5A to the cells did not influence proliferation (**Figure 30B** and **Table A- 2**, $n = 24$, two-way ANOVA with Bonferroni post-hoc test: DMSO vs. LGK974^{pre}: $p > 0.9999$, DMSO vs. LGK974^{pre} + WNT5A, $p > 0.9999$).

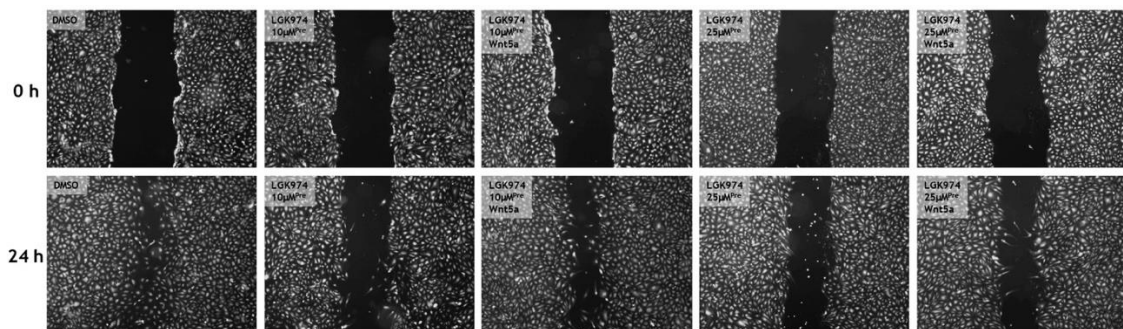


Figure 29: Scratch assay: Application of recombinant WNT5A to migrating HD-LECs. The cells were pre-treated with either 10 µM or 25 µM LGK974. After scratching, the cells were treated with constant amounts of LGK974 and 500 ng/ml recombinant WNT5A. Representative pictures after 0 h (upper row) and 24 h (lower row) are shown. Controls were performed with solvent DMSO.

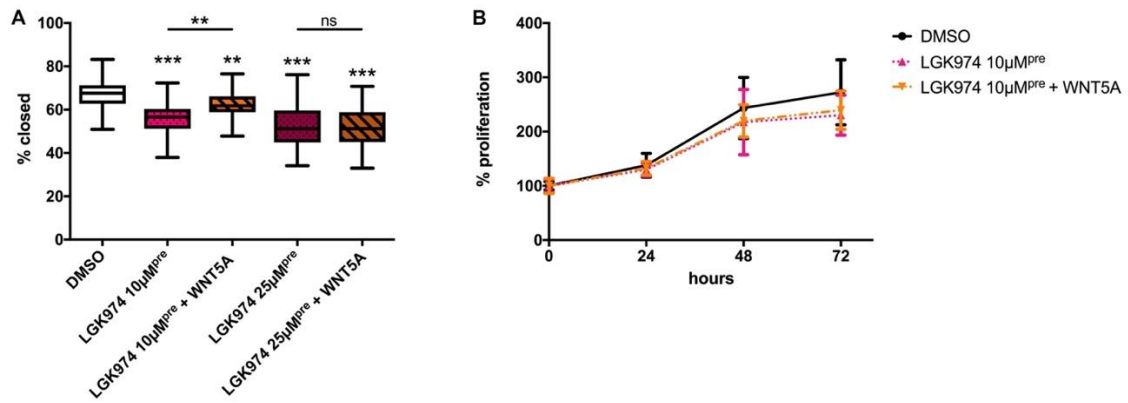


Figure 30: Effects of recombinant WNT5A protein on migration and proliferation of HD-LECs. (A) Quantification of scratch closure in scratch assays with HD-LECs. The cells were pre-treated with either 10 μ M or 25 μ M LGK974. After scratching, the cells were treated with constant amounts of LGK974 plus 500 ng/ml recombinant WNT5A. After 24 h the scratch closure rate was determined. Inhibition with 10 μ M LGK974 reduced migration significantly ($n \geq 26$ each; t-test, $***p \leq 0.001$), which was rescued by the application of 500 ng/ml WNT5A (t-test, LGK974^{pre} vs. LGK974^{pre} + WNT5A, $**p \leq 0.01$). Cells treated with 25 μ M LGK974 plus WNT5A showed no improvement of migration ($n \geq 27$ each; t-test, $***p \leq 0.001$). **(B)** Proliferation studies with LGK974 pre-treated HD-LECs after application of 500 ng/ml recombinant WNT5A for 24, 48 and 72 h as compared to DMSO controls (mean with SD, $n = 24$ each, two-way ANOVA with Bonferroni post-hoc test: no differences after 24 h). ns = not significant.

The results show that application of 25 μ M LGK974 had severe effects on LEC migration, which could not be rescued with WNT5A protein. In contrast, the effects of 10 μ M LGK974 could be significantly reversed by WNT5A.

3.2.3.2.2 Horizontal migration of HD-LECs is mediated through the planar-cell-polarity (PCP) pathway via RAC and JNK

In the next set of experiments, I sought to characterise which arm of the WNT pathway was specifically involved in the control of LEC migration. Therefore, I applied activators and inhibitors of both the β -catenin-dependent and the β -catenin-independent WNT pathways.

Firstly, I tested an inhibitor (FH535) and two activators (BIO and IM-12) of the β -catenin-dependent WNT pathway in the scratch assay. Results are shown in **Figure 31** and **Figure 32A**. FH535, an inhibitor of the β -catenin-dependent WNT signalling pathway that antagonises the β -catenin/TCF-mediated transcription, did not influence horizontal migration of HD-LECs ($n \geq 37$; t-test, DMSO vs. FH535: $p = 0.2168$, DMSO vs. Bio: $p < 0.0001$, DMSO vs. IM-12: $p = 0.0013$). In proliferation assays the used concentration of FH535 showed an inhibitory effect (**Figure 32B** and **Table A- 3**, $n \geq 23$, two-way ANOVA with Bonferroni post-hoc

test after 24 hours: DMSO vs. FH535: $p = 0.0161$). This is a clear proof that the scratch assay only measures migration but not proliferation effects.

Both activators Bio and IM-12 did not have a significant effect on proliferation after 24 hours (**Table A- 3**, $N \geq 23$, two-way ANOVA with Bonferroni post-hoc test, DMSO vs. Bio: $p = 0.2098$, DMSO vs. IM-12: $p > 0.9999$), but reduced migration of LECs significantly (**Figure 31** and **Figure 32A.**)

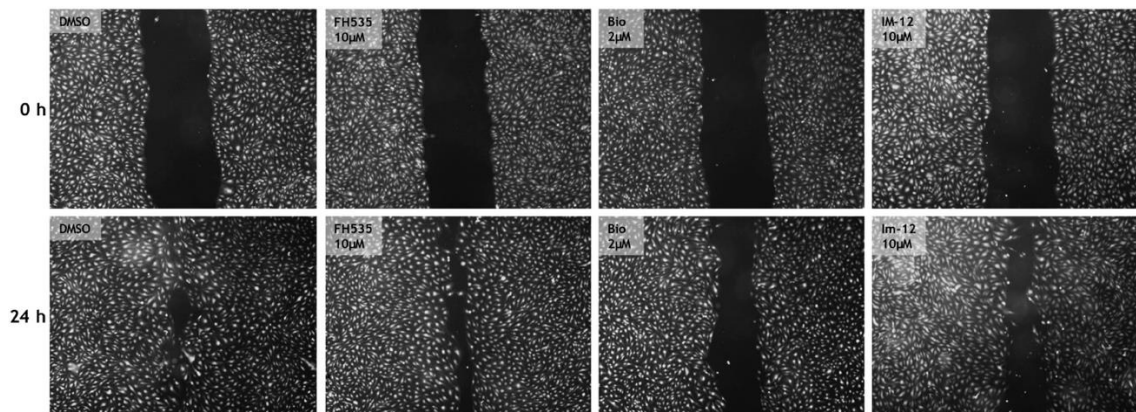


Figure 31: Is migration of HD-LECs mediated by β -catenin-dependent WNT signalling? Representative pictures of scratch assays with HD-LECs after 0 (upper row) and 24 (lower row) hours are shown. HD-LECs were treated with an inhibitor (FH535), and two activators (Bio and IM-12) of the β -catenin-dependent WNT signalling. Bio and IM-12 inhibit migration.

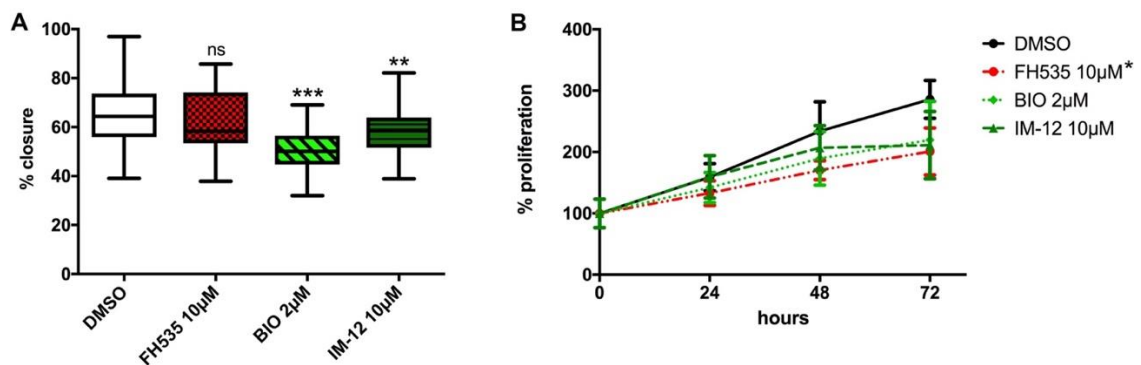


Figure 32: Activation of the β -catenin-dependent WNT signalling inhibits migration of HD-LECs, but does not influence their proliferation. (A) Quantification of the closed area in scratch assays with HD-LECs after application of FH535 (β -catenin-dependent WNT signalling inhibitor), Bio and IM-12 (β -catenin-dependent WNT signalling activators) after 24 hours. Percentage of closed area is shown. Activation of β -catenin-dependent WNT signalling with Bio and IM-12 reduces migration significantly ($n \geq 37$; t-test, $**p \leq 0.01$, $***p \leq 0.001$). **(B)** Proliferation studies with HD-LECs treated with FH535, Bio and IM-12 for 24, 48 and 72 hours compared to DMSO controls (mean with SD, $n \geq 23$, two-way ANOVA with Bonferroni post-hoc test: inhibition β -catenin-dependent WNT signalling decreases proliferation significantly after 24 h ($*p \leq 0.05$), whereas activation of β -catenin-dependent WNT signalling does not influence the proliferation after 24 h).

In the next step, I studied PCP-pathway-members in greater detail. Therefore, I also used small molecule inhibitors. The first pathway member I was interested in was ROCK. In many cases ROCK is involved in the regulation of migration (Riento and Ridley, 2003). I used two inhibitors (Y-27632 and Fasudil) and tested them in scratch assays with HD-LECs (**Figure 33** and **Figure 34A**). Both did not influence the migration of HD-LECs (**Figure 34A**, $n \geq 31$; t-test, DMSO vs. Y-27632: $p = 0.2904$, DMSO vs. Fasudil: $p = 0.3595$).

I also analysed these inhibitors in proliferation assays. Fasudil did not change the proliferation significantly (**Figure 34B** and **Table A- 4**, $n \geq 27$, two-way ANOVA with Bonferroni post-hoc test: DMSO vs. Fasudil: $p = 0.7906$), but Y-27632 inhibited the proliferation significantly after 24 hours ($n \geq 27$, two-way ANOVA with Bonferroni post-hoc test: DMSO vs. Y-27632: $p = 0.0069$).

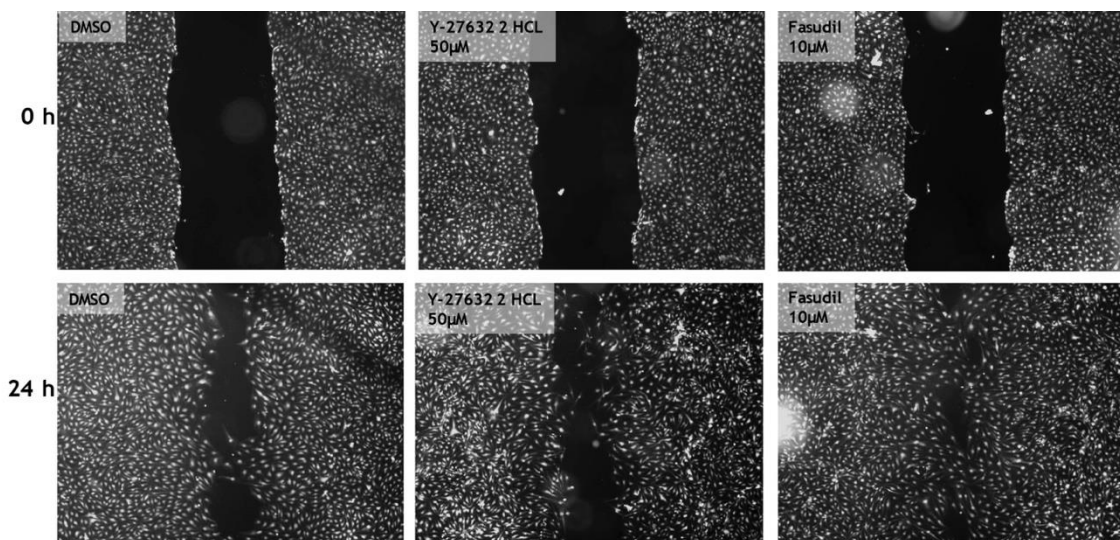


Figure 33: Migration of HD-LECs is independent of ROCK. Representative pictures of scratch assays with HD-LECs after 0 (upper row) and 24 (lower row) hours are shown. HD-LECs were treated with two ROCK inhibitors (Y-27632 and Fasudil) after scratching.

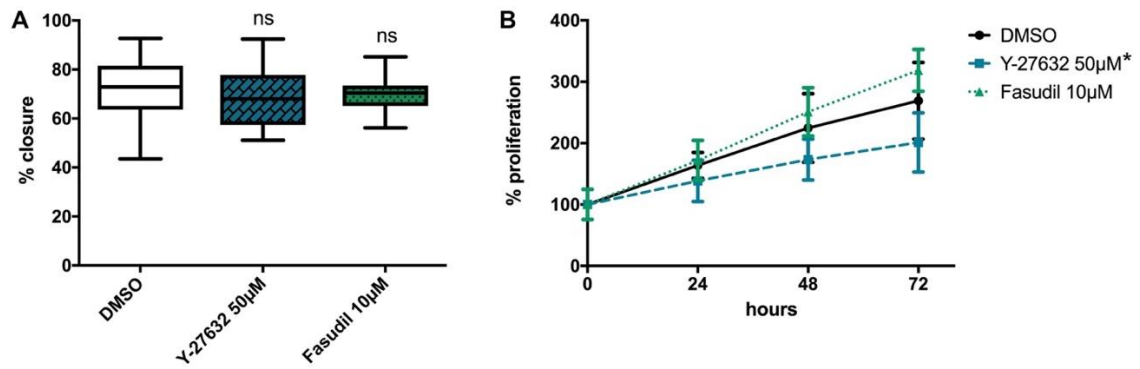


Figure 34: Horizontal migration of HD-LECs is independent of ROCK signalling. (A) Quantification of scratch closure of HD-LECs after application of the ROCK inhibitors Y-2763 and Fasudil after 24 h. Percentage of closure is shown. Inhibition of ROCK does not influence migration ($n \geq 31$; t-test, not significant). (B) Proliferation studies with HD-LECs treated for 24, 48 and 72 hours with Y-27632 and Fasudil compared to DMSO controls (mean with SD, $n \geq 27$, two-way ANOVA with Bonferroni post-hoc test: inhibition of ROCK with Y-27632 decreases proliferation significantly after 24 h ($*p \leq 0.05$), whereas Fasudil did not influence proliferation after 24 h).

The next PCP signalling molecule I was interested in was RAC. RAC is also known to be involved in the regulation of migration of several cell types (Sadok and Marshall, 2014). To investigate the influence of RAC on horizontal migration, I used two RAC inhibitors (EHT 1864 and NSC23766) in scratch assays and tested their influence on the migration of HD-LECs. The results are shown in **Figure 35** and **Figure 36A**. Both inhibitors significantly reduced the horizontal migration ($n \geq 33$; t-test, DMSO vs. EHT 1864: $p < 0.0001$, DMSO vs. NSC23766: $p < 0.0001$).

I also tested if the inhibitors had an influence on proliferation (**Figure 36B** and **Table A- 5**). EHT 1864 did not reduce proliferation after 24 hours ($n \geq 24$, two-way ANOVA with Bonferroni post-hoc test: DMSO vs. EHT 1864: $p = 0.0621$), but NSC23766 decreased proliferation significantly ($n \geq 24$, two-way ANOVA with Bonferroni post-hoc test: DMSO vs. NSC23766: $p = 0.0094$).

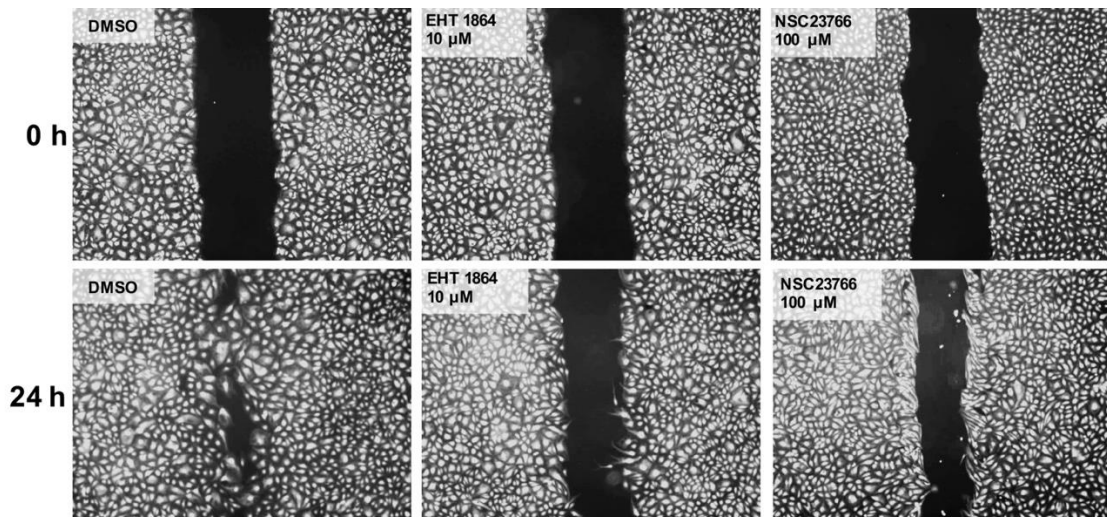


Figure 35: Migration of HD-LECs is RAC-mediated. Representative pictures of scratch assays with HD-LECs after 0 h (upper row) and 24 h (lower row) are shown. HD-LECs were treated with RAC inhibitors (EHT 1864 and NSC23766) after scratching. Both inhibited migration significantly after 24 hours.

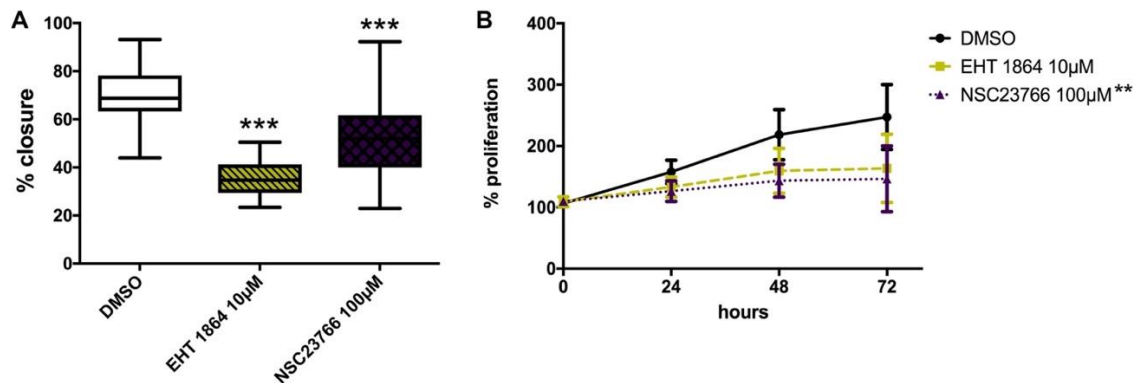


Figure 36: Horizontal migration of HD-LECs depends on RAC signalling. (A) Quantification of scratch assays with HD-LECs after application of the RAC inhibitors EHT 1864 and NSC23766 after 24 hours. Percentage of closure is shown. Inhibition of RAC significantly reduces migration ($n \geq 33$; t-test, $***p \leq 0.001$). (B) Proliferation studies with HD-LECs treated for 24, 48 and 72 hours with EHT 1864 or NSC23766 compared to DMSO controls (mean with SD, $n \geq 24$, two-way ANOVA with Bonferroni post-hoc test). Inhibition of RAC with EHT 1864 did not influence proliferation after 24 h, whereas inhibition of RAC with NSC23766 decreases proliferation significantly after 24 h, $**p \leq 0.01$.

JNK is a downstream signalling molecule of RAC. JNK is also often mentioned in the context of migration. So, my next step was to analyse if JNK influences the migration of HD-LECs. Therefore, I used two JNK inhibitors (SP600125 and JNK-IN-8) and analysed their influence on migration of HD-LECs in scratch assays. **Figure 37** and **Figure 38A** show the results. Both, SP600125 and JNK-IN-8 inhibited the horizontal migration of HD-LECs significantly ($n \geq 26$; t-test, DMSO vs. SP600125: $p < 0.0001$, DMSO vs. JNK-IN-8: $p < 0.0001$).

I also tested if the inhibitors would have an effect on proliferation (**Figure 38B** and **Table A-6**). Both inhibitors did not decrease proliferation significantly after

24 hours ($n \geq 31$, two-way ANOVA with Bonferroni post-hoc test: DMSO vs. SP600125: $p = 0.8913$; DMSO vs. JNK-IN-8: $p > 0.9999$).

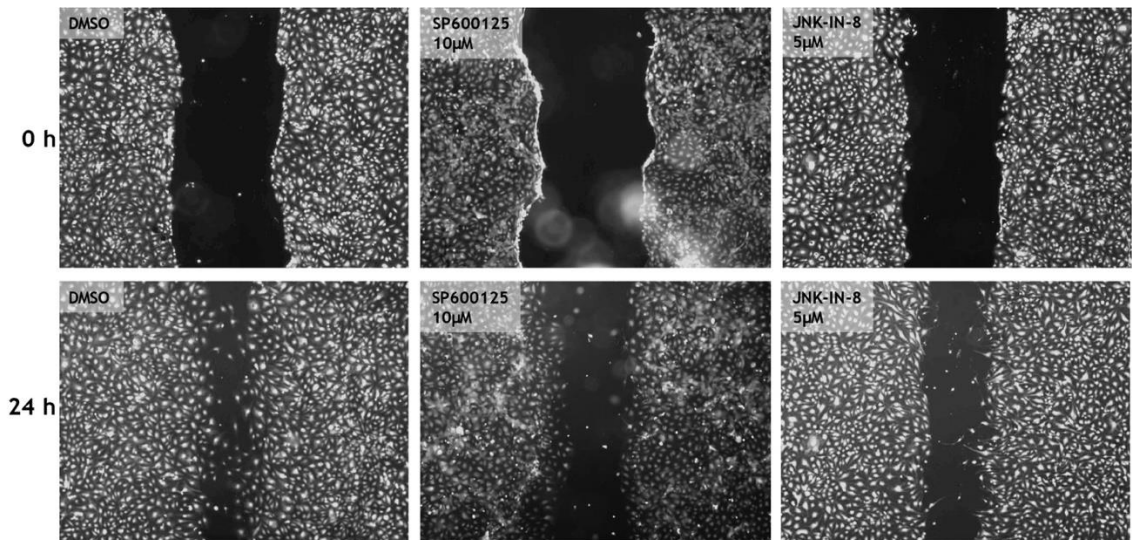


Figure 37: Migration of HD-LECs is JNK-mediated. Representative pictures of scratch assays with HD-LECs after 0 h (upper row) and 24 h (lower row) are shown. HD-LECs were treated with JNK inhibitors (SP600125 and JNK-IN-8) after scratching, and both inhibited the migration.

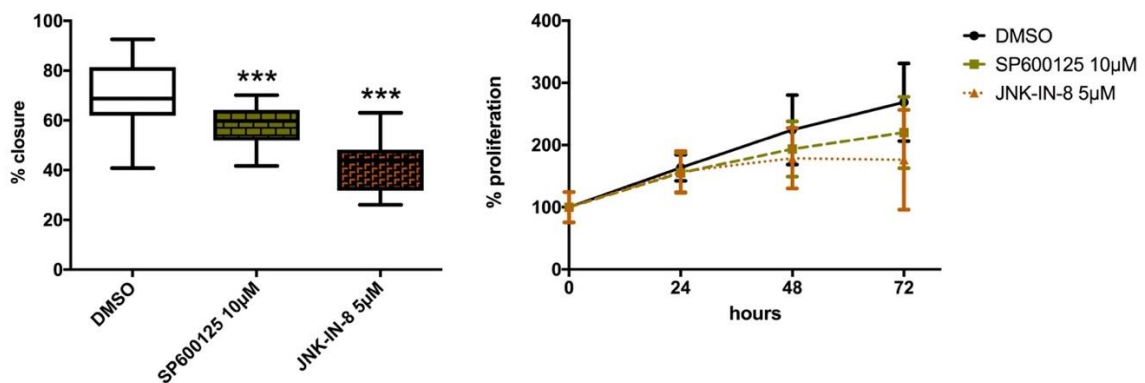


Figure 38: Horizontal migration of HD-LECs depends on JNK signalling. (A) Quantification of scratch assays with HD-LECs after application of the JNK inhibitors SP600125 and JNK-IN-8 after 24 hours. Percentage of closure is shown. Inhibition of JNK significantly reduces the migration ($n \geq 26$; t-test, $***p \leq 0.001$). (B) Proliferation studies with HD-LECs treated for 24, 48 and 72 hours with SP600125 and JNK-IN-8 compared to DMSO controls (mean with SD, $n \geq 31$, two-way ANOVA with Bonferroni post-hoc test) Inhibition of JNK did not influence proliferation after 24 h.

3.2.3.3 WNT5A induces phosphorylation of JNK

The migration studies of HD-LECs with scratch assays had shown that horizontal migration of the cells is mediated by RAC and JNK. To analyse if WNT5A can directly activate the JNK pathway by inducing JNK phosphorylation, I studied

LGK974-pre-treated HD-LECS and stimulated them with 500 ng/ml recombinant WNT5A. I prepared cell lysates and studied Western blots for JNK phosphorylation. Since the supplementation of the growth medium with FBS led to an overall phosphorylation of JNK, I starved the cells for 24 h in serum-free medium before the WNT5A application. The results clearly show that WNT5A induced a strong phosphorylation of JNK after 15 and 30 minutes, whereas after 2 h the level of phosphorylation was nearly back to the initial value (**Figure 39**). This shows explicitly that WNT5A is a potent activator of JNK in HD-LECs.

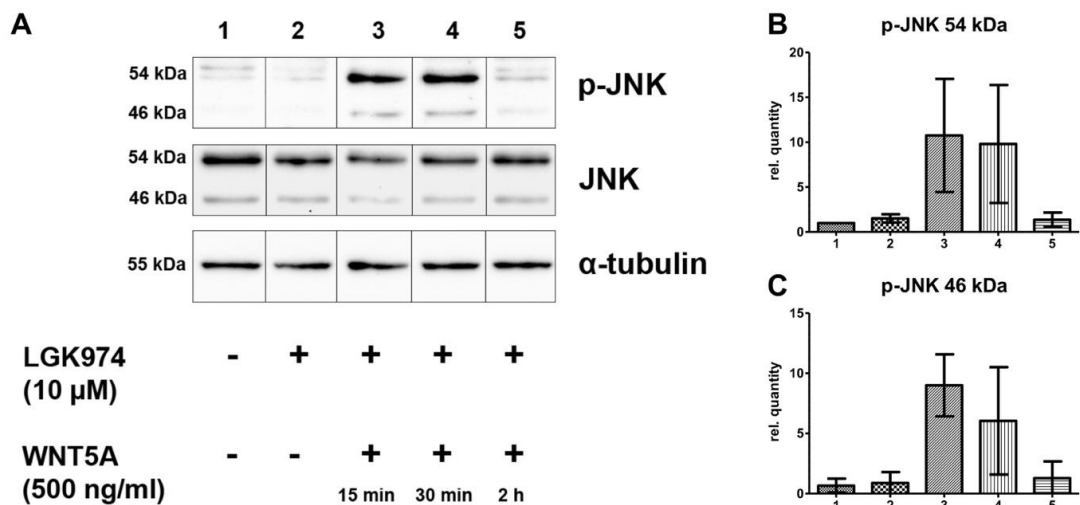


Figure 39: WNT5A induces phosphorylation of JNK in HD-LECs. Western blot analysis of HD-LEC lysates. HD-LECs were treated with LGK974 for 3 d and starved for 24h in serum-free medium before WNT5A application. **(A)** Application of 500 ng/ml WNT5A induces a transient phosphorylation (p) of JNK (lanes 3-5). α -tubulin was used as loading control. **(B, C)** Relative quantification of p-JNK at 46 kDa and at 54 kDa. (Mean \pm SD from 3 independent experiments). Note that WNT5A induces a transient phosphorylation of JNK after 15 min and 30 min (lanes 3 and 4).

3.2.3.4 Tube Formation Assay – WNT5A increases network formation

The tube formation assays were performed as described in 2.2.3.5. Normal, healthy HD-LECs (HD-LEC-C2, HD-LEC-C3, HD-LEC-C4) were used and pre-treated with 10 μ M LGK974 for 3 days. For better visibility, cells were labelled with CellTracker. The results are shown in **Figure 40**. LGK974 alone induced network formation (n = 15; DMSO vs. LGK974: cell-covered area: Mann Whitney test: p = 0.0063, number of tubes: t-test: p < 0.0001, total length of tubes: t-test:

$p = 0.0004$ and number of branching points: t-test: $p = 0.0003$), which was an unexpected result. However, application of WNT5A to the inhibited cells significantly improved all measured aspects of network formation like cell-covered area ($n = 15$; DMSO vs. LGK974 + WNT5A: Mann Whitney test: $p < 0.0001$), number of tubes ($n = 15$; DMSO vs. LGK974 + WNT5A: t-test: $p < 0.0001$), total length of tubes ($n = 15$; DMSO vs. LGK974 + WNT5A: t-test: $p < 0.0001$), and number of branching points ($n = 15$; DMSO vs. LGK974 + WNT5A: t-test: $p < 0.0001$). This is also the case for the comparison to the inhibited cells ($n = 15$; LGK974 vs. LGK974 + WNT5A: cell-covered area: Mann Whitney test: $p = 0.0059$, number of tubes: t-test: $p = 0.0118$, total length of tubes: t-test: $p = 0.0021$ and number of branching points: t-test: $p = 0.02$).

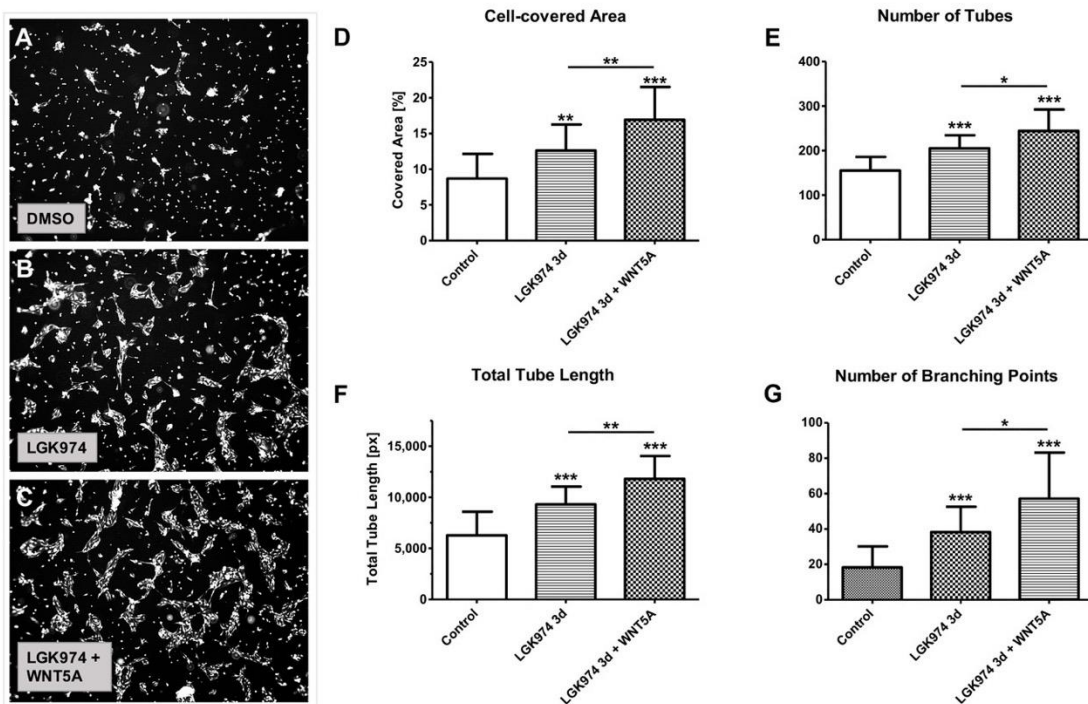


Figure 40: WNT5A increases network formation. (A-C) Representative pictures of tube formation assays with HD-LECs 9 hours after seeding. Quantification revealed a significant increase in cell-covered area (D), number of tubes (E), total length of tubes (F) and number of branching points after autocrine WNT-inhibition with 10 μ M LGK974 (for 3 days), and after application of 500 ng/ml recombinant WNT5A to the pre-treated cells compared to the solvent control. Note the significant increase of all parameters after WNT5A application ($n = 15$; Mann Whitney test (D) or t-test (E-F), * $p \leq 0.05$, ** $p \leq 0.01$, *** $p \leq 0.001$).

3.2.4 mRNA sequencing analyses of LGK974-treated HD-LECs

Next, I was interested in the genes that were regulated by WNTs in HD-LECs. Therefore, I worked together with the Transcriptome and Genome Analysis Laboratory (TAL) of the UMG, Göttingen. We performed stranded mRNA sequencing (mRNAseq) of LGK974-treated vs. non-treated (control) HD-LECs (each three HD-LEC lines with two samples each). The treatment group received the application of 10 μ M LGK974 for three days to inhibit autocrine WNT signalling and the controls received equal amounts of the solvent DMSO. All cells were grown in MV2 with 5% FBS. The corresponding gene sets were compared and differentially regulated genes in HD-LECs without autocrine WNT signalling were depicted. This led to the identification of 116 genes differently regulated in the treatment group. The top 50 regulated genes are presented in **Figure 41**. The whole list of genes is shown in **Table A-7** in the appendix.

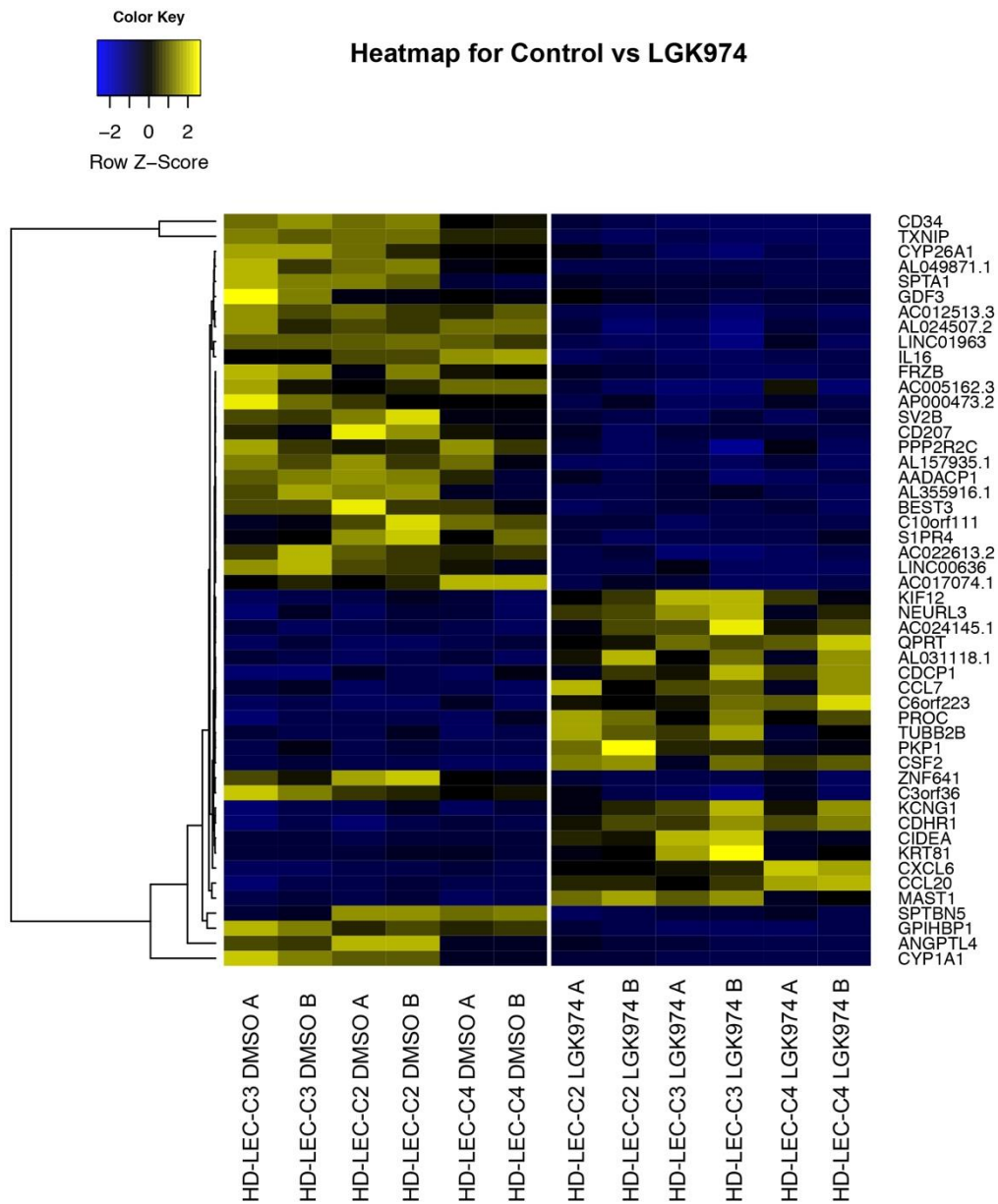


Figure 41: Heatmap of the top 50 differentially expressed genes in HD-LECs treated with 10 μ M LGK974 compared to DMSO controls. Log₂ fold-change is shown.

The obtained data set was also used for a gene set enrichment analysis (GSEA) with a tool from the Broad Institute (<http://software.broadinstitute.org/gsea/>). Three gene sets were overrepresented in the gene list and belonged to the gene ontology terms (GO)/gene sets: “GO: response to an external stimulus”, “GO: movement of cell or subcellular component” and “GO: extracellular space” (**Table 11**).

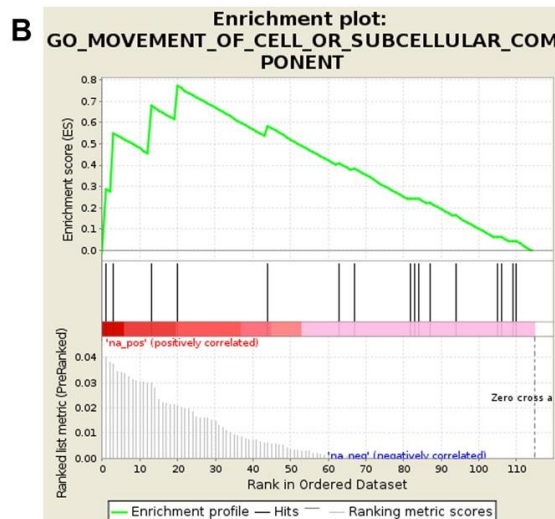
Table 11: Results of the GSEA. Three gene sets are overrepresented in the gene list control vs. LGK974-treated.

NAME	SIZE	ES	NES	NOM p-val	FDR q-val	FWER p-val	RANK AT MAX
GO_MOVEMENT_OF_CELL_OR_SUBCELLULAR_COMPONENT	16	0.7705442	11.934.462	0.0	0.0	0.0	20
GO_RESPONSE_TO_EXTERNAL_STIMULUS	17	0.68736356	10.571.826	0.3	0.45000002	0.7	13
GO_EXTRACELLULAR_SPACE	17	0.6336669	0.9820182	0.6	0.5333334	0.9	27

Especially the “GO: movement of cell or subcellular component” appeared to be of great interest, because it revealed down-regulation of migration-related transcripts after the application of LGK974, which is in line with my experimental studies (**Figure 43**).

A

Dataset	Control_vs_Treatment
Phenotype	NoPhenotypeAvailable
Upregulated in class	na_pos
GeneSet	GO_MOVEMENT_OF_CELL_OR_SUBCELLULAR_COMPONENT
Enrichment Score (ES)	0.7705442
Normalized Enrichment Score (NES)	1,1934462
Nominal p-value	0
FDR q-value	0
FWER p-Value	0



C

PROBE	RANK IN GENE LIST	RANK METRIC SCORE	RUNNING ES	CORE ENRICHMENT	UP REGULAEAD	DOWN REGULATED
IGF1	1	0.039900001138448715	0.28523463	Yes		x
CYP1B1	3	0.03700000047683716	0.5490038	Yes		x
FPR3	13	0.0296999983906746	0.67793095	Yes	x	
KLC3	20	0.02070000022649765	0.7705442	Yes	x	
KIF4B	44	0.00590999832510948	0.5819661	No		x
VAV1	63	9,97E+11	0.40752763	No	x	
CCL7	67	7,18E+11	0.38253915	No	x	
PROC	82	4,81E+11	0.24148105	No	x	
KIF12	83	4,81E+11	0.24183708	No	x	
SPTA1	84	4,61E+10	0.2421783	No		x
SPTBN5	87	2,80E+11	0.22218354	No		x
TUBB2B	94	5,23E+09	0.16161619	No	x	
CCL20	105	1,57E+03	0.060606092	No	x	
CXCL6	106	4,29E+02	0.060606092	No	x	
IL16	109	1,24E-01	0.04040407	No		x
CD34	110	1,24E-01	0.04040407	No		x

Figure 42: GSEA for the gene set “Movement of cell or subcellular component”. (A) Results of the GSEA for the gene set “Movement of cell or subcellular component”. (B) Enrichment plot. (C) Overrepresented genes in the gene set “Movement of cell or subcellular component”.

3.2.4.1 Validation of WNT-regulated genes in LECs by qRT-PCR

Three genes (IGF1, SPTA1, and SPTBN5) of the gene set “Movement of cell or subcellular component” caught our special attention. Insulin-like growth factor 1 (IGF-1) is a hormone that has an important role in the growth of the musculo-skeletal system, as exemplified by the fact that mutations in the gene and its receptors cause the Laron Syndrome (mainly visible as dwarfism; reviewed in Laron (2004)). SPTA1 and SPTBN5 encode for spectrins, which are cytoskeletal proteins important for stability of the cell membrane and migration.

To validate the results of the mRNAseq analysis, I repeated the experiments and treated the three HD-LEC lines again for three days with 10 μ M LGK974 (vs. controls) and analysed the expression of IGF1, SPTA1 and SPTBN5 with qRT-PCR. The results are shown in **Figure 43**. This analysis confirmed the mRNAseq results. All three genes were down-regulated in the probes, which were treated with LGK974 for autocrine WNT inhibition.

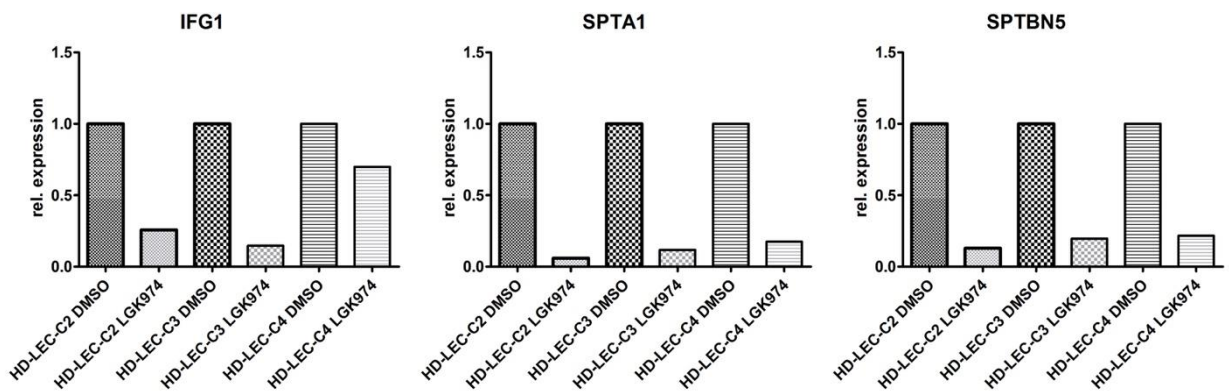


Figure 43: Validation of the mRNAseq analysis with qRT-PCR. In a second round, HD-LECs were treated in the same way as for mRNAseq analysis and investigated with qRT-PCR. Treatment with 10 μ M LGK974 led to a down-regulation of the three investigated genes.

4 Discussion

Wnt signalling is an important regulator of angiogenesis. In several studies, it has been shown that many Wnt ligands, their receptors and co-receptors, and also several other Wnt-related molecules play essential roles during the development and growth of the blood vascular system (reviewed in: Dejana (2010); Olsen et al. (2017)). And a small number of studies has also shown that Wnts play important roles in the regulation of lymphangiogenesis (e.g. Buttler et al., 2013; Cha et al., 2016; Muley et al., 2017), but the mechanisms how they regulate the behaviour of lymphatic endothelial cells remained unclear.

In my thesis, I have been able to show that dermal lymphatics of murine embryos exhibit several Wnt-related molecules and that Wnts and especially Wnt5a are important for their development. In my *in vitro* studies, I could show that this holds true also for human lymphatic endothelial cells (LECs), where WNTs have essential functions in the regulation of angiogenic processes like sprouting, migration and tube formation. Thereby, I could show that WNT5A mediates horizontal migration via RAC and JNK. And finally, my global analyses of WNT-regulated genes have shown that WNTs control divers of angiocrine pathways in LECs.

4.1 Development of murine dermal lymphatics is Wnt5a-mediated

That Wnts are important for the development and function of blood and lymphatic vessels in mice has been shown in previous studies. For example, Wnt signalling is needed for the precise vascular patterning in organs and the remodelling and organization of the vasculature in murine embryos (Cattelino et al., 2003; Corada et al., 2010; Descamps et al., 2012). Korn et al. (2014) have shown that in mice with EC-specific deletion of the pan-Wnt-secretion factor Evenness Interrupted (Evi; also known as Wntless, Wls), the regulation of endothelial cell survival, proliferation and the vascular density are defective. The cell-specific knock-out of

WIs in myeloid cell revealed that Wnts are important for normal development of dermal lymphatics (Muley et al., 2017). Additionally, Wnt signalling controls the correct formation of lymphatic and lymphovenous valves (Cha et al., 2016) and can directly interact with Vegf-C, the vascular endothelial growth factor with high specificity for lymphatics (Niederleithner et al., 2012; Sessa et al., 2016). Among the 19 WNT ligands, Wnt5a has a special significance for the development of blood and lymphatic vessels, which has been shown in studies of mice (Buttler et al., 2013; Muley et al., 2017), and in human ECs (Cheng et al., 2008; Cirone et al., 2008; Masckauchan et al., 2006).

The mouse-related part of my thesis based mainly on previous observations of our lab, published by Buttler et al. (2013). There it was shown that Wnt5a is an important regulator of lymphangiogenesis of dermal lymphatics. They analysed the initial lymphatics of Wnt5a-null-mice and noted that these vessels were massively dilated. Compared to the dermal lymphatics of the healthy wild-type littermates the number and diameter of the vessels were significantly altered in the Wnt5a-null-mice. The authors concluded that these effects occurred due to a morphogenesis defect but not due to proliferation defects, since the number of LECs and the total vessel-covered area were not significantly altered in ED 18.5 embryos.

To examine these findings in greater detail, I characterised the expression of several Wnt-related molecules in dermal lymphatics of embryonic mice using immunofluorescence staining, analysed the function of initial lymphatics and lymphatic collectors in earlier developmental stages, and used a new *ex vivo* assay to study the influence of activators and inhibitors of Wnt-signalling on lymphangiogenesis in embryonic murine dermis.

My immunofluorescence staining with several antibodies revealed that the dermal lymphatics of mice express Wnt5a, Fzd5, Fzd8 and Vangl2. My findings are in line with previous results of our lab, who have shown in tissue slices that LECs are positive for Wnt5a. My staining results also support their findings that LECs show a stronger expression of Wnt5a than BECs (Buttler et al., 2013).

The expression of Fzd5 and Fzd8 is in line with findings of other studies, which demonstrate that Fzds are typical receptors for Wnts (Niehrs, 2012). Thereby, Fzd5 is a high-affinity receptor for Wnt5a (Dijksterhuis et al., 2015; Xi He et al., 1997), which is supported by the Reference sequence (RefSeq) database (RefSeq, Jul 2008; (O'Leary et al., 2016)). The expression of Fzd receptors on many cell types is not surprising due to the fact that Wnt signalling is a complex system, and it has been shown for many cell types in the dermis that they communicate via Wnt signalling.

Vangl2 is a protein with important functions in planar-cell-polarity (PCP). It transmits directional signals to individual cells or groups of cells in epithelial sheets (Findlay et al., 2016; Gao et al., 2018). LECs are also organised as epithelial sheets, and their directed migration seems to be a prerequisite for lymphangiogenesis.

I also strengthened the functional analysis of Buttler et al. (2013) with further fluorescence microlymphangiographic studies of younger mouse embryos. I could show that in mice of ED 17.5 the lymphatic vascular system is functional, and that in Wnt5a-null-mice of this age interstitially injected FITC-dextran is not transported centripetally. Thereby, I could demonstrate that mice possess functional superficial lymphatic collectors in the dermis of the trunk, which connect the axillary with the inguinal region. This interconnexion is the reason why metastases of tumours placed on the hip of nude-mice are regularly found in axillary lymph nodes. In the human, comparable collectors do not exist.

In a new *ex vivo* assay I analysed if WNT5A is capable of rescuing the phenotype of dermal lymphatics that occurred through the general loss of the *Wnt5a* gene. The application of recombinant WNT5A protein to *ex vivo* cultures of dermis from ED 15.5 Wnt5a-null mice induced a flow-independent development from an immature plexus into a slender, elongated lymphatic network after two days. This maturation was measurable (significant reduction of vessel-covered area) and characterized by thinner and longer vessels, with less but larger “loops” and longer interconnections. The cell shape in the vessels changed from round in immature to elongated and longitudinally directed in the mature vessels.

Working with dermal specimens from Wnt5a-null mice was difficult, because of their soft and oedematous texture. Many of the specimens showed a strong background after whole-mount immunostaining with anti-Lyve-1 antibody, and finally, only one-fifth of the specimens could in the end be used for quantification in comparison to the non-treated controls of the contra-lateral side. Although the number of quantified specimens was low, results were statistically significant, and, as shown in the representative pictures, the changes were very obvious.

With the same type of assay, I also did a reverse experiment. I used the small molecule PORCN inhibitor LGK974, which prevents secretion of all Wnt proteins, and applied it to wt-mouse dermis. I used two concentrations and the higher one (50 μM) induced significant changes. The dermal lymphatic vessels of the untreated specimens were more mature. They were thin and only a small number of "loops" and interconnections between individual vessels were present. While the specimens treated with the lower concentration (25 μM) only occasionally showed immature "loops", the ones treated with the higher concentration regularly presented with large-diameter vessels with numerous immature "loops" and connections between neighbouring vessels. I interpret the emerge of larger vessel diameters with more and smaller "loops" as a deceleration or stop of maturation.

The defects of the dermal lymphatics in Wnt5a-null mouse embryos seem to occur through a failure during the elongation of the lymphatics during maturation or through a failure of connectivity of the lymphatic vessels. This results in an immature lymphatic plexus and the frequent formation of isolated cyst-like lymphatics, which I could demonstrate by whole-mount staining of dermal lymphatics with Lyve-1 antibody.

My findings suggest that during lymphangiogenesis Wnts have the same or similar functions as during early embryogenesis, e.g. during gastrulation. There, the effects of Wnts have been summarized as 'convergent extension' (Djiane et al., 2000; Topczewski et al., 2001). This describes the migration of cells towards each other, followed by movements that result in the elongation of a structure, e.g. the primitive streak.

The convergence of angioblasts and the extension of a primitive vascular plexus into a network are important mechanisms during both (haem)angiogenesis and lymphangiogenesis. It has been shown that haemangioblasts emerge from various extra- and intra-embryonic compartments, assemble (converge and build the so-called blood islands), extend into vascular tubes and form a primitive vascular plexus. The lumen of the early vessels is very wide, so they have been assigned as sinusoidal, primary or 'primitive'. A variety of mechanisms take place in the further development of the vascular plexus, like the integration of more angioblasts (convergence), fusion of vessels, sprouting, splitting and intussusception (Jain, 2003; Risau, 1997; Wilting et al., 1995). Elongation of vessels (extension) is also a widely observed mechanism, but has mostly been called vascular branching, pruning, and remodelling (Ribatti, 2006; Risau, 1997).

The same mechanisms obviously also take place during lymphangiogenesis. There lymphangioblasts, either originating from veins or from mesenchymal sources (e.g. Martinez-Corral et al., 2015) assemble (converge) into primary lymphatic networks, which mature (elongate, extend) into lymphatic capillaries and collectors. A function for Wnt-signalling during lymphangiogenesis has been noted earlier (Buttler et al., 2013; Dejana, 2010; Nicenboim et al., 2015), but the significance of convergent extension movements for lymphangiogenesis has not been discussed before. My studies clearly support the importance of these mechanisms. In the dermal lymphatics of *Wnt5a*-null-mice these mechanisms are disturbed. Similar defects could also be found in the dermal lymphatics of *Wnt5a*-null-mice after *ex vivo* culturing. There, the application of WNT5A normalised lymphangiogenesis, and induced elongation of LECs.

4.2 WNT signalling potential of human lymphatic endothelial cells

To analyse the potential of WNT signalling during lymphangiogenesis in humans, I first characterised human, foreskin-derived and lymphangioma-derived LECs. Therefore, I used immunocytology, qRT-PCR and Western blot analyses.

With anti-PROX1 and anti-CD31 staining of LECs I could demonstrate that the cells, which were used in all following studies, are LECs, and not BEC or fibroblast, which may contaminate the cultures during the isolation process. In the next step, I analysed three human dermal (HD)-LEC lines by qRT-PCR and investigated the mRNA expression of WNT-related molecules. I used a pool of neuroblastoma cell lines, BECs and LECs as positive control. It has been shown that WNT signalling is high in many neuroblastoma cell lines (Jürgen Becker and Wilting, 2018), and Buttler et al. (2013) have previously shown that BEC and LY-LECs also express several WNT-related molecules. The analysed HD-LECs show a wide variety of WNT-related mRNAs, and many of these could be verified at protein level with Western blots and immunocytology. Because of the fact that WNT5A is often found in the context of PCP, I was mainly interested in molecules that belong to the PCP pathway, and, in fact, many of them are expressed in HD-LECs. I could also clearly confirm that HD-LECs express WNT5A.

In e.g. *Drosophila* and mouse it has been shown that some PCP-molecules are expressed in a polarized manner. Thereby, Fzd and Vangl can form a so-called Fzd/PCP core complex (or Fzd-Vangl/PCP module in vertebrates). In general, Fzd and Vangl are localised at opposite cell membranes, and the two molecules interact with each other across neighbouring cells. There are also antagonistic effects of both molecules in the cell, which stabilises their polarized expression (reviewed in: Y Yang and Mlodzik (2015)). Because of the fact that endothelial cells cultured as a confluent monolayer show no strong polarization, I induced polarization. Therefore, I used the scratch assay, which is a migration assay. For directed migration the cells need to become polarized (Horwitz and Webb, 2003).

Vladar et al. (2012) have shown that in tracheal epithelial cells of mice Fzd6 and Vangl1 are expressed in a polarized manner. Therefore, I used antibodies against FZDs and VANGL and stained migrating cells. I found polarized expression of FZD5 and VANGL2 in migrating HD-LECs. FZD5 is predominantly expressed in the trailing end of the cells and VANGL2 in the leading end. Both molecules do not show the expected clear expression at the cell membrane. This could be due to the fact that migration of cells *in vitro* differs from migration *in vivo* (Horwitz and Webb, 2003). And, the expression of Fzd6 and Vangl1 in tracheal epithelial cells was not a result of migration, but of pre-existing polarisation. Lim et al. (2016) showed nicely the expression of PRICKLE1 at the trailing end of human gastric cancer cells with the same antibody I used in my studies. Correspondingly, in migrating HD-LECs I observed PRICKLE1 expression at the trailing end.

Taken together, my results clearly show that migrating LECs in scratch assays are polarized, and this can be demonstrated by the polarized expression of PCP-related proteins.

4.3 PORCN inhibition with LGK974 prevents WNT5A secretion in HD-LECs

I used the PORCN inhibitor LGK974 in almost all of my studies to prevent WNT secretion. LGK974 was discovered by J Liu et al. (2013) and proposed as a possible drug for cancer treatment. Today, LGK974 is in phase 1 clinical trials for WNT-related cancers like melanoma, breast cancer and neuroepithelioma. LGK974 is a small molecule drug that inhibits PORCN. PORCN is a membrane-bound O-acyltransferases located at the ER. It palmitoylates WNT ligands, and this palmitoylation is needed for the secretion of the WNT ligands.

J Liu et al. (2013) showed in their studies that LGK974 is able to block secretion of Wnt1, -2, -3, -3A, -6, -7A, and -9A, and that this inhibition is highly specific for WNTs. They also stated that the inhibitory effect of LGK974 is consistent with the genetic loss of the PORCN phenotype (J Liu et al., 2013). They did not test if

LGK974 is able to block WNT5A secretion. Therefore, I tested if LGK974 inhibits WNT5A secretion in HD-LECs. I collected supernatants of HD-LECs, which had been treated for three days with 10 μ M LGK974, concentrated them and analysed them with Western blots (WB) for the presences of WNT5A. The amount of WNT5A in the supernatants after LGK974 treatment was significantly decreased or almost absent, which clearly shows that LGK974 blocks WNT5A secretion.

I had added LGK974 to the normal growth medium, which contains FBS. This led to a strong BSA fraction on the WB, and it appeared that this might have influenced the results. Therefore, I repeated this analysis, and applied LGK974 to LECs in serum-free culture medium. To exclude any effects of culturing under serum-free conditions, I collected supernatants already after 24 h and repeated the experiment three times. Again, the application of LGK974 led also to a significant reduction of WNT5A in the supernatants, which clearly shows that LGK974 blocks WNT5A secretion in LECs.

I also tested the cell lysates of the treated LECs for WNT5A expression. I expected, like shown by J Liu et al. (2013) for Wnt3a, that no change in the amount of WNT5A occurred, or that eventually an increase would be seen, because of an accumulation of WNT5A in the cells. However, my studies show that LGK974 also reduced the amount of WNT5A in the cells (in both conditions, w/wo serum). I can only speculate why LGK974 induced this effect. One reason could be the concentration of LGK974. I used 10 μ M (the concentration that showed inhibitory effects in the *in vitro* assays), while the highest concentration used by J Liu et al. (2013) was 0,5 μ M. However, they noted that there was no cytotoxicity up to 20 μ M. Furthermore, I treated the cells for up to three days, whereas J Liu et al. (2013) treated the cells in the reporter assay only for 24 h. Taken together, my studies show that LGK974 is able to inhibit WNT5A production and secretion in HD-LECs.

LGK974 is not the only available PORCN inhibitor. There are others like Wnt-C59 or IWP-3. I tested Wnt-C59 initially in the spheroid assays, and there I observed that LGK974 showed a stronger inhibitory effect. Therefore, I concentrated on LGK974 in all assays performed thereafter.

4.4 WNT signalling regulates various mechanisms of lymphangiogenesis

My studies on mouse dermis and the studies by Buttler et al. (2013) provided the hypothesis that in *Wnt5a*-null-mice the morphogenesis of lymphatic networks is defective. To analyse the underlying mechanisms more deeply, I used *in vitro* angiogenesis assays with human LECs and studied isolated aspects of lymphangiogenesis. There are established angiogenesis assays (for BECs) that provide a way of measuring these mechanisms e.g. proliferation, migration, sprouting, and network (tube) formation. I adapted these angiogenesis assays to lymphangiogenesis. I focussed on three different assays and analysed the influence of WNT signalling on lymphangiogenic aspects in greater detail.

The first assay I performed was the spheroid assay, which measures sprouting of LECs. In this assay, EC are allowed to assemble into aggregates (spheroids). Then, these aggregates are transferred into extracellular matrix (ECM), like Matrigel. The cells of the outer layer of the spheroids behave like tip-cells of developing/growing vessels and sprout into the ECM (Korff and Augustin, 1998). I performed the initial assays with lymphangioma-derived LY-LECs (which were previously also used by Buttler et al. (2013)) and tested two PORCN inhibitors (*Wnt-C59* and *LGK974*). Both of the inhibitors significantly prevented sprouting. This clearly shows that sprouting of LY-LECs is WNT-dependent, which may provide a new therapeutic strategy for the lymphangioma patients.

During my studies, our lab analysed the LY-LECs in greater detail and it was found that the cells possess a monoallelic activating mutation of the *PIK3CA* gene (Blesinger et al., 2018). Since there may be interactions between the *PIK3CA* pathway and the WNT-signalling pathway, I switched to LECs, which were isolated from healthy donors. It was confirmed that the HD-LECs used in my further studies do not possess activating mutations of the *PIK3CA* gene (Blesinger et al., 2018).

Therefore, I performed the spheroid assays with HD-LECs from a healthy donor. I observed that healthy LECs needed a stimulation with growth factors, especially VEGF-C, for sprouting. That sprouting of LECs can be stimulated with VEGF-C has been shown before (Bruyère et al., 2008). Like in the studies of Bruyère et al. (2008), I was able to block sprouting by application of soluble VEGF receptors, which bind VEGF-C. Interestingly, I could also inhibit the VEGF-C-induced sprouting with the two PORCN inhibitors (Wnt-C59 and LGK974). This again shows that sprouting of LECs is WNT-dependent and supports the hypothesis of a connection/interplay between WNT and VEGF signalling (Olsen et al., 2017; Zhang et al., 2016).

I further studied if the WNT-inhibition effects by LGK974 can be rescued by the application of recombinant WNT5A, but this was not successful. This could have multiple reasons. Most likely, WNT ligands are very sticky proteins with a lipid anchor, and signal only in direct cell contact or over short distances. There was probably not enough active WNT5A protein reaching the cell membranes through the Matrigel. WNTs are difficult to purify (van Amerongen et al., 2012) and expensive, therefore the studies could be repeated using supernatants from WNT5A overexpressing cells.

The second mechanisms of lymphangiogenesis I investigated in greater detail with a focus on WNT signalling was migration. As mentioned before, migration is an important mechanism of lymphangiogenesis. To analyse migration, I performed scratch assays. In this assay, a gap is scratched into a monolayer of cells and after a certain time-point the cells start to migrate towards this gap and close it. This type of migration also been called directed, or horizontal migration. I used several WNT-related activators and inhibitors in this assay and analysed their influence on migration.

In a first step, I used the PORCN inhibitor LGK974 in this assay, and the results clearly show that horizontal migration of HD-LECs is WNT-dependent. In a second step, I treated the HD-LECS for three days before scratching with LGK974 (to prevent autocrine WNT signalling) and applied recombinant WN5A after scratching. I observed that WNT5A is able to rescue the inhibitory effect of

LGK974. That the LGK974 inhibition is reversible, has also been shown for Wnt3a by J Liu et al. (2013). This clearly shows that WNT5A mediates horizontal migration of HD-LECs.

Discussing the scratch assays often leads to the question if the measured results exclusively reflect migration or if proliferation plays a role during the closure of the gap. It is known for quite some time that both migration and proliferation are important processes of vessel repair *in vivo* (Ausprunk and Folkman, 1977; Folkman and Haudenschild, 1980) and *in vitro* (Coomber and Gotlieb, 1990). It has also been shown that the first 3 - 4 rows of cells adjacent to the scratch are the ones that migrate (Ettenson and Gotlieb, 1994). To analyse the influence of proliferation, I also performed proliferation assays with all used drugs. These assays clearly reveal that HD-LECs need more than 24 h to double their cell number, and 24 h was the time-point where I stopped the scratch assays and analysed the scratch closure.

I tested two concentrations (10 μ M and 25 μ M) of LGK974 in proliferation assays. Thereby, the lower concentration did not show significant effects on the proliferation of HD-LECs after 24 h, 48 h and 72 h. Cells treated with 25 μ M showed reduced proliferation after 48 h and 72 h, but not after 24 h. These results are in line with the cytotoxicity level of 20 μ M determined by J Liu et al. (2013).

I also analysed the influence of pre-treatment with LGK974 and the application of recombinant WNT5A on proliferation. Again, there was no influence of both treatments on proliferation after 24 h and 48 h.

Having shown that horizontal migration is WNT-mediated, I analysed the downstream signalling of WNT5A. WNT5A is the most prominent member of β -catenin-independent WNT signalling pathway, but it has also been shown that WNT5A can activate the β -catenin-dependent WNT signalling pathway, depending upon the receptor context (AJ Mikels and Nusse, 2006). Therefore, in the next assays I applied two activators of the β -catenin-dependent WNT signalling pathway (IM-12 and Bio) and one inhibitor of the β -catenin-dependent WNT signalling pathway (FH535). Both activators inhibited the horizontal migration of HD-LECs significantly, whereas the application of the inhibitor of the β -catenin-dependent WNT

signalling did not influence LEC migration. It is well known that the two WNT signalling pathways can antagonize each other (Torres et al., 1996). And therefore, my results imply that activation of the β -catenin-dependent pathway leads to an inhibition of the β -catenin-independent pathway, which in turn inhibits migration. Taken together, my results suggest that horizontal migration of HD-LECs is mediated through WNT5A, which activates the β -catenin-independent pathway.

The inhibition of migration can also have a second reason. Both activators (IM-12 and Bio) are GSK3 inhibitors. Previously, Grumolato et al. (2010); and Yamamoto et al. (2007) have shown that GSK3 can phosphorylate ROR receptors in a WNT5A-dependent manner. So, this can also mean that the GSK3 inhibition leads to an inhibition of the β -catenin-independent pathway.

And GSK3 can phosphorylate more than 100 substrates (Beurel et al., 2015), which implies that inhibition of GSK3 can also interfere with other signalling pathways and cellular functions.

Additionally, I always tested if these drugs used in the scratch assays had an influence on the proliferation of HD-LECs. Both activators of the β -catenin-dependent signalling (IM-12 and Bio) did not change the proliferation significantly after 24 h. Interestingly, FH535, the inhibitor of the β -catenin-dependent signalling significantly inhibited the proliferation after 24 h, but did not influence the migration in the scratch assays. Again, this proves that the scratch assays performed here exclusively measured migration and not proliferation.

4.5 WNT5A mediates horizontal migration of HD-LECs via RAC and JNK

Because of the fact that the hints that horizontal migration of HD-LECs is regulated through β -catenin-independent signalling via WNT5A, my next focus was to analyse the downstream signalling cascade of the WNT5A/ β -catenin-independent signalling in greater detail.

For this purpose, I also used scratch assays and small molecule inhibitors. The first investigated downstream signalling molecule was ROCK. Numerous studies have shown that this kinase plays an important part in the control of migration (e.g. reviewed in Amano et al. (2010)). I tested two commonly used small molecule inhibitors, Fasudil and Y-27632. Both of them did not block the migration of HD-LECs. I tested the drugs also in proliferation assays. Thereby, Y-27632 did and Fasudil did not reduced the proliferation of HD-LECs after 24 h. But, like for FH535, this clearly proves that the scratch assay specifically measures migration.

There is a potential explanation why inhibition of ROCK does not influence the migration of HD-LECs. In fact, several studies have shown that ROCK mediates migration of cells by influencing the cytoskeleton, also called amoeboid-like migration (Sahai and Marshall, 2003). A second form of migration is called mesenchymal migration. During this type of migration the cells form protrusions/filopodia, which has often been associated with RAC (Sahai and Marshall, 2003). And because of the fact that I observed filopodia in migrating HD-LECs, I assume that horizontal migration of HD-LECs represents mesenchymal type of migration.

Therefore, in the next set of scratch assay I tested two RAC inhibitor – EHT 1864 and NSC 234766. Both of the inhibitors significantly reduced the migration of HD-LECs. I performed proliferation assay as well. One inhibitor decreased proliferation (NSC 234766), whereas EHT 1864 did not have any effects. Again, it is highly unlikely that this reduced proliferation influenced the measured migration.

In the last set of scratch assays, I used inhibitors for JNK, a downstream signalling molecule of RAC. Both of the inhibitors – SP600125 and JNK-IN-8 – reduced the migration of LECs significantly, and did not have any effect on proliferation. This clearly shows that horizontal migration of HD-LECs is regulated by RAC and JNK.

To test if WNT5A is the ligand that activates this pathway, I used Western blot analysis and studied if JNK becomes phosphorylated after stimulation of HD-LECs with WNT5A. I used LGK974-pre-treated HD-LECs and stimulated them with recombinant WNT5A. Because of the fact that under normal growth conditions an overall phosphorylation of JNK was detectable, I had to starved the

cells for 24 h in serum-free medium before WNT5A application. The WB clearly showed that WNT5A induced a strong phosphorylation of JNK after 15 and 30 minutes, whereas after 2 h the level of phosphorylation was nearly back to normal. This shows clearly that WNT5A is a potent activator of JNK in HD-LECs and that WNT5A mediates horizontal migration via RAC and JNK.

That WNT5A mediates horizontal migration of cells via RAC and JNK is not a completely new finding. Nomachi et al. (2008) have shown that Wnt5a induces polarized migration of murine fibroblasts, which is mediated by JNK. However, it has not been shown before that horizontal migration of HD-LECs is mediated through this pathway.

4.6 WNT5A increases network formation of HD-LECs *in vitro*

In a third angiogenesis assay, I analysed the influence of WNT signalling on network formation. Therefore, I used the widely accepted tube-formation assay. I used LGK974 pre-treated HD-LECs and then stimulated the cells with recombinant WNT5A. The application of WNT5A led to a significant increase in cell-covered area, number of tubes, number of branching points, and total tube length. Interestingly, already the pre-treatment with LGK974 induced increased network formation. This was weaker than the stimulation with WNT5A, but also significant. I have no clear explanation for this. One hypothesis may be that network formation of HD-LECs is regulated by an alternative pathway in the complete absence of WNT signalling. Probably, GSK3 is part of this pathway. As noted before, GSK3 is capable of phosphorylating numerous substrates. And in the absence of WNTs, when GSK3 is not inhibited by the WNT pathway, GSK3 may phosphorylate c-JUN (Sutherland, 2011), a transcription factor that is the downstream signalling molecule of JNK. Thereby, c-Jun regulates Receptor for Activated C Kinase 1 (RACK1) (López-Bergami et al., 2005), which in turn can regulate JNK. If this pathway induces network formation of LECs needs to be studied in future experiments.

4.7 WNTs regulate migration-associated and lymphangiocrine pathways

In the last part of my studies I investigated, which genes were regulated by auto-crine WNT signalling. For this part of my thesis I worked together with the TAL, Göttingen, and used mRNA-Sequencing. I analysed the regulation of genes in HD-LECs after treatment with LGK974, to inhibit autocrine WNT signalling of the cells.

Treatment with LGK974 induced the differential expression of 116 genes. To get an overview of the function of the genes listed, a gene-set-enrichment analysis was performed. This analysis produced a list of 3 regulated gene sets. Of note, one of these was the gene set “GO: movement of cell or subcellular component”. This gene set revealed the down-regulation of migration-related transcripts after the application of LGK974, which is in line with my experimental studies.

Three genes (IGF1, SPTA1, and SPTBN5) of the gene set caught my special attention. Insulin-like growth factor 1 (IGF-1) has important functions for the growth of the skeletal system. Mutations of the IGF-1 gene cause the Laron Syndrome, which is characterised by dwarfism (reviewed in Laron (2004)). Of note, *Wnt5a*-null mice have massive defects of the skeletal system. This implies that LECs control neighbouring cells (which is the function of the so-called angiocrine signalling), e.g. the cells of the developing skeleton in the limb buds.

Additionally, I observed down-regulation of SPTA1 and SPTBN5, which encode for spectrins, a group of cytoskeletal proteins, which are important for migration and also for the stability of the cell membrane.

In a first step, I started to validate the mRNAseq results. I repeated the experiments and analysed the expression of these three genes with qRT-PCR. The results confirmed the mRNAseq results. Again, all three genes were down regulated after treatment of HD-LECs with LGK974.

Further analyses have to be performed to analysis these findings in greater detail.

5 Summary and Conclusions

Lymphangiogenesis – the development of lymphatic vessels – takes place in response to lymphangiogenic growth factors during embryogenesis, wound healing, inflammation and cancer. It has been shown that WNT signalling plays important roles during embryonic development and cancer, and there are also a number of studies that have shown that WNT signalling controls angiogenesis. However, only very few investigations on WNT signalling on lymphangiogenesis exist, and these have not provided detailed analyses on the mechanisms how WNTs regulate the formation of lymphatics.

A previous study of my lab has revealed that *Wnt5a*, a member of the β -catenin-independent Wnt pathway, is an essential regulator of lymphatic development in the dermis of mice. At embryonic day (ED) 18.5, *Wnt5a*-null-mice possess non-functional, highly dilated lymphatics, in contrast to functional lymphatics with small lumen observed in *Wnt5a*^{+/-} and wild-type mice.

A) With whole-mount immunofluorescence staining, I show that *Wnt5a*^{-/-} embryos exhibit blood-filled, often cyst-like lymphatics in their dermis, which fail to form proper interconnections. With fluorescence micro-lymphangiography I can show that these lymphatics are non-functional, whereas in *Wnt5a*^{+/-} and wt-embryos lymphatic drainage is functional already at ED 17.5.

B) With various immunostaining techniques, I demonstrate that dermal lymphatics of murine embryos express several Wnt-related molecules, including *Wnt5a* and its Fzd receptors.

C) With a newly developed *ex vivo* culture of embryonic dermis I show that Wnts, and especially *Wnt5a*, are important regulators of lymphangiogenesis. The application of WNT5A protein to the dermis of ED 15.5 *Wnt5a*-null mice induces flow-independent development of slender, elongated lymphatic networks after two days, in contrast to an immature lymphatic plexus in the controls. Thereby, mor-

phology of individual LECs changes from round to elongated. Reversely, the application of the PORCN-inhibitor LGK974 (which prevents the secretion of WNTs, which I confirmed for WNT5A in human LECs) to wild type-mouse dermis significantly disrupts lymphatic network maturation and elongation.

D) Using various *in vitro* lymphangiogenesis assays with three different human LEC lines, I was able to show that WNTs, and prominently WNT5A, are potent regulators of lymphangiogenic mechanisms including sprouting, migration and tube formation. These mechanisms are independent of proliferation, which shows that non-canonical WNT signalling regulates various aspects of the morphogenesis of lymphatics. I also show that activation of the canonical pathway inhibits the effects of the non-canonical pathway.

E) My studies on the intracellular cascade of WNT5A signalling in migrating LECs with scratch assays show that pharmacological inhibition of the RHO-GTPase RAC, or the c-Jun N-terminal kinase JNK significantly reduce migration, which leads to the assumption that WNT5A regulates morphogenesis of lymphatics via RAC and JNK. This is supported by the finding that WNT5A induces transient phosphorylation of JNK.

F) Finally, global mRNAseq analyses of LECs show that WNTs regulate 116 genes. Among these there are genes that control migration, but also angiocrine growth factors that indicate an active control of LECs for the growth of neighbouring tissues.

Taken together, my data clearly show that WNT signalling is an essential regulator of lymphovascular morphogenesis.

6 Appendix

Additional Macrophotographs of a *Wnt5a*-null-mice and a wt-litterate control (ED 16,5) are shown in **Figure A- 1**.

Additional the 2way ANOVAs of proliferation studies are shown in **Table A- 1** to **Table A- 6**.

Table A-7 shows the all differentially regulated genes in HD-LECs treated with LGK974 compared to controls, determined with mRNAseq.

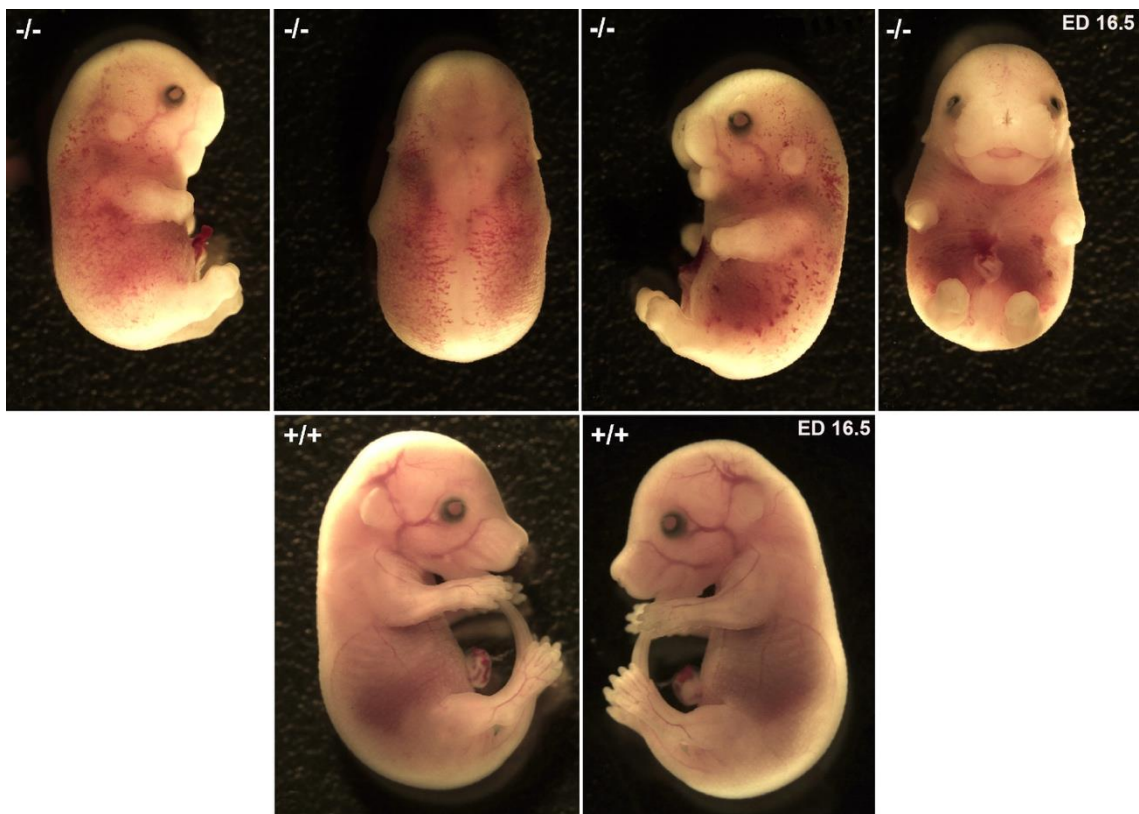


Figure A- 1: Macrophotographs of a *Wnt5a*-null-mouse embryo (upper row) and a littermate control (lower row). Note the petechial bleedings in the skin of the *Wnt5a*-null-mouse embryo.

Table A- 1: 2way ANOVA of proliferation studies with HD-LECs and the PORCN inhibitor LGK974.

2way ANOVA of Proliferation Studies with LGK974						
Within each row, compare columns (simple effects within rows)						
Number of families	4					
Number of comparisons per family	2					
Alpha	0.05					
Bonferroni's multiple comparisons test	Mean Diff.	95.00% CI of diff.	Significant?	Summary	Adjusted P Value	
0 h						
DMSO vs. LGK974 10 μ M	0	-8.647 to 8.647	No	ns	>0.9999	
DMSO vs. LGK974 25 μ M	0	-8.647 to 8.647	No	ns	>0.9999	
24 h						
DMSO vs. LGK974 10 μ M	2.385	-16.1 to 20.87	No	ns	>0.9999	
DMSO vs. LGK974 25 μ M	12.42	-6.063 to 30.91	No	ns	0.3216	
48h						
DMSO vs. LGK974 10 μ M	-8.846	-27.33 to 9.641	No	ns	0.7535	
DMSO vs. LGK974 25 μ M	25.58	7.09 to 44.06	Yes	**	0.0028	
72 h						
DMSO vs. LGK974 10 μ M	-9.409	-27.9 to 9.078	No	ns	0.6668	
DMSO vs. LGK974 25 μ M	26.5	8.018 to 44.99	Yes	**	0.0019	

Table A- 2: 2way ANOVA of proliferation studies with LGK974 pre-treated (10 μ M) HD-LECs and 500ng/ml WNT5A.

2way ANOVA of Proliferation Studies with WNT5A						
Within each row, compare columns (simple effects within rows)						
Number of families	4					
Number of comparisons per family	2					
Alpha	0.05					
Bonferroni's multiple comparisons test	Mean Diff.	95.00% CI of diff.	Significant?	Summary	Adjusted P Value	
0 h						
DMSO vs. LGK974 10 μ M ^{pre}	2.50E-06	-26.1 to 26.1	No	ns	>0.9999	
DMSO vs. LGK974 10 μ M ^{pre} + WNT5A	9.17E-06	-26.1 to 26.1	No	ns	>0.9999	
24 h						
DMSO vs. LGK974 10 μ M ^{pre}	7.879	-18.22 to 33.98	No	ns	>0.9999	
DMSO vs. LGK974 10 μ M ^{pre} + WNT5A	5.53	-20.57 to 31.63	No	ns	>0.9999	
48h						
DMSO vs. LGK974 10 μ M ^{pre}	26.01	-0.0954 to 52.11	No	ns	0.0512	
DMSO vs. LGK974 10 μ M ^{pre} + WNT5A	23.75	-2.352 to 49.85	No	ns	0.0878	
72h						
DMSO vs. LGK974 10 μ M ^{pre}	42.22	16.11 to 68.32	Yes	***	0.0004	
DMSO vs. LGK974 10 μ M ^{pre} + WNT5A	33	6.902 to 59.11	Yes	**	0.0076	

Table A- 3: 2way ANOVA of proliferation studies with an inhibitor of the β -catenin-dependent WNT signalling pathway (FH535) and two activators (Bio and IM-12).

2way ANOVA of Proliferation Studies with IM-12, Bio and FH535						
Within each row, compare columns (simple effects within rows)						
Number of families	4					
Number of comparisons per family	2					
Alpha	0.05					
Bonferroni's multiple comparisons test	Mean Diff.	95.00% CI of diff.	Significant?	Summary	Adjusted Value	P
0 h						
DMSO vs. IM-12 10 μ M	0	-12.67 to 12.67	No	ns	>0.9999	
DMSO vs. BIO 2 μ M	0	-12.67 to 12.67	No	ns	>0.9999	
DMSO vs. FH535 10 μ M	0	-12.67 to 12.67	No	ns	>0.9999	
24 h						
DMSO vs. IM-12 10 μ M	-0.5325	-22.95 to 21.88	No	ns	>0.9999	
DMSO vs. BIO 2 μ M	16.95	-5.464 to 39.37	No	ns	0.2098	
DMSO vs. FH535 10 μ M	26.09	3.677 to 48.51	Yes	*	0.0161	
48 h						
DMSO vs. IM-12 10 μ M	26.95	4.535 to 49.36	Yes	*	0.0121	
DMSO vs. BIO 2 μ M	44.46	22.05 to 66.88	Yes	***	<0.0001	
DMSO vs. FH535 10 μ M	63.66	41.25 to 86.08	Yes	***	<0.0001	
72 h						
DMSO vs. IM-12 10 μ M	74.84	52.43 to 97.26	Yes	***	<0.0001	
DMSO vs. BIO 2 μ M	66.27	43.85 to 88.68	Yes	***	<0.0001	
DMSO vs. FH535 10 μ M	85.05	62.63 to 107.5	Yes	***	<0.0001	

Table A- 4: 2way ANOVA of proliferation studies with the ROCK inhibitors Y-27632 and Fasudil.

2way ANOVA of Proliferation Studies with Y-27632 and Fasudil						
Within each row, compare columns (simple effects within rows)						
Number of families	4					
Number of comparisons per family	2					
Alpha	0.05					
Bonferroni's multiple comparisons test	Mean Diff.	95.00% CI of diff.	Significant?	Summary	Adjusted P Value	
0 h						
DMSO vs. Y-27632 50 μ M	0	-11.69 to 11.69	No	ns	>0.9999	
DMSO vs. Fasudil 10 μ M	0	-11.69 to 11.69	No	ns	>0.9999	
24 h						
DMSO vs. Y-27632 50 μ M	25.34	5.962 to 44.72	Yes	**	0.0069	
DMSO vs. Fasudil 10 μ M	-8.125	-29.6 to 13.35	No	ns	0.7906	
48 h						
DMSO vs. Y-27632 50 μ M	51.24	31.7 to 70.78	Yes	***	<0.0001	
DMSO vs. Fasudil 10 μ M	-26.31	-47.92 to -4.695	Yes	*	0.0129	
72 h						
DMSO vs. Y-27632 50 μ M	67.89	48.19 to 87.59	Yes	***	<0.0001	
DMSO vs. Fasudil 10 μ M	-49.64	-71.11 to -28.17	Yes	***	<0.0001	

Table A- 5: 2way ANOVA of proliferation studies with the RAC inhibitors EHT 1864 and NSC23766.

2way ANOVA of Proliferation Studies with EHT 1864 and NSC23766						
Within each row, compare columns (simple effects within rows)						
Number of families	4					
Number of comparisons per family	2					
Alpha	0.05					
Bonferroni's multiple comparisons test	Mean Diff.	95.00% CI of diff.	Significant?	Summary	Adjusted P Value	
0 h						
DMSO vs. EHT 1864 10 μ M	-2.65	-27.96 to 22.66	No	ns	>0.9999	
DMSO vs. NSC23766 100 μ M	-3.448	-28.76 to 21.87	No	ns	>0.9999	
24 h						
DMSO vs. EHT 1864 10 μ M	24.46	-0.8565 to 49.77	No	ns	0.0621	
DMSO vs. NSC23766 100 μ M	31.29	5.976 to 56.6	Yes	**	0.0094	
48 h						
DMSO vs. EHT 1864 10 μ M	59	33.69 to 84.32	Yes	***	<0.0001	
DMSO vs. NSC23766 100 μ M	75.1	49.78 to 100.4	Yes	***	<0.0001	
72 h						
DMSO vs. EHT 1864 10 μ M	83.65	58.34 to 109	Yes	***	<0.0001	
DMSO vs. NSC23766 100 μ M	100.8	75.45 to 126.1	Yes	***	<0.0001	

Table A- 6: 2way ANOVA of proliferation studies with the JNK inhibitors SP600125 and JNK-IN-8.

2way ANOVA of Proliferation Studies with SP600125 and JNK-IN-8						
Within each row, compare columns (simple effects within rows)						
Number of families	4					
Number of comparisons per family	2					
Alpha	0.05					
Bonferroni's multiple comparisons test	Mean Diff.	95.00% CI of diff.	Significant?	Summary	Adjusted P Value	
0 h						
DMSO vs. SP600125 10 μ M	0	-13.65 to 13.65	No	ns	>0.9999	
DMSO vs. JNK-IN-8 5 μ M	0	-13.65 to 13.65	No	ns	>0.9999	
24 h						
DMSO vs. SP600125 10 μ M	8.298	-16.14 to 32.74	No	ns	0.8913	
DMSO vs. JNK-IN-8 5 μ M	6.213	-16.42 to 28.84	No	ns	>0.9999	
48 h						
DMSO vs. SP600125 10 μ M	30.78	5.87 to 55.69	Yes	*	0.0113	
DMSO vs. JNK-IN-8 5 μ M	45.58	22.59 to 68.57	Yes	***	<0.0001	
72 h						
DMSO vs. SP600125 10 μ M	48.7	24.26 to 73.14	Yes	***	<0.0001	
DMSO vs. JNK-IN-8 5 μ M	92.43	69.8 to 115.1	Yes	***	<0.0001	

Table A-7: List of differentially regulated genes in HD-LECs treated with LGK974 compared to controls, ranked according to the adjusted p value (padj).

ensembl gene id	external gene name	description	baseMean	log2FoldChange	padj
ENSG00000164949	GEM	GTP binding protein overexpressed in skeletal muscle [Source:HGNC Symbol;Acc:HGNC:4234]	2.85	2.16	4.58E-02
ENSG00000017427	IGF1	insulin like growth factor 1 [Source:HGNC Symbol;Acc:HGNC:5464]	2.66	-2.57	3.99E-02
ENSG00000196557	CACNA1H	calcium voltage-gated channel subunit alpha 1 H [Source:HGNC Symbol;Acc:HGNC:1395]	6.73	2.15	3.80E-02
ENSG00000138061	CYP1B1	cytochrome P450 family 1 subfamily B member 1 [Source:HGNC Symbol;Acc:HGNC:2597]	3.03	-3.59	3.70E-02
ENSG00000224745	AC063965.1		2.73	2.35	3.43E-02
ENSG00000173862	AC008080.1		2.86	-2.32	3.41E-02
ENSG00000048545	GUCA1A	guanylate cyclase activator 1A [Source:HGNC Symbol;Acc:HGNC:4678]	4.19	2.19	3.35E-02
ENSG00000253649	PRSS51	protease, serine 51 [Source:HGNC Symbol;Acc:HGNC:37321]	3.09	-2.20	3.22E-02
ENSG00000218896	TUBB8P2	tubulin beta 8 class VIII pseudogene 2 [Source:HGNC Symbol;Acc:HGNC:42334]	2.63	2.29	3.10E-02
ENSG00000267655	AC125437.1		2.65	-2.16	3.07E-02
ENSG00000179772	FOXS1	forkhead box S1 [Source:HGNC Symbol;Acc:HGNC:3735]	122.49	2.52	3.03E-02
ENSG00000231231	LINC01423	long intergenic non-protein coding RNA 1423 [Source:HGNC Symbol;Acc:HGNC:50732]	3.49	2.26	3.02E-02
ENSG00000172986	GXYLT2	glucosyl xylosyltransferase 2 [Source:HGNC Symbol;Acc:HGNC:33383]	2.65	2.40	2.98E-02
ENSG00000187474	FFR3	formyl peptide receptor 3 [Source:HGNC Symbol;Acc:HGNC:3828]	3.39	2.04	2.97E-02
ENSG00000141698	CP1A2	cerebellin 2 precursor [Source:HGNC Symbol;Acc:HGNC:1544]	9.32	-2.02	2.76E-02
ENSG00000240244	GAPDH P33	glyceraldehyde 3 phosphate dehydrogenase pseudogene 33 [Source:HGNC Symbol;Acc:HGNC:37785]	3.19	-2.31	2.71E-02
ENSG00000188263	IL17REL	interleukin 17 receptor E like [Source:HGNC Symbol;Acc:HGNC:33808]	3.25	2.16	2.71E-02
ENSG00000235442	AL391845.2		3.31	-2.18	2.70E-02
ENSG00000255189	GLYATL1P1	glycine-N-acyltransferase like 1 pseudogene 1 [Source:HGNC Symbol;Acc:HGNC:37866]	11.50	-2.10	2.70E-02
ENSG00000278396	AL122023.1		3.85	-2.12	2.70E-02
ENSG00000104892	KLC3	kinesin light chain 3 [Source:HGNC Symbol;Acc:HGNC:20717]	5.68	2.20	2.07E-02
ENSG00000065325	GLP2R	glucagon like peptide 2 receptor [Source:HGNC Symbol;Acc:HGNC:4325]	4.93	-2.63	1.98E-02
ENSG00000156804	FBXO32	F-box protein 32 [Source:HGNC Symbol;Acc:HGNC:16731]	402.09	-2.22	1.96E-02
ENSG00000276846	AC016590.3		2.98	-2.45	1.94E-02
ENSG00000272076	AC090186.1		2.94	-2.36	1.82E-02
ENSG00000229308	AC010737.1		5.53	-2.12	1.63E-02
ENSG00000175899	A2M	alpha-2-macroglobulin [Source:HGNC Symbol;Acc:HGNC:7]	703.69	-2.81	1.59E-02
ENSG00000225401	TGIF2P1	TGFB induced factor homeobox 2 pseudogene 1 [Source:HGNC Symbol;Acc:HGNC:33317]	3.18	-2.25	1.58E-02
ENSG00000047457	CP	ceruloplasmin [Source:HGNC Symbol;Acc:HGNC:2295]	6.13	-2.09	1.58E-02
ENSG00000128655	PDE11A	phosphodiesterase 11A [Source:HGNC Symbol;Acc:HGNC:8773]	2.73	-3.41	1.50E-02
ENSG00000286220	AL365277.2		3.42	2.21	1.47E-02
ENSG00000270462	AC005034.2		2.74	3.23	1.29E-02
ENSG00000125285	SOX21	SRY-box 21 [Source:HGNC Symbol;Acc:HGNC:11197]	7.40	-2.97	1.21E-02
ENSG00000273062	AL449106.1		2.88	-2.66	1.11E-02
ENSG00000106302	HYAL4	hyaluronoglucosaminidase 4 [Source:HGNC Symbol;Acc:HGNC:5323]	32.24	-2.19	1.02E-02
ENSG00000066813	ACSM2B	acyl-CoA synthetase medium-chain family member 2B [Source:HGNC Symbol;Acc:HGNC:30931]	3.82	-3.07	9.48E-03
ENSG00000225407	AC025188.1		3.05	-3.09	8.89E-03
ENSG00000179817	MRGPRX4	MAS related GPR family member X4 [Source:HGNC Symbol;Acc:HGNC:17617]	3.13	-2.84	8.56E-03
ENSG00000159450	TCHH	trichohyalin [Source:HGNC Symbol;Acc:HGNC:11791]	3.66	-2.29	7.73E-03
ENSG00000140009	ESR2	estrogen receptor 2 [Source:HGNC Symbol;Acc:HGNC:3468]	4.60	-2.68	7.49E-03
ENSG00000143001	TMEM61	transmembrane protein 61 [Source:HGNC Symbol;Acc:HGNC:27296]	3.81	2.21	7.44E-03
ENSG00000204291	COL15A1	collagen type XV alpha 1 chain [Source:HGNC Symbol;Acc:HGNC:2192]	27.79	-4.21	7.22E-03
ENSG00000277883	NLRP3P1	NLR family pyrin domain containing 3 pseudogene 1 [Source:HGNC Symbol;Acc:HGNC:29886]	3.67	-2.24	6.71E-03
ENSG00000230519	HMGBP1A9	high mobility group box 1 pseudogene 49 [Source:HGNC Symbol;Acc:HGNC:39282]	3.67	-2.79	6.13E-03
ENSG00000226650	KIF4B	kinesin family member 4B [Source:HGNC Symbol;Acc:HGNC:6322]	4.05	-2.27	5.91E-03
ENSG00000185739	SRL	sarcalumenin [Source:HGNC Symbol;Acc:HGNC:11295]	4.71	2.73	5.57E-03
ENSG00000280639	LINC02204	long intergenic non-protein coding RNA 2204 [Source:HGNC Symbol;Acc:HGNC:53070]	3.87	-2.86	5.54E-03
ENSG00000154133	DPEP1	dipeptidase 1 (renal) [Source:HGNC Symbol;Acc:HGNC:3002]	6.37	-2.53	5.26E-03
ENSG00000279881	AC041040.2		5.44	-2.07	5.20E-03
ENSG00000255843	AP000593.3		4.41	2.47	3.87E-03
ENSG00000230400	LINC01747	long intergenic non-protein coding RNA 1747 [Source:HGNC Symbol;Acc:HGNC:52536]	3.88	-3.17	3.76E-03
ENSG00000270022	Z93241.1		6.40	-2.02	3.41E-03
ENSG00000196209	SIRPB2	signal regulatory protein beta 2 [Source:HGNC Symbol;Acc:HGNC:16247]	10.30	-3.33	3.31E-03
ENSG00000119891	ULBP1	UL16 binding protein 1 [Source:HGNC Symbol;Acc:HGNC:14893]	10.63	2.15	2.87E-03
ENSG00000242173	ARHGDI3	Rho GDP dissociation inhibitor gamma [Source:HGNC Symbol;Acc:HGNC:680]	8.22	2.10	2.96E-03
ENSG00000269101	LINC00565	long intergenic non-protein coding RNA 565 [Source:HGNC Symbol;Acc:HGNC:43709]	3.15	-3.63	2.71E-03
ENSG00000279807	AC011472.5		7.68	2.28	1.97E-03
ENSG00000007314	CACNA4	sodium voltage-gated channel alpha subunit 4 [Source:HGNC Symbol;Acc:HGNC:10591]	4.02	2.79	1.85E-03
ENSG00000074181	NOTCH3	notch 3 [Source:HGNC Symbol;Acc:HGNC:7883]	639.62	2.70	1.48E-03
ENSG00000203280	AL022323.1		4.56	-3.11	1.27E-03
ENSG00000270587	AC046185.2		4.51	-2.47	1.21E-03
ENSG00000106066	CPVL	carboxypeptidase, vitellogenic like [Source:HGNC Symbol;Acc:HGNC:14399]	5.00	-2.46	1.04E-03
ENSG00000100583	SAMD15	sterile alpha motif domain containing 15 [Source:HGNC Symbol;Acc:HGNC:18631]	5.86	-2.09	1.03E-03
ENSG00000141968	VAV1	vav guanine nucleotide exchange factor 1 [Source:HGNC Symbol;Acc:HGNC:12657]	5.13	2.52	9.97E-04
ENSG00000132933	SLC7A14	solute carrier family 7 member 14 [Source:HGNC Symbol;Acc:HGNC:29326]	69.90	2.34	8.92E-04
ENSG00000163814	CDCP1	CUB domain containing protein 1 [Source:HGNC Symbol;Acc:HGNC:24357]	8.89	2.62	8.64E-04
ENSG00000204423	LINC00636	long intergenic non-protein coding RNA 636 [Source:HGNC Symbol;Acc:HGNC:27702]	4.69	-3.20	7.64E-04
ENSG00000108688	CCL7	C-C motif chemokine ligand 7 [Source:HGNC Symbol;Acc:HGNC:10634]	5.01	2.93	7.18E-04
ENSG00000250548	AL355916.1		7.95	-2.39	5.70E-04
ENSG00000125910	S1PR4	sphingosine-1-phosphate receptor 4 [Source:HGNC Symbol;Acc:HGNC:3170]	7.44	-2.19	4.31E-04
ENSG00000184344	GDF3	growth differentiation factor 3 [Source:HGNC Symbol;Acc:HGNC:4218]	47.19	-2.67	4.20E-04
ENSG0000027359	AC017074.1		5.34	-2.77	3.96E-04
ENSG00000272568	AC005162.3		8.87	-2.13	3.62E-04
ENSG00000181577	C6orf223	chromosome 6 open reading frame 223 [Source:HGNC Symbol;Acc:HGNC:28692]	4.57	4.07	2.95E-04
ENSG00000176236	C10orf111	chromosome 10 open reading frame 111 [Source:HGNC Symbol;Acc:HGNC:28582]	7.98	-2.42	2.83E-04
ENSG00000116031	CD207	CD207 molecule [Source:HGNC Symbol;Acc:HGNC:17935]	11.20	-2.14	2.15E-04
ENSG00000240602	AADACP1	arylacetamide deacetylase pseudogene 1 [Source:HGNC Symbol;Acc:HGNC:50305]	9.89	-2.11	1.94E-04
ENSG00000221972	C3orf36	chromosome 3 open reading frame 36 [Source:HGNC Symbol;Acc:HGNC:26170]	26.26	-2.19	1.55E-04
ENSG00000259523	AC022613.2		7.34	-2.09	1.39E-04
ENSG00000140465	CYP1A1	cytochrome P450 family 1 subfamily A member 1 [Source:HGNC Symbol;Acc:HGNC:2595]	1123.46	-3.21	1.24E-04
ENSG00000270093	AP000473.2		12.56	-2.04	1.16E-04
ENSG00000081277	PKP1	plakophilin 1 [Source:HGNC Symbol;Acc:HGNC:9023]	10.75	3.17	6.40E-05
ENSG00000115718	PROC	protein C, inactivator of coagulation factors Va and VIIIa [Source:HGNC Symbol;Acc:HGNC:9451]	8.06	2.31	4.81E-05
ENSG00000136883	KIF12	kinesin family member 12 [Source:HGNC Symbol;Acc:HGNC:21495]	13.69	2.05	4.81E-05
ENSG00000163554	SPTA1	spectrin alpha, erythrocytic 1 [Source:HGNC Symbol;Acc:HGNC:11272]	59.54	-2.85	4.61E-05
ENSG00000127325	BEST3	bestrophin 3 [Source:HGNC Symbol;Acc:HGNC:17105]	8.07	-2.40	4.59E-05
ENSG00000163121	NEURL3	neuronal E3 ubiquitin protein ligase 3 [Source:HGNC Symbol;Acc:HGNC:25162]	11.63	2.05	4.28E-05
ENSG00000137877	SPTBN5	spectrin beta, non-erythrocytic 5 [Source:HGNC Symbol;Acc:HGNC:15680]	259.12	-2.06	2.80E-05
ENSG00000162998	FRZB	frizzled-related protein [Source:HGNC Symbol;Acc:HGNC:3959]	9.24	-2.61	2.26E-05
ENSG00000205426	KRT81	keratin 81 [Source:HGNC Symbol;Acc:HGNC:6458]	22.90	6.06	2.19E-05
ENSG00000185518	SV2B	synaptic vesicle glycoprotein 2B [Source:HGNC Symbol;Acc:HGNC:16874]	12.07	-2.80	1.71E-05
ENSG00000085596	CYP28A1	cytochrome P450 family 26 subfamily A member 1 [Source:HGNC Symbol;Acc:HGNC:2603]	53.20	-2.07	1.54E-05
ENSG00000271755	AL031118.1		9.28	3.18	1.44E-05
ENSG00000176194	CIDEA	cell death-inducing DFFA-like effector a [Source:HGNC Symbol;Acc:HGNC:1976]	31.12	2.44	6.64E-06
ENSG00000137285	TUBB2B	tubulin beta 2B class Iib [Source:HGNC Symbol;Acc:HGNC:30829]	16.28	2.88	5.23E-06
ENSG00000074211	PPP2R2C	protein phosphatase 2 regulatory subunit Bgamma [Source:HGNC Symbol;Acc:HGNC:9306]	17.28	-2.05	4.95E-06
ENSG00000255968	AC024145.1		16.10	2.28	1.28E-06
ENSG00000167772	ANGPTL4	angiopoietin like 4 [Source:HGNC Symbol;Acc:HGNC:16039]	527.50	-2.28	8.03E-07
ENSG00000206559	KCNG31	potassium voltage-gated channel modifier subfamily G member 1 [Source:HGNC Symbol;Acc:HGNC:6248]	34.46	2.07	7.86E-07
ENSG00000167528	ZNF641	zinc finger protein 641 [Source:HGNC Symbol;Acc:HGNC:31834]	26.51	-2.06	1.91E-07
ENSG00000103485	OPRT	quinolinate phosphoribosyltransferase [Source:HGNC Symbol;Acc:HGNC:9755]	13.57	2.51	1.85E-07
ENSG00000227218	AL157935.1		15.64	-2.25	6.81E-08
ENSG00000164400	CSF2	colony stimulating factor 2 [Source:HGNC Symbol;Acc:HGNC:2434]	19.92	2.70	1.68E-08
ENSG00000105613	MAST1	microtubule associated serine/threonine kinase 1 [Source:HGNC Symbol;Acc:HGNC:19034]	113.81	2.05	1.69E-09
ENSG00000260804	LINC01963	long intergenic non-protein coding RNA 1963 [Source:HGNC Symbol;Acc:HGNC:25283]	121.43	-2.13	1.02E-11
ENSG00000115009	CCL20	C-C motif chemokine ligand 20 [Source:HGNC Symbol;Acc:HGNC:10619]	137.29	2.18	1.57E-13
ENSG00000124875	CXCL6	C-X-C motif chemokine ligand 6 [Source:HGNC Symbol;Acc:HGNC:10643]	56.83	3.31	4.29E-14
ENSG00000272476	AL024507.2		51.03	-2.17	2.10E-14
ENSG00000148600	CDHR1	cadherin related family member 1 [Source:HGNC Symbol;Acc:HGNC:14550]	29.82	2.98	8.60E-15
ENSG00000172349	IL16	interleukin 16 [Source:HGNC Symbol;Acc:HGNC:5960]	91.73	-2.60	1.24E-17
ENSG00000174059	CD34	CD34 molecule [Source:HGNC Symbol;Acc:HGNC:1662]	4217.67	-2.22	1.24E-17
ENSG00000258943	AL049871.1		42.41	-4.75	2.42E-18
ENSG00000277494	GPIHBP1	glycosylphosphatidylinositol anchored high density lipoprotein binding protein 1 [Source:HGNC Symbol;Acc:HGNC:24945]	224.05	-2.84	6.48E-21
ENSG00000279348	AC012513.3		68.40	-2.25	4.18E-24
ENSG00000265972	TXNIP	thioredoxin interacting protein [Source:HGNC Symbol;Acc:HGNC:16952]	3214.84	-2.27	6.89E-40

7 Bibliography

Aebischer D, Iolyeva M, Halin C (2014): The inflammatory response of lymphatic endothelium *Angiogenesis* 17, 383-393

Alitalo K, Tammela T, Petrova TV (2005): Lymphangiogenesis in development and human disease *Nature* 438, 946-953

Amano M, Nakayama M, Kaibuchi K (2010): Rho-kinase/ROCK: A key regulator of the cytoskeleton and cell polarity *Cytoskeleton (Hoboken, N.J.)* 67, 545-554

Andersson ER, Bryjova L, Biris K, Yamaguchi TP, Arenas E, Bryja V (2010): Genetic interaction between Lrp6 and Wnt5a during mouse development *Dev Dyn* 239, 237-245

Asem MS, Buechler S, Wates RB, Miller DL, Stack MS (2016): Wnt5a Signaling in Cancer *Cancers (Basel)* 8

Aspelund A, Antila S, Proulx ST, Karlsen TV, Karaman S, Detmar M, Wiig H, Alitalo K (2015): A dural lymphatic vascular system that drains brain interstitial fluid and macromolecules *J Exp Med* 212, 991-999

Ausprunk DH, Folkman J (1977): Migration and proliferation of endothelial cells in preformed and newly formed blood vessels during tumor angiogenesis *Microvasc Res* 14, 53-65

Bafico A, Liu G, Goldin L, Harris V, Aaronson SA (2004): An autocrine mechanism for constitutive Wnt pathway activation in human cancer cells *Cancer Cell* 6, 497-506

Baluk P, Fuxe J, Hashizume H, Romano T, Lashnits E, Butz S, Vestweber D, Corada M, Molendini C, Dejana E, et al. (2007): Functionally specialized junctions between endothelial cells of lymphatic vessels *J Exp Med* 204, 2349-2362

Becker J, Erdlenbruch B, Noskova I, Schramm A, Aumailley M, Schorderet DF, Schweigerer L (2006): Keratopithelin suppresses the progression of experimental human neuroblastomas *Cancer Res* 66, 5314-5321

Becker J, Wilting J (2018): WNT signaling, the development of the sympathoadrenal–paraganglionic system and neuroblastoma *Cellular and Molecular Life Sciences* 75, 1057-1070

Beurel E, Grieco SF, Jope RS (2015): Glycogen synthase kinase-3 (GSK3): regulation, actions, and diseases *Pharmacology & therapeutics* 148, 114-131

Blesinger H, Kaulfuss S, Aung T, Schwoch S, Prantl L, Rossler J, Wilting J, Becker J (2018): PIK3CA mutations are specifically localized to lymphatic endothelial cells of lymphatic malformations *PLoS One* 13, e0200343

Bruyère F, Melen-Lamalle L, Blacher S, Roland G, Thiry M, Moons L, Frankenne F, Carmeliet P, Alitalo K, Libert C, et al. (2008): Modeling lymphangiogenesis in a three-dimensional culture system *Nature Methods* 5, 431

Bryja V, Andersson ER, Schambony A, Esner M, Bryjova L, Biris KK, Hall AC, Kraft B, Cajanek L, Yamaguchi TP, et al. (2009): The extracellular domain of Lrp5/6 inhibits noncanonical Wnt signaling in vivo *Mol Biol Cell* 20, 924-936

Buttler K, Becker J, Pukrop T, Wilting J (2013): Maldevelopment of dermal lymphatics in Wnt5a-knockout-mice *Dev Biol* 381, 365-376

Card CM, Yu SS, Swartz MA (2014): Emerging roles of lymphatic endothelium in regulating adaptive immunity *J Clin Invest* 124, 943-952

Cattelino A, Liebner S, Gallini R, Zanetti A, Balconi G, Corsi A, Bianco P, Wolburg H, Moore R, Oreda B, et al. (2003): The conditional inactivation of the beta-catenin gene in endothelial cells causes a defective vascular pattern and increased vascular fragility *The Journal of cell biology* 162, 1111-1122

Cervantes S, Yamaguchi TP, Hebrok M (2009): Wnt5a is essential for intestinal elongation in mice *Dev Biol* 326, 285-294

Cha B, Geng X, Mahamud MR, Fu J, Mukherjee A, Kim Y, Jho E-H, Kim TH, Kahn ML, Xia L, et al. (2016): Mechanotransduction activates canonical Wnt/ β -catenin signaling to promote lymphatic vascular patterning and the development of lymphatic and lymphovenous valves *Genes & development* 30, 1454-1469

Cheng CW, Yeh JC, Fan TP, Smith SK, Charnock-Jones DS (2008): Wnt5a-mediated non-canonical Wnt signalling regulates human endothelial cell proliferation and migration *Biochemical and Biophysical Research Communications* 365, 285-290

Cirone P, Lin S, Griesbach HL, Zhang Y, Slusarski DC, Crews CM (2008): A role for planar cell polarity signaling in angiogenesis *Angiogenesis* 11, 347-360

Coomber BL, Gotlieb AI (1990): In vitro endothelial wound repair. Interaction of cell migration and proliferation *Arteriosclerosis* 10, 215-222

Corada M, Nyqvist D, Orsenigo F, Caprini A, Giampietro C, Taketo MM, Iruela-Arispe ML, Adams RH, Dejana E (2010): The Wnt/ β -catenin pathway modulates vascular remodeling and specification by upregulating Dll4/Notch signaling *Dev Cell* 18, 938-949

Dejana E (2010): The role of wnt signaling in physiological and pathological angiogenesis *Circ Res* 107, 943-952

Descamps B, Sewduth R, Ferreira Tojais N, Jaspard B, Reynaud A, Sohet F, Lacolley P, Allieres C, Lamaziere JM, Moreau C, et al. (2012): Frizzled 4 regulates

arterial network organization through noncanonical Wnt/planar cell polarity signaling
Circ Res 110, 47-58

Dijksterhuis JP, Baljinnyam B, Stanger K, Sercan HO, Ji Y, Andres O, Rubin JS, Hannoush RN, Schulte G (2015): Systematic mapping of WNT-FZD protein interactions reveals functional selectivity by distinct WNT-FZD pairs J Biol Chem 290, 6789-6798

Djjane A, Riou J, Umbhauer M, Boucaut J, Shi D (2000): Role of frizzled 7 in the regulation of convergent extension movements during gastrulation in *Xenopus laevis* Development 127, 3091-3100

<https://www.gnu.org/software/octave/doc/v4.4.1/>; Zugriff

Ettenson DS, Gotlieb AI (1994): Endothelial wounds with disruption in cell migration repair primarily by cell proliferation Microvasc Res 48, 328-337

Findlay AS, Panzica DA, Walczysko P, Holt AB, Henderson DJ, West JD, Rajnicek AM, Collinson JM (2016): The core planar cell polarity gene, *Vangl2*, directs adult corneal epithelial cell alignment and migration Royal Society open science 3, 160658-160658

Folkman J (1995): Angiogenesis in cancer, vascular, rheumatoid and other disease Nat Med 1, 27-31

Folkman J, Haudenschild C (1980): Angiogenesis in vitro Nature 288, 551-556

Gao B, Ajima R, Yang W, Li C, Song H, Anderson MJ, Liu RR, Lewandoski MB, Yamaguchi TP, Yang Y (2018): Coordinated directional outgrowth and pattern formation by integration of Wnt5a and Fgf signaling in planar cell polarity Development 145

Grumolato L, Liu G, Mong P, Mudbhary R, Biswas R, Arroyave R, Vijayakumar S, Economides AN, Aaronson SA (2010): Canonical and noncanonical Wnts use a common mechanism to activate completely unrelated coreceptors Genes Dev 24, 2517-2530

Hasselhof V, Sperling A, Buttler K, Strobel P, Becker J, Aung T, Felmerer G, Wilting J (2016): Morphological and Molecular Characterization of Human Dermal Lymphatic Collectors PLoS One 11, e0164964

He TC, Sparks AB, Rago C, Hermeking H, Zawel L, da Costa LT, Morin PJ, Vogelstein B, Kinzler KW (1998): Identification of c-MYC as a target of the APC pathway Science 281, 1509-1512

He X, Saint-Jeannet J-P, Wang Y, Nathans J, Dawid I, Varmus H (1997): A Member of the Frizzled Protein Family Mediating Axis Induction by Wnt-5A Science 275, 1652-1654

He X, Semenov M, Tamai K, Zeng X (2004): LDL receptor-related proteins 5 and 6 in Wnt/beta-catenin signaling: arrows point the way *Development* 131, 1663-1677

Ho HY, Susman MW, Bikoff JB, Ryu YK, Jonas AM, Hu L, Kuruvilla R, Greenberg ME (2012): Wnt5a-Ror-Dishevelled signaling constitutes a core developmental pathway that controls tissue morphogenesis *Proc Natl Acad Sci U S A* 109, 4044-4051

Horwitz R, Webb D (2003): Cell migration *Curr Biol* 13, R756-759

Huntington GS, McClure CFW (1910): The anatomy and development of the jugular lymph sacs in the domestic cat (*Felis domestica*) *American Journal of Anatomy* 10, 177-312

Jain RK (2003): Molecular regulation of vessel maturation *Nat Med* 9, 685-693

Katoh M, Katoh M (2017): Molecular genetics and targeted therapy of WNT-related human diseases (Review) *Int J Mol Med* 40, 587-606

Kikuchi A, Yamamoto H, Sato A, Matsumoto S (2011): New insights into the mechanism of Wnt signaling pathway activation *Int Rev Cell Mol Biol* 291, 21-71

Klotz L, Norman S, Vieira JM, Masters M, Rohling M, Dube KN, Bollini S, Matsuzaki F, Carr CA, Riley PR (2015): Cardiac lymphatics are heterogeneous in origin and respond to injury *Nature* 522, 62-67

Korff T, Augustin HG (1998): Integration of endothelial cells in multicellular spheroids prevents apoptosis and induces differentiation *J Cell Biol* 143, 1341-1352

Korn C, Scholz B, Hu J, Srivastava K, Wojtarowicz J, Arnsperger T, Adams RH, Boutros M, Augustin HG, Augustin I (2014): Endothelial cell-derived non-canonical Wnt ligands control vascular pruning in angiogenesis *Development* 141, 1757-1766

Kubota Y, Kleinman HK, Martin GR, Lawley TJ (1988): Role of laminin and basement membrane in the morphological differentiation of human endothelial cells into capillary-like structures *J Cell Biol* 107, 1589-1598

Kurayoshi M, Yamamoto H, Izumi S, Kikuchi A (2007): Post-translational palmitoylation and glycosylation of Wnt-5a are necessary for its signalling *Biochem J* 402, 515-523

Laemmli UK (1970): Cleavage of structural proteins during the assembly of the head of bacteriophage T4 *Nature* 227, 680-685

Laron Z (2004): Laron syndrome (primary growth hormone resistance or insensitivity): the personal experience 1958-2003 *J Clin Endocrinol Metab* 89, 1031-1044

Li J, Ying J, Fan Y, Wu L, Ying Y, Chan AT, Srivastava G, Tao Q (2010): WNT5A antagonizes WNT/beta-catenin signaling and is frequently silenced by promoter CpG methylation in esophageal squamous cell carcinoma *Cancer Biol Ther* 10, 617-624

Lim BC, Matsumoto S, Yamamoto H, Mizuno H, Kikuta J, Ishii M, Kikuchi A (2016): Prickle1 promotes focal adhesion disassembly in cooperation with the CLASP-LL5beta complex in migrating cells *J Cell Sci* 129, 3115-3129

Liu J, Pan S, Hsieh MH, Ng N, Sun F, Wang T, Kasibhatla S, Schuller AG, Li AG, Cheng D, et al. (2013): Targeting Wnt-driven cancer through the inhibition of Porcupine by LGK974 *Proc Natl Acad Sci U S A* 110, 20224-20229

Liu WC, Chen S, Zheng L, Qin L (2017): Angiogenesis Assays for the Evaluation of Angiogenic Properties of Orthopaedic Biomaterials - A General Review *Adv Healthc Mater* 6

Livak KJ, Schmittgen TD (2001): Analysis of relative gene expression data using real-time quantitative PCR and the 2^{-Delta Delta C(T)} Method *Methods* 25, 402-408

Logan CY, Nusse R (2004): The Wnt signaling pathway in development and disease *Annu Rev Cell Dev Biol* 20, 781-810

López-Bergami P, Habelhah H, Bhoumik A, Zhang W, Wang L-H, Ronai Ze (2005): RACK1 mediates activation of JNK by protein kinase C [corrected] *Molecular cell* 19, 309-320

Louveau A, Smirnov I, Keyes TJ, Eccles JD, Rouhani SJ, Peske JD, Derecki NC, Castle D, Mandell JW, Lee KS, et al. (2015): Structural and functional features of central nervous system lymphatic vessels *Nature* 523, 337-341

Martinez-Corral I, Ulvmar MH, Stanczuk L, Tatin F, Kizhatil K, John SW, Alitalo K, Ortega S, Makinen T (2015): Nonvenous origin of dermal lymphatic vasculature *Circ Res* 116, 1649-1654

Masckauchan TN, Agalliu D, Vorontchikhina M, Ahn A, Parmalee NL, Li CM, Khoo A, Tycko B, Brown AM, Kitajewski J (2006): Wnt5a signaling induces proliferation and survival of endothelial cells in vitro and expression of MMP-1 and Tie-2 *Mol Biol Cell* 17, 5163-5172

Mikels A, Minami Y, Nusse R (2009): Ror2 receptor requires tyrosine kinase activity to mediate Wnt5A signaling *J Biol Chem* 284, 30167-30176

Mikels AJ, Nusse R (2006): Purified Wnt5a protein activates or inhibits beta-catenin-TCF signaling depending on receptor context *PLoS Biol* 4, e115

Modlich U, Kaup FJ, Augustin HG (1996): Cyclic angiogenesis and blood vessel regression in the ovary: blood vessel regression during luteolysis involves endothelial cell detachment and vessel occlusion *Lab Invest* 74, 771-780

Muley A, Odaka Y, Lewkowich IP, Vemaraju S, Yamaguchi TP, Shawber C, Dickie BH, Lang RA (2017): Myeloid Wnt ligands are required for normal development of dermal lymphatic vasculature PLoS One 12, e0181549

Nicenboim J, Malkinson G, Lupo T, Asaf L, Sela Y, Maysel O, Gibbs-Bar L, Senderovich N, Hashimshony T, Shin M, et al. (2015): Lymphatic vessels arise from specialized angioblasts within a venous niche Nature 522, 56-U100

Niederleithner H, Heinz M, Tauber S, Bilban M, Pehamberger H, Sonderegger S, Knöfler M, Bracher A, Berger W, Loewe R, et al. (2012): Wnt1 Is Anti-Lymphangiogenic in a Melanoma Mouse Model Journal of Investigative Dermatology 132, 2235-2244

Niehrs C (2012): The complex world of WNT receptor signalling Nat Rev Mol Cell Biol 13, 767-779

Nomachi A, Nishita M, Inaba D, Enomoto M, Hamasaki M, Minami Y (2008): Receptor tyrosine kinase Ror2 mediates Wnt5a-induced polarized cell migration by activating c-Jun N-terminal kinase via actin-binding protein filamin A J Biol Chem 283, 27973-27981

Norgall S, Papoutsi M, Rossler J, Schweigerer L, Wilting J, Weich HA (2007): Elevated expression of VEGFR-3 in lymphatic endothelial cells from lymphangiomas BMC Cancer 7, 105

Nusse R (2005): Wnt signaling in disease and in development Cell Res 15, 28-32

Ny A, Koch M, Schneider M, Neven E, Tong RT, Maity S, Fischer C, Plaisance S, Lambrechts D, Heligon C, et al. (2005): A genetic *Xenopus laevis* tadpole model to study lymphangiogenesis Nat Med 11, 998-1004

O'Leary NA, Wright MW, Brister JR, Ciufo S, Haddad D, McVeigh R, Rajput B, Robbertse B, Smith-White B, Ako-Adjei D, et al. (2016): Reference sequence (RefSeq) database at NCBI: current status, taxonomic expansion, and functional annotation Nucleic acids research 44, D733-D745

Olsen JJ, Pohl SÖ-G, Deshmukh A, Visweswaran M, Ward NC, Arfuso F, Agostino M, Dharmarajan A (2017): The Role of Wnt Signalling in Angiogenesis The Clinical biochemist. Reviews 38, 131-142

Pansky B: Review of Medical Embryology. Macmillan, New York 1982

Polakis P (2012): Wnt signaling in cancer Cold Spring Harb Perspect Biol 4

Proffitt KD, Madan B, Ke Z, Pendharkar V, Ding L, Lee MA, Hannoush RN, Virshup DM (2013): Pharmacological inhibition of the Wnt acyltransferase PORCN prevents growth of WNT-driven mammary cancer Cancer Res 73, 502-507

Ribatti D (2006): Genetic and epigenetic mechanisms in the early development of the vascular system *Journal of anatomy* 208, 139-152

Riento K, Ridley AJ (2003): ROCKs: multifunctional kinases in cell behaviour *Nature Reviews Molecular Cell Biology* 4, 446

Risau W (1997): Mechanisms of angiogenesis *Nature* 386, 671-674

Risau W, Flamme I (1995): Vasculogenesis *Annu Rev Cell Dev Biol* 11, 73-91

Sabin FR (1902): On the origin of the lymphatic system from the veins and the development of the lymph hearts and thoracic duct in the pig *Am. J. Anat.* 1, 367-389

Sadok A, Marshall CJ (2014): Rho GTPases *Small GTPases* 5, e983878

Sahai E, Marshall CJ (2003): Differing modes of tumour cell invasion have distinct requirements for Rho/ROCK signalling and extracellular proteolysis *Nature Cell Biology* 5, 711

Schindelin J, Arganda-Carreras I, Frise E, Kaynig V, Longair M, Pietzsch T, Preibisch S, Rueden C, Saalfeld S, Schmid B, et al. (2012): Fiji: an open-source platform for biological-image analysis *Nat Methods* 9, 676-682

Schlange T, Matsuda Y, Lienhard S, Huber A, Hynes NE (2007): Autocrine WNT signaling contributes to breast cancer cell proliferation via the canonical WNT pathway and EGFR transactivation *Breast Cancer Res* 9, R63

Schneider M, Othman-Hassan K, Christ B, Wilting J (1999): Lymphangioblasts in the avian wing bud *Dev Dyn* 216, 311-319

Sessa R, Yuen D, Wan S, Rosner M, Padmanaban P, Ge S, Smith A, Fletcher R, Baudhuin-Kessel A, Yamaguchi TP, et al. (2016): Monocyte-derived Wnt5a regulates inflammatory lymphangiogenesis *Cell research* 26, 262-265

Shtutman M, Zhurinsky J, Simcha I, Albanese C, D'Amico M, Pestell R, Ben-Ze'ev A (1999): The cyclin D1 gene is a target of the beta-catenin/LEF-1 pathway *Proc Natl Acad Sci U S A* 96, 5522-5527

Srinivasan RS, Dillard ME, Lagutin OV, Lin FJ, Tsai S, Tsai MJ, Samokhvalov IM, Oliver G (2007): Lineage tracing demonstrates the venous origin of the mammalian lymphatic vasculature *Genes Dev* 21, 2422-2432

Sutherland C (2011): What Are the bona fide GSK3 Substrates? *Int J Alzheimers Dis* 2011, 505607

Tahergorabi Z, Khazaei M (2012): A review on angiogenesis and its assays *Iran J Basic Med Sci* 15, 1110-1126

Takada R, Satomi Y, Kurata T, Ueno N, Norioka S, Kondoh H, Takao T, Takada S (2006): Monounsaturated fatty acid modification of Wnt protein: its role in Wnt secretion *Dev Cell* 11, 791-801

Takeuchi S, Takeda K, Oishi I, Nomi M, Ikeya M, Itoh K, Tamura S, Ueda T, Hatta T, Otani H, et al. (2000): Mouse Ror2 receptor tyrosine kinase is required for the heart development and limb formation *Genes Cells* 5, 71-78

Tammela T, Alitalo K (2010): Lymphangiogenesis: Molecular mechanisms and future promise *Cell* 140, 460-476

Topczewski J, Sepich DS, Myers DC, Walker C, Amores A, Lele Z, Hammerschmidt M, Postlethwait J, Solnica-Krezel L (2001): The zebrafish glypican knypek controls cell polarity during gastrulation movements of convergent extension *Dev Cell* 1, 251-264

Topol L, Jiang X, Choi H, Garrett-Beal L, Carolan PJ, Yang Y (2003): Wnt-5a inhibits the canonical Wnt pathway by promoting GSK-3-independent beta-catenin degradation *J Cell Biol* 162, 899-908

Torres MA, Yang-Snyder JA, Purcell SM, DeMarais AA, McGrew LL, Moon RT (1996): Activities of the Wnt-1 class of secreted signaling factors are antagonized by the Wnt-5A class and by a dominant negative cadherin in early *Xenopus* development *J Cell Biol* 133, 1123-1137

van Amerongen R, Fuerer C, Mizutani M, Nusse R (2012): Wnt5a can both activate and repress Wnt/beta-catenin signaling during mouse embryonic development *Dev Biol* 369, 101-114

Vladar EK, Bayly RD, Sangoram AM, Scott MP, Axelrod JD (2012): Microtubules enable the planar cell polarity of airway cilia *Curr Biol* 22, 2203-2212

Wiese KE, Nusse R, van Amerongen R (2018): Wnt signalling: conquering complexity *Development* 145

Wigle JT, Oliver G (1999): Prox1 function is required for the development of the murine lymphatic system *Cell* 98, 769-778

Wilting J, Aref Y, Huang R, Tomarev SI, Schweigerer L, Christ B, Valasek P, Papoutsis M (2006): Dual origin of avian lymphatics *Dev Biol* 292, 165-173

Wilting J, Brand-Saberi B, Kurz H, Christ B (1995): Development of the embryonic vascular system *Cell Mol Biol Res* 41, 219-232

Wilting J, Chao TI: Integrated anatomy of the vascular system: PanVascular Medicine; hrsg v. Lanzer P; Springer-Verlag Berlin Heidelberg, Heidelberg, New York 2015, 193-242

Wilting J, Papoutsi M, Christ B, Nicolaides KH, von Kaisenberg CS, Borges J, Stark GB, Alitalo K, Tomarev SI, Niemeyer C, et al. (2002): The transcription factor Prox1 is a marker for lymphatic endothelial cells in normal and diseased human tissues *FASEB J* 16, 1271-1273

Yamada M, Udagawa J, Matsumoto A, Hashimoto R, Hatta T, Nishita M, Minami Y, Otani H (2010): Ror2 is required for midgut elongation during mouse development *Dev Dyn* 239, 941-953

Yamaguchi TP, Bradley A, McMahon AP, Jones S (1999): A Wnt5a pathway underlies outgrowth of multiple structures in the vertebrate embryo *Development* 126, 1211-1223

Yamamoto H, Yoo SK, Nishita M, Kikuchi A, Minami Y (2007): Wnt5a modulates glycogen synthase kinase 3 to induce phosphorylation of receptor tyrosine kinase Ror2 *Genes Cells* 12, 1215-1223

Yang DH, Yoon JY, Lee SH, Bryja V, Andersson ER, Arenas E, Kwon YG, Choi KY (2009): Wnt5a is required for endothelial differentiation of embryonic stem cells and vascularization via pathways involving both Wnt/beta-catenin and protein kinase Calpha *Circ Res* 104, 372-379

Yang Y, Mlodzik M (2015): Wnt-Frizzled/planar cell polarity signaling: cellular orientation by facing the wind (Wnt) *Annu Rev Cell Dev Biol* 31, 623-646

Yang Y, Oliver G (2014): Development of the mammalian lymphatic vasculature *J Clin Invest* 124, 888-897

Yaniv K, Isogai S, Castranova D, Dye L, Hitomi J, Weinstein BM (2006): Live imaging of lymphatic development in the zebrafish *Nat Med* 12, 711-716

Zhang Z, Nör F, Oh M, Cucco C, Shi S, Nör JE (2016): Wnt/ β -Catenin Signaling Determines the Vasculogenic Fate of Postnatal Mesenchymal Stem Cells *Stem cells (Dayton, Ohio)* 34, 1576-1587

Zudaire E, Gambardella L, Kurcz C, Vermeren S (2011): A computational tool for quantitative analysis of vascular networks *PLoS One* 6, e27385

Acknowledgements

First, I would like to thank Prof. Dr. Jörg Wilting for his support and supervision during the time of my thesis. I am very thankful for the advices he gave me and for the time he invested.

Furthermore, I am very grateful for the support, advice and new perspectives of my thesis committee members Prof. Dr. Gregor Eichele and Prof. Dr. Ahmed Mansouri.

I would also like to thank our cooperation partners. Dr. Gabriela Salinas and Kaamini Raithatha from the Microarray and Deep-Sequencing Core Facility of the UMG for performing the mRNA sequencing analysis, providing us with the statistical analysis and for their support. Moreover, I want to thank Prof. Dr. Dieter Kube and his team for the good collaboration, not only in work-related matters, and Dr. Ivo Chao and Rod Dungan for taking the macrophotographs of the mouse embryos. I thank Adem Saglam, who provided the script for Octave, which was used for the evaluation of the scratch assays. Without his support, this analysis would have taken months instead of minutes.

My special thank goes to Dr. Kerstin Buttler. I do not know what I would have done without her support and help during all these years.

I also want thank Dr. Jürgen Becker and Dr. Martina Vockerodt for all the practical and theoretical help and for all the inspiring and motivating discussions of the last years.

My sincere thank also goes to Berti Manshausen, Sonja Schwoch and Christina Zelent, for their practical, but also for their personal help in the last years. And I also like to thank and acknowledge all our former and current lab members, who supported and motivated me throughout the years.

Finally, I want to thank my family, my friends, my former flat mates and my boyfriend Andreas, who were there for me all the time. Without their support, I would never have finished this work.

Curriculum Vitae

Grit Lutze

Personal Information

Date of birth	September 9 th , 1986
Place of birth	Erfurt
Nationality	German

Education

07/2014 till present	Doctoral thesis at the University Medical Centre of the Georg-August University of Göttingen:
----------------------	---

“Regulation of lymphangiogenesis by WNT signalling: focus on WNT5A” (Institute of Anatomy and cell biology, supervisor: Prof. Dr. J. Wilting)

10/2006 - 09/2013	Diploma Studies of Biology at the Friedrich-Schiller University/Jena,
-------------------	---

Title of the Diploma thesis:

„Funktioneller Atlas des Antennallobus von Manduca sexta (Sphingidae, Lepidoptera)“ (MPI for Chemical Ecology, Department Evolutionary Neuroethology, supervisor: Dr. S. Bisch-Knaden)

09/2003 - 07/2006	Abitur (A-levels) Gutenberg Gymnasium Erfurt
09/1997 - 07/2003	Realschulabschluss (GCSE) Willy-Brandt Realschule Erfurt

Awards and Honours

Poster Prize for “Wnt5a in Lymphangiogenesis” at the Joint Dutch-German Microcirculation Meeting 2015/37th Annual Meeting of the German Society for Microcirculation and Vascular Biology (GfMVB), Sep 24, 2015 - Sep 26, 2015, Hannover